T H E U N I V E R S I T Y O F M I C H I G A N

COLLEGE OF ENGINEERING
Department of Engineering Mechanics
Meteorological Laboratories

Interim Report

VISUAL RESOLUTION AND OPTICAL SCINTILLATION OVER SNOW, ICE, AND FROZEN GROUND

Donald J. Portman
Associate Research Meteorologist

Edward Ryznar
Assistant Research Meteorologist

Floyd C. Elder
Assistant Research Meteorologist

Vincent E. Noble
Associate Research Physicist

ORA Project 03372

under contract with:

U. S. ARMY COLD REGIONS RESEARCH AND ENGINEERING LABORATORY
CORPS OF ENGINEERS
HANOVER, NEW HAMPSHIRE
CONTRACT NO. DA-11-190-ENG-78

administered through:

OFFICE OF RESEARCH ADMINISTRATION ANN ARBOR

September 1961

PREFACE

The work described in this report was conducted under U. S. Army Cold Regions Research and Engineering Laboratory, Corps of Engineers, Contract No. DA-11-190-ENG-78. The purpose was to investigate visual resolution and optical scintillation over snow, ice and frozen ground in such a way as to contribute, in general, to their predictability for various meteorological conditions. Only horizontal optical paths in clear air, one to two meters above the surfaces, were considered. Work on the contract included specifically (1) measurement of visual resolution, optical scintillation, and micrometeorological variables over snow, ice and frozen ground and (2) processing and analysis of the data obtained. This report gives the results of the analysis and measurement programs, a description of the equipment and procedures used, and a tabulation of the data obtained.

The authors wish to express their appreciation to Mr. Dwight Meeks for assistance in the measurement phase of the investigation, Mr. William Tank of Boeing Aircraft Company for his valuable assistance in the comparison of methods of spectral analysis, (Mrs.) Ruth Baehr for her work in data processing and (Mrs.) Joy Beil for typing the final report.

TABLE OF CONTENTS

TABLE OF CONTENTS (Continued)

LIST OF TABLES

LIST OF FIGURES

LIST OF FIGURES (Continued)

ABSTRACT

Optical scintillation, visual resolution, and wind and temperature profiles were measured over snow, ice, and frozen ground. The data were analyzed to determine relationships between (1) scintillation and visual resolution and (2) scintillation and meteorological and surface conditions.

The experimental results included (1) estimates of the limit of visual resolution, (2) telephotometer measurements of the apparent fluctuations in brightness (scintillation) of an artificial light source, and (3) measurements of wind direction and of the vertical distributions of wind speed and temperature. The optical path was 543 meters long and 1.5 meters above uniform horizontal surfaces. All scintillation and meteorological data are given in an appendix.

The principal results of the analysis showed that for turbulent flow in stable stratification over snow (1) visual resolution deteriorated systematically as scintillation increased in intensity and (2) scintillation intensity increased with increase in vertical temperature gradient. Scintillation was at a minimum in the absence of thermal stratification and at a maximum in very stable thermal stratification during the transition from laminar to turbulent flow. For a given temperature gradient, scintillation increased with increase in wind speed. When wind and temperature gradients were combined in terms of Richardson number and related to scintillation it was found that the data obtained over snow indicated a critical Richardson number of about 0.35.

Scintillation power spectra for eight periods revealed characteristics that could be related to visual resolution, Richardson number and the mean wind speed component normal to the optical path.

These and other relationships are discussed and equipment and measurement procedures are described.

1. INTRODUCTION

1.1 The Problem

Visual detection and recognition of distant objects is critically dependent on atmospheric conditions in the line of sight. In addition to contrast attenuation due to absorption and scattering of light by suspended particles and droplets, there are important diffraction and refraction effects caused by fluctuations in atmospheric density. To an observer viewing a distant object these effects appear as rapid changes in brightness (or intensity), position, and size. The net effect is to blur the image and, effectively, to reduce the apparent contrast between an object and its background. Brightness fluctuations are termed scintillation and image motion is called shimmer. These phenomena are most pronounced in clear weather, when the visual resolution otherwise would be unimpeded. They act, therefore, as the limiting factors in the ultimate resolution obtainable with optical devices for distant viewing.

The atmospheric density fluctuations responsible for scintillation and shimmer are the result of incomplete turbulent mixing of thermally stratified layers. The condition is common in the lower atmosphere because (1) it is nearly always turbulent and (2) during the day, the sun is constantly heating the ground surface more than the air, and at night, the surface is cooling faster than the air. Thermal stratification is absent only in very cloudy and windy conditions and during brief periods near sunrise and sunset (in most climates) when the vertical temperature gradient changes sign. Scintillation and shimmer appear to vary in a complex manner with turbulence and thermal stratification. They are absent in isothermal conditions and have a maximum intensity, dependent upon wind and surface roughness conditions, for maximum vertical temperature gradients.

The dependence of scintillation and shimmer on meteorological conditions near the ground suggests that if quantitative relationships were known, it would be possible to predict the deterioration in visual resolution from meteorological and surface data for any time and region of concern. The information gained would have a variety of applications in cold region operations and investigations. It could be applied, for example, to operational problems in surveying, military surveillance, and communications methods utilizing light propagation. In addition, the testing of optical systems in variable environmental conditions might require that scintillation and shimmer be isolated from other attenuation effects.

1.2 Previous Work

Work for the U. S. Army Cold Regions Research and Engineering Laboratories (then SIPRE) on relationships between visual resolution and meteorological and surface conditions was begun by the University of Michigan personnel in early 1960. In effect, it was a continuation of earlier work directed toward the design of optical sensors for combat area surveillance. In that work a series of field experiments were based on the measurement of scintillation of a spot-

light directed along a 2000 ft horizontal path to a telephotometer. The light path was about 1.5 meters above the ground on the eastern edge of Willow Run airfield. This location assured a relatively horizontal and homogeneous trajectory for air moving through the optical path from the west. In this way it was possible to characterize turbulence and thermal stratification in the optical path by measuring vertical wind and temperature gradients at a single location.

Results of the measurements confirmed early predictions that scintillation (1) would be absent when there is no height variation in average potential temperature, (2) could be as severe at night when temperature increases with height (inversion) as during the day when temperature decreases with height (lapse) and (3) increases with increase in length of optical path. Further consideration of the dependency of scintillation on turbulence and thermal stratification suggested that, for constant average density and for a given light source and optical system the degree of scintillation should depend on the following parameters:

1. Mean vertical gradient in potential temperature;
2. Mean wind speed;
3. Mean wind direction relative to the optical path;
4. Surface roughness;
5. Height of optical path;
6. Length of optical path.

1.3 Plan of the Investigation

Field experiments were based on the idea that empirical relationships among the six parameters and measured scintillation would make it possible to predict or estimate scintillation from ordinary meteorological and terrain information. Then from relationships between scintillation and visual resolution the desired goal could be achieved.

A more direct approach would include measurements of visual resolution and the appropriate meteorological variables only. There is an important difficulty in this approach, however. Since the meteorological variables have a wide range of values and exist in a wide range of combinations, it is necessary to conduct a large number of experiments to establish general relationships for reliable predictors. At the same time statistically reliable measurements of visual resolution must be made for each experiment. Since the latter require direct visual observations for realistic application to practical problems, they are subject to both psychological and physiological influences and should, ideally, be conducted with suitable replication. The combination of meteorological variability and experimental replication would require an impractically large number of experiments.

The direct recording of scintillation reduces, therefore, the number of field observations required. If a unique relationship between scintillation

and visual resolution can be established, then scintillation measurements, free from subjectivity, can be easily made for a wide variety of meteorological variables.

The reasoning developed for determining general relationships between visual resolution and meteorological and surface conditions is summarized schematically in Figure 1. Field experiments are conducted to determine relationships indicated by arrows b and c. These, with general micrometeorological knowledge of relationships shown by arrow a make it possible to estimate visual resolution directly from meteorological and surface data.

Figure 1

Predicting Visual Resolution from Meteorological and Surface Conditions

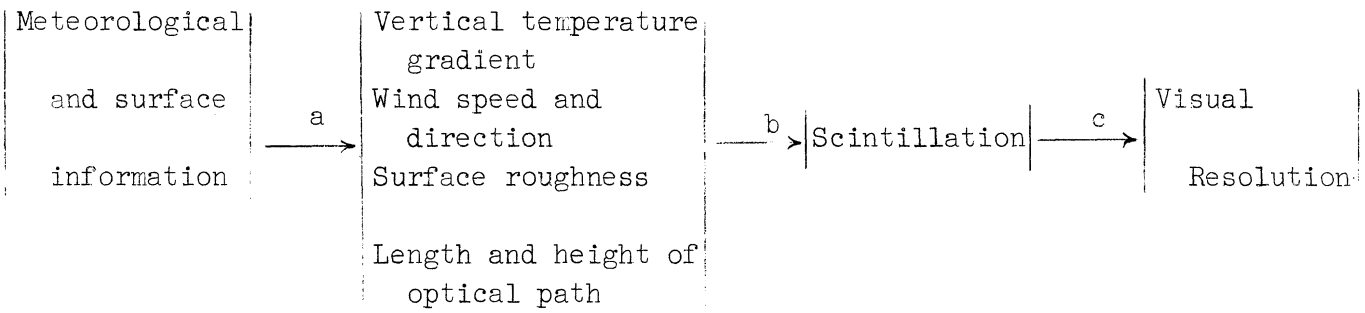

Most of the observations reported and discussed in this report were made at the CRREL Keweenaw Field Station in February and March 1960. The field was covered with snow about 0.5 meters deep and the optical path was about 1.5 meters above the snow and 543 meters long. Scintillation and average vertical wind and temperature gradients were measured as in the experiments at the Willow Run field station mentioned earlier. Visual resolution was determined by an observer viewing a Landolt broken-ring resolution chart through a 12-power telescope. The observer was positioned at the light source and the resolution chart near the telephotometer.

The observations were made mainly at night to avoid undesirable influences of background light on the telephotometer and to obtain data for a wide range of stable thermal gradients (inversions). The resolution chart was uniformly illuminated with flood lights for all nighttime observations.

The fact that nocturnal vision is necessarily restricted does not limit the significance of findings based on these observations. As indicated above, the analysis seeks to relate visual resolution to meteorological conditions independent of time of day. Since, however, inversions are common over high latitude snow surfaces, even in daylight, the results should be particularly

useful for cold region operations.

The conclusions listed in the following section are general statements relating visual resolution to scintillation and to wind and temperature conditions over snow and frozen ground in the absence of significant absorption or scattering by suspended materials. They are based on the results of simultaneous field measurements of (1) visual resolution and scintillation and (2) scintillation and wind and temperature conditions. The results themselves are described and discussed in following sections, and, finally, the equipment and procedures are described.

2. CONCLUSIONS

2.1 Visual Resolution and Scintillation

a. Visual resolution and scintillation (apparent brightness fluctuations of a distant light source) are inversely related; visual resolution deteriorates as scintillation increases and vice-versa.

b. Limited results from spectral measurements of scintillation suggest that visual resolution depends specifically on the product of (1) the relative amount of scintillation caused by turbulent inhomogeneities whose sizes are equal to and smaller than the size of the element being resolved and (2) the wind speed component normal to the line of sight.

2.2 Visual Resolution and Wind, Temperature and Surface Conditions

a. Because of the dependence of the index of refraction on air density, visual resolution is poorer at low temperatures and at high pressures than for the opposite condition (high temperatures and low pressures) for equivalent conditions of turbulence and thermal stratification.

b. In turbulent flow visual resolution deteriorates with increase in average vertical temperature gradient. Best resolution exists in the absence of temperature gradients and, therefore, in windy and cloudy conditions for all seasons, times of day and kinds of surface.

c. Visual resolution deteriorates with increasing mean wind speed for conditions otherwise constant. Since, however, in turbulent flow mean wind speed and vertical temperature gradient are inversely related, the effect is not apparent except at very low wind speeds when small increases in speed cause initial mixing of stably stratified layers.

d. The combined effect of stable thermal stratification (inversion condition) and turbulence on visual resolution may be expressed through the following relationships between scintillation and a characteristic Richardson number: The relative amount of scintillation per unit temperature gradient decreases rapidly as the Richardson number increases from near zero to a critical value and decreases less rapidly at higher Richardson numbers. The critical value was found to be about +0.35 for the experiments conducted over snow.

e. For positive Richardson numbers greater than about 0.35, visual resolution is apparently controlled by distortions in image caused by internal gravity waves in the transition between laminar and turbulent flow. Because of the random occurrence of the internal waves and the high variability of very low wind speeds visual resolution is extremely variable under these conditions.

f. Visual resolution deteriorates with increase in aerodynamic roughness of the underlying surface for equivalent conditions of wind speed and thermal

stratification. Since snow and ice surfaces are relatively smooth and often overlain with stably stratified air, their roughness effects on visual resolution are relatively insignificant at heights of the order of one meter or greater. The greater roughness of frozen ground, on the other hand, may be expected to influence turbulence in such a way that, for equivalent thermal stratification and mean wind speed, visual resolution over it would be inferior to that over snow and ice surfaces. The effect, however, would most likely be masked by differences in thermal stratification caused by both the roughness and thermal characteristics of the different surfaces.

g. Visual resolution is optimum for wind direction parallel to the optical path and minimum for the wind normal to the path.

2.3 Visual Resolution and Height and Length of Optical Path

a. Visual resolution improves with increase in height of the optical path since temperature gradient, wind shear and roughness effects decrease with height.

b. Visual resolution deteriorates with increase of length of optical path independently of image size effects.

3. RESULTS

3.1 Measurement Program

3.1.1 Visual Resolution and Scintillation Data--Data from simultaneous measurements of visual resolution and scintillation are listed for various periods of observation in Table I. Most of the data were obtained at the CRREL Keweenaw Field Station, Houghton, Michigan in February and March, 1960, over a snow surface at night. There are a few data, however, obtained in the daytime. The remainder of the observations, except for a very few over ice on Ford Lake near Ypsilanti, Michigan, were made over frozen ground at the University of Michigan Micrometeorological Field Station located at the Willow Run Airport. The latter are about equally divided between day and night.

Visual resolution was measured in terms of the smallest broken ring whose orientation could be positively identified by an observer with a 24 power telescope at a distance of 1780 feet. For convenience the broken rings are numbered according to size as shown in Table II. A detailed description of the equipment and procedures used in this measurement is given in Section 5.1.

Scintillation is measured in terms of per cent modulation (Pm or % mod.) a measure of the relative intensity of brightness fluctuations as "seen" by the telephotometer. It is 100 times the ratio of the average equivalent sine wave peak-to-peak voltage output (A.C. component) of the phototube to its average output level (D.C. component). A description of the measuring circuit is given in Section 5.2.

3.1.2 Scintillation and Meteorological Data--All scintillation and micrometeorological data obtained over snow at Keweenaw Field Station, over frozen ground at the Willow Run Airport and over ice at Ford Lake are tabulated in the Appendix. The data include total anemometer revolutions at 0.5, 1, 2 and 4 meters (nominal) above the surface for successive two-minute intervals and simultaneous averages of temperature differences between 0.5 meters and 1, 2 and 4 meters, wind direction and scintillation per cent modulation (Pm). Approximately 42 hours of data were obtained over snow, 18 hours over frozen ground and 3 hours over ice.

(a) Dates and times for all measurement periods are listed in Table III with information on cloudiness, wind, temperature, humidity and station pressure for each period. The meteorological data for the snow observations were taken from the standard WBAN form prepared at the Houghton Airport FAA weather station. The remaining data were taken from the WBAN form prepared at the Weather Bureau Station at Willow Run Airport.

(b) Figures 2 and 3 show the observed distributions of scintillation intensity for various wind speed and sky conditions over snow at night. The percentage frequency of occurrence of values of Pm are shown for various wind speeds for overcast (Figure 2) and clear or scattered (less than 0.6 cloudiness)

sky conditions (Figure 3). With an overcast sky the most frequently occurring values of Pm increased with increasing wind speed but did not exceed 35% mod. With a wind speed less than 2 mph these values were less than 10% mod about 85 per cent of the time and with a wind speed between 2 mph and 4 mph they were between 10 and 20% mod about 75 per cent of the time, etc. With a clear or scattered sky condition, and a wind speed less than 2 mph, values varied from less than 10 to about 85% mod. As the wind speed increased, the distributions became less skewed, and at wind speeds of 6-8 mph, a distinct peak occurred at about 35% mod with no occurrence above about 45% mod.

3.1.3 Magnetic Tape Recordings--Direct magnetic tape recordings of the telephotometer output were made for approximately 10 hours and 18 minutes over snow, 1 hour and 19 minutes over frozen ground and 21 minutes over ice. The periods of recording are listed in Table IV and descriptions of the recording equipment and procedures are given in Section 5.2.4. The recordings are contained in a total of 12 reels of tape which are filed at the University of Michigan Meteorological Laboratory at Willow Run.

3.2 Analysis Program

3.2.1 Visual Resolution and Scintillation Relationships

(a) The results of grouping and plotting visual resolution and scintillation data for observations over snow at night are shown in Figure 4 and are discussed in Section 4.2.1. Average values of Pm for various broken ring slot sizes (visual resolution limits) are shown in relation to slot size. The slot size (Table II) is the length of a side of the approximately square gap in the broken ring. Each point on the graph corresponds to the slot size for the smallest broken ring whose orientation could be identified positively in a series of trials during the two-minute period for which the average Pm was measured. The equipment and procedures for visual resolution determination are described in Section 5.1.

The number at the base of each vertical line segment refers to the number of observations included in computing the average Pm. Each vertical line segment, measured on the ordinate scale, equals two times the standard deviation for the mean on which it is centered.

The results shown in Figure 4 reveal a consistent deterioration in visual resolution as scintillation increases in intensity. They form the primary basis for relating visual resolution to wind and temperature conditions over snow during inversion conditions, i.e., for stable stratification.

The following statements summarize the observer's experiences in identifying broken ring orientations for the nighttime observations shown in Figure 4:

(1) During very low scintillation (1-15% mod) the observer discerned the orientation of all rings as large as or larger than number 11 at all

times and as small as number 13 some of the time.

(2) During low scintillation (16-30% mod) the observer discerned the orientation of all rings as large as or larger than number 7 at all times and as small as number 13 some of the time.

(3) During moderate scintillation (31-45% mod) the observer discerned the orientation of all rings as large as or larger than number 7 at at all times but seldom as small as number 9.

(4) During high scintillation 46-60% mod) the observer discerned the orientation of all rings as large as or larger then number 6 at all times but seldom as small as number 9.

(5) During very high scintillation (greater than 60% mod) the observer discerned the orientation of rings as large as or larger than number 5 at all times, but very seldom as small as number 7.

(b) The daytime observations of visual resolution over snow were too limited in range to permit analysis for systematic relationships with scintillation or meteorological conditions. As discussed in Section 4.2.2, the results show a correspondence between a very low average scintillation level (5-20% mod) and relatively good visual resolution. Ring numbers 13 and 14 were nearly always visible.

(c) The results for visual resolution and scintillation measured over frozen ground are shown in Figure 5 and are discussed in Sections 4.2.2 and 4.2.4. Curves for both daytime and nighttime observations are included. Standard deviations were not computed because of the relatively small number of observations for each plotted point. The nighttime results over frozen ground, although restricted in range, appear quite similar to those obtained over snow.

(d) The daytime results over frozen ground show a smaller variation in visual resolution with the same range of Pm than do the nighttime results for either snow or frozen ground. The differences may be due to measurement techniques as explained in Section 4.2.4.

The following statements summarize the observer's experiences in identifying broken ring orientations for the daytime observations over frozen ground shown in Figure 5:

(1) During very low scintillation (1-15% mod) the observer discerned the orientation of all rings as large or larger than number 14 at all times and number 15 occasionally.

(2) During low scintillation (16-30% mod) the observer discerned the orientation of all rings as large as or larger than number 14 at all times.

(3) During moderate scintillation (31-45% mod) the observer discerned the orientation of all rings as large as or larger than number 12 at all times and number 13 quite often.

(4) During high scintillation (46-60% mod) the observer discerned the orientation of all rings as large as or larger than number 10 at all times and number 11 occasionally.

(5) During very high scintillation (greater than 60% mod) the observer discerned the orientation of ring number 8 most of the time. Occasionally number 10 was discernible.

(e) Figure 6 shows a relationship between visual resolution and a spectral resolution factor for eight selected 2 minute measurement periods. Scintillation power spectra for the eight periods are given in Section 3.2.3. Slot size scaled on the ordinate is, as before, the size of the slot on the smallest broken ring whose orientation could be identified positively. The spectral resolution factor is the product of (1) the average component of the wind speed normal to the line of sight and (2) a measure of the total relative power due to thermal discontinuity elements whose length scales are equal to and less than the slot size at the limit of resolution. Specifically, the spectral resolution factor, F, is given by

$$F = \bar{V}_n \int_{1/s}^{\infty} W_p(k)\, d\,k = 2\pi \int_{\bar{V}_n/2\pi s}^{\infty} W_p(f)\, d\,f$$

in which $\bar{V}_n$ = wind speed component normal to line of sight, cm/sec

s = slot size at the limit of resolution, cm.

$W_p(k)$ = power per unit wavelength $(mv)^2/cm^{-1}$

k = wave number = $2\pi f/\bar{V}_n$, cycles/cm

f = scintillation frequency, cycles/sec

$W_p(f)$ = power per unit and width $(mv)^2$/cps

The results shown in this figure as discussed in Section 4.2.1 are based on limited data and no account has been taken of the "aperture integration."

3.2.2 Scintillation and Micrometeorological Relationships--

(a) Figure 7 shows the observed relationship between scintillation (Pm) and inversion magnitude between 4 and 0.5 meters for all data obtained at night over snow. Each plotted point represents the mean of all Pm observations for each one-degree temperature difference interval. The number of cases for each point is indicated in the figure in addition to the standard logarithmic deviation for each point.

The results, discussed in Section 4.1.2, show a systematic increase in scintillation with increasing inversion magnitude. The same data plotted in linear coordinates are shown in Figure 8.

(b) The observed relationship between scintillation (Pm) and the wind speed at 2 meters for all data obtained at night over snow is shown in Figure 9 and is discussed in Section 4.1.3. The data were grouped for wind speed intervals of 0.9 mph and the number of two-minute periods, averaged for each point is indicated, as in previous figures.

Except for winds less than 2 mph and between 8 and 10 mph, Pm shows a general tendency to decrease as the wind speed increases. For 0-2 and 8-10 mph there is an increase in Pm with increasing wind speed.

(c) Figure 10 shows the average relationship of wind speed, temperature difference and Pm. It is discussed in Section 4.1.4. Two-minute average values of Pm were averaged for wind speed intervals of one mph and temperature difference intervals of one degree C and isolines of Pm were drawn. The dashed lines are estimates of the behavior of the isolines in an apparently narrow region separating the area that includes all observations from that which includes none.

The figure shows that, in general:

(1) For a given temperature difference, Pm increases with increasing wind speed, and

(2) For a given wind speed, Pm increases with increase in temperature difference.

(d) Aerodynamic roughness parameters, computed from wind profiles during five separate adiabatic periods for the KFS snow surface, are given in Table V.

Table V

Feb., 1960	EST	z_o, cm.
5	1540-1556	0.014
9	1118-1134	0.008
12	(afternoon)	0.010
18	1500-1516	0.006
19	2220-2236	0.037

The method of computation and a brief discussion are given in Section 4.1.5.

(e) A relationship between Pm and Richardson number for the observations made in inversion conditions over snow is shown in Figure 11. Plotted in

logarithmic coordinates are Pm per unit temperature difference, Pm/ΔT, and positive Richardson numbers, +Ri. As indicated, ΔT is the temperature difference between one and two meters (nominal). Richardson numbers were computed according to Lettau's definition (Lettau, 1957) from wind and temperature data from the same two heights.

Thus $$Ri = \frac{g}{\overline{T}} \quad \frac{\partial\theta / \partial z}{(\partial\overline{u} / \partial z)^2}$$

$$\frac{2g\, z_{1,2}\, (\overline{\theta}_2 - \overline{\theta}_1) \ln n}{\overline{T}_2\, (\overline{u}_2 - \overline{u}_1)^2}$$

in which g = acceleration due to gravity, cm/sec^2.
$\overline{T}$ = average temperature, deg. A.
$\overline{\theta}$ = average potential temperature, deg. C.
$\overline{u}$ = average wind speed, cm/sec.
$z_{1.2} = (z_1 \cdot z_2)^{1/2}$, cm.
$n = (z_2/z_1)^{1/2}$

The number of two-minute periods averaged for each point is indicated in the figure, and the standard linear deviation for each mean is indicated by the length of the vertical line segment extending above and below each point. It should be noted that because the standard deviations were computed on a linear basis and shown on a logarithmic scale, the line segments are not directly comparable for different regions of the scale. The two lines whose equations are shown in the figure were obtained by linear regression with each point weighted according to the number of observations averaged.

The results of this analysis shows that Pm/ΔT varies as $Ri^{-0.72}$ for $+0.005 > Ri < +0.35$ and as $Ri^{-0.08}$ for $+0.35 < Ri < +150$. The significance of the apparent discontinuity and other aspects of the results are discussed in Section 4.1.6.

3.2.3 Scintillation Power Spectra--Power spectra for eight selected two-minute periods are shown in Figure 12. The relative power per unit frequency is scaled in terms of the square of the millivolt output of the harmonic wave analyzer and graphed for frequencies ranging from 2.5 to 100 cycles per second. A detailed description of the method of analysis is given in Section 5.4.3.

The eight periods were selected mainly on the basis of visual resolution and Pm data. They provide the basic data for computing spectral resolution

factors presented in Figure 6. For the eight periods there is a visual resolution range corresponding to a slot size range of 0.61 to 3.68 cm. Pm ranged from 11 to 62 for the eight periods. These and other appropriate data are included in Table VI.

Table VI

Summary of Meteorological Measurements Coincident with Power Spectra of Scintillation

Group	Period	Date 1960	Time EST	$\bar{U}_{1.5m}$ cm/sec	$\bar{V}_n$ cm/sec	+Ri	$T_{2m}-T_{1m}$ Deg.C	Sky	% Mod	$+\overline{Ri}$	$\bar{\bar{V}}_n$ cm/sec
3	I	2/13	2131-33	137.2	68.6	0.19	1.7	Clear	62	0.17	64.4
	III	2/13	2054-56	94.0	60.3	0.16	1.3	Clear	39		
4	IV	2/23	2125-27	309.9	130.9	0.13	0.9	Clear	40	0.24	121.4
	VIII	2/24	2031-33	146.1	111.9	0.35	0.4	1500 ft Ovcst	13		
1	II	3/8	0632-34	53.0	50.9	0.60	2.0	Clear	62	1.65	63.4
	V	2/20	2017-19	71.9	46.2	3.77	0.8	Hi Sctd	28		
	VI	2/12	2336-38	96.5	93.2	0.59	1.5	Clear	29		
2	VII	2/19	2031-33	462.3	264.3	0.01	0.05	1500 ft Brkn	11	0.01	264.3

In general, the spectra show large variations in relative power for frequencies between 2.5 and 20 cps. Except for periods VII and VIII, maxima appear to be at frequencies less than 2.5 cps. The maximum for period VII is at 5 cps and that for period VIII at 7.5 cps.

To make more direct comparisons, the spectra were normalized by a factor

$$\int_{2.5}^{200} W_p(f)\, df$$

for an arbitrary reference spectrum. The normalized spectra are displayed in Figure 13, grouped in four categories according to similarities in shapes. Shown also are the appropriate average Richardson numbers and wind components normal to the optical path. The similarities of the spectra within each group are clearly evident. It is significant to note, in this regard, that the spectra are essentially statistically independent samples insofar as they are widely separated in time.

Figure 14 shows the same normalized power spectra in terms of wave number, k, defined by

$$k = \frac{2 \pi f}{\overline{V}_n}$$

These spectra may be compared with those in Figure 13 to see the effect of the wind component normal to the optical path.

3.2.4 Scintillation and Path Length--Figure 15 shows data obtained over grass on two separate nights (curves 1 and 3) and one day (curve 2) with individual light sources at 400, 800 1200, 1600 and 2000 feet from the telephotometer. Richardson numbers (Ri), wind speed at 2 meters ($\overline{u}_{2m}$), wind direction relative to the optical path (α), average temperature difference between 2 and 1 meters ($\overline{T}_{2m} - \overline{T}_{1m}$), and the slope of each curve computed by a least squares method are also given. The results, as discussed in Section 4.1.8, show that scintillation increases systematically with increase in length of optical path according to the relationship $Pm \propto L^p$ in which $p \approx 0.9$ for $T_{2m} - T_{1m} \approx \pm 0.2°C$ and $p \approx 0.8$ for $T_{2m} - T_{1m} = +0.8°C$.

Table I

VISUAL RESOLUTION AND SCINTILLATION DATA

Nighttime over snow, KFS, 1960

Date	Time EST	Slot No.	Pm	Time EST	Slot No.	Pm
12 Feb.	1926	11	19	2344	12	21
	1942	11	20	2346	13	20
	1946	11	17	2348	12	23
	2002	11	24	2352	13	18
	2016	11	22	2358	13	18
	2032	12	19	0000	11	31
	2048	9	36	0006	11	22
	2102	10	24	0008	12	16
	2218	10	29	0016	11	20
	2226	10	26	0022	11	18
	2326	11	34	0024	10	23
	2336	11	29	0030	9	29
	2338	11	29	0036	11	29
	2340	10	29	0040	9	36
	2342	10	25			
13 Feb.	2030	8	39	2116	9	45
	2034	8	39	2120	8	45
	2040	7	39	2124	7	69
	2042	7	45	2126	7	59
	2046	7	52	2128	6	59
	2050	8	39	2130	6	62
	2052	9	38	2132	5	63
	2056	6	43	2136	7	59
	2058	6	49	2140	9	41
	2104	6	59	2142	8	43
	2112	6	72			
14 Feb.	2018	12	12	2114	11	21
	2028	12	23	2140	11	10
	2048	11	16	2304	11	21
19 Feb.	2214	11	12	2222	11	12
20 Feb.	2012	9	28	2040	7	27
	2018	8	28	2044	7	24
	2020	10	29	2050	7	30
	2026	9	23	2056	7	26
	2036	8	22	2206	8	48
	2038	8	23	2207	7	53

VISUAL RESOLUTION AND SCINTILLATION DATA (Continued)

Nighttime over snow, KFS, 1960, (Continued)

Date	Time EST	Slot No.	Pm	Time EST	Slot No.	Pm
20 Feb.	2208	6	55	2228	10	24
(Continued)	2210	7	52	2230	11	20
	2212	8	56	2232	10	21
	2214	8	54	2236	9	22
	2216	8	52	2238	11	20
	2222	8	32	2240	11	17
	2226	9	32			
23 Feb.	2114	9	36	2152	9	36
	2124	9	42	2238	10	30
	2130	9	39	2258	11	26
	2148	10	34			
24 Feb.	2016	11	25	2034	12	13
	2024	12	20	2038	12	13
	2026	13	15	2042	12	13
	2032	13	13			
29 Feb.	2122	8	28	2124	9	30
2 Mar.	1952	11	21	2002	12	20
	1954	11	22	2018	11	17
	2000	12	20	2026	12	16
7 Mar.	1832	11	34	1900	13	18
	1836	13	26	1904	13	26
	1840	13	15	1910	12	34
	1848	13	19	1912	13	30
	1854	13	16	1914	13	29
8 Mar.	0628	9	76	0718	9	47
	0632	9	63	0720	9	40
	0640	8	47	0732	9	55
	0710	8	45			

VISUAL RESOLUTION AND SCINTILLATION DATA (Continued)

Daytime over snow, KFS, 1960

Date	Time EST	Slot No.	Pm	Time EST	Slot No.	Pm
5 Feb.	1558	14	4	1602	13	4
	1600	13	4			
9 Feb.	1142	13	5	1144	13	5
12 Feb.	1500	13	10	1530	13	12

Nighttime over frozen ground, WRL, 1961

Date	Time EST	Slot No.	Pm	Time EST	Slot No.	Pm
25 Jan.	1956	12	13	2042	11	14
	2014	13	10	2052	12	5
	2016	12	12	2054	13	5
	2038	12	7	2108	12	20
	2040	11	17	2110	12	22
6 Feb.	1946	11	35			
14 Feb.	2020	12	24	2120	12	32
	2028	12	32	2126	12	31
	2114	13	23	2152	12	26
15 Mar.	2044	13	27	2146	13	28
	2108	13	23			

Daytime over frozen ground, WRL, 1961

Date	Time EST	Slot No.	Pm	Time EST	Slot No.	Pm
8 Feb.	1424	14	12	1532	14	20
	1436	14	18	1538	15	12

VISUAL RESOLUTION AND SCINTILLATION DATA (Continued)

Daytime over frozen ground, WRL, 1961 (Continued)

Date	Time EST	Slot No.	Pm	Time EST	Slot No.	Pm
16 Mar.	1440	7	90	1511	8	94
	1446	11	53	1536	7	83
	1448	7	83	1537	10	65
	1454	7	83	1538	11	47
	1506	8	94	1540	10	58
	1507	10	78	1541	9	82
	1508	8	95	1542	8	90
	1509	8	85	1543	7	88
	1510	10	83	1544	7	83

Nighttime over ice, Ford Lake, 1961

Date	Time EST	Slot No.	Pm	Time EST	Slot No.	Pm
20 Feb.	2050	14	7	2146	14	4

Daytime over ice, Ford Lake, 1961

Date	Time EST	Slot No.	Pm	Time EST	Slot No.	Pm
21 Feb.	1506	16	11			

Table II

LANDOLT BROKEN RING RESOLUTION CHART DATA

Slot No.	Diam. (in.)	Slot Size (in.)	Slot No.	Diam. (in.)	Slot Size (in.)
1	17.76	3.55	12	1.53	.30
2	14.21	2.84	13	1.22	.24
3	11.37	2.27	14	.98	.196
4	9.10	1.82	15	.78	.156
5	7.28	1.45	16	.625	.125
6	5.82	1.17	17	.50	.10
7	4.66	.93	18	.40	.080
8	3.73	.75	19	.32	.064
9	2.98	.59	20	.26	.051
10	2.38	.46	21	.20	.041
11	1.91	.38			

Table III

OBSERVATION PERIODS AND WEATHER SUMMARIES

Over snow, KFS, 1960

Date	Time (EST)	Cloudiness	Ave. Wind Vel.(mph)	Ave. Temp. °C	Ave. Dew Pt. °C	Ave. Sta. Press. (mb)
Feb.						
3	2125-2324	Clear	SSW 11	-6	-8	985
4	1545-1815	Hi sctd	E 8	-4	-7	983
	2130-2230	500 ft ovcst	E 11	-3	-4	982
5	1520-1650	10,000 ft ovcst	NW 6	-1	-2	970
9	1115-1200	2000 ft ovcst/lt snw	N 9	-12	-14	962
	2130-2220	1600 ft ovcst/lt snw	ENE 10	-12	-13	967
12	1900-13/0100	Hi sctd	NW 6	-12	-14	989
13	1917-2210	Clear	Lt/vrbl	-15	-17	983
14	1930-2307	Hi sctd becoming 2800 ft ovcst	ESE 5	-8	-12	976
18	1405-1611	1200 ft ovcst/lt snw	NW 12	-8	-9	972
19	2141-2248	2000 ft ovcst/lt snw	NW 13	-9	-12	983
20	2000-2250	Clear	NNE 4	-15	-17	985
23	2100-2300	Clear	N 8	-10	-13	985
24	2000-2130	1500 ft brkn vrbl ovcst	NW 1	-10	-12	984
27	1820-2100	1500 ft brkn becoming clear	NW 1	-13	-15	982
29	2020-2140	Clear becoming 1200 ft ovcst	WNW 4	-14	-16	986
Mar.						
1	1925-2210	1500 ft brkn becoming clear	Lt/vrbl	-15	-16	992
2	1840-2030	1500 ft brkn vrbl ovcst	Lt/vrbl	-10	-14	990
7	1820-1920	Hi thin ovcst	NNW 1	-10	-16	990

OBSERVATION PERIODS AND WEATHER SUMMARIES (Continued)

Over snow, KFS, 1960 (Continued)

Date	Time (EST)	Cloudiness	Ave. Wind Vel.(mph)	Ave. Temp. °C	Ave. Dew Pt. °C	Ave. Sta. Press. (mb)
Mar.						
8	0545-0745	Clear	NW 1	-18	-20	990
14	0945-1030	2000 ft brkn	Lt/vrbl	-5	-8	988

Over frozen ground, WRL, 1961

Date	Time (EST)	Cloudiness	Ave. Wind Vel.(mph)	Ave. Temp. °C	Ave. Dew Pt. °C	Ave. Sta. Press. (mb)
Jan.						
25	1954-2117	Hi sctd	Lt/vrbl	-11	-17	1005
Feb.						
6	1944-2214	Clear	N 8	-1	-10	1000
8	1404-1540	Clear	NW 10	+7	-7	987
14	1956-2152	Hi thin brkn	WNW 6	+1	-4	996
Mar.						
15	1932-2144	6000 ft sctd becoming 5500 ft brkn	WNW 12	+1	-8	979
16	1434-1608	4000 ft sctd becoming 5000 ft brkn	NW 18	-1	-12	986
30	1344-1600	Clear	W 7	+8	-10	988
	1658-2226		S 8	+6	-8	988

Over ice, Ford Lake, 1961

Date	Time (EST)	Cloudiness	Ave. Wind Vel.(mph)	Ave. Temp. °C	Ave. Dew Pt. °C	Ave. Sta. Press. (mb)
Feb.						
20	1958-2156	Hi thin brkn	Lt/vrbl	-2	-6	1001
21	1502-1528	Hi thin brkn	SSE 6	+9	-7	993

Table IV

PERIODS OF MAGNETIC TAPE RECORDINGS

Over snow, KFS, 1960

Date	Time (EST)	Date	Time (EST)
12 Feb.	1915-1920	20 Feb.	1845-1850
	1930-1935		1910-1915
	1945-1950		2013-2026
	2000-2005		2156-2246
	2015-2020		
	2026-2027:35	23 Feb.	2108-2156
	2030-2035:30		2237-2245
	2037-2039:15		2252-2302
	2045-2052		
	2103-2105	24 Feb.	2015-2020
	2230-2235		2029-2043
	2245-2254:15		
	2300-2308:15	27 Feb.	1840-1845
	2315-2323		1855-1900
	2330-2338		1920-1925
	2345-2348		1950-1955
			2000-2005
13 Feb.	0001-0005		2015-2025
	0015-0023		2045-2053
	0030-0036		
	0045-0050	29 Feb.	2040-2110
	2030-2035		2120-2134:30
	2039-2056		
	2101-2149	1 Mar.	1950-2015
			2025-2030
14 Feb.	2010-2020		2040-2045
	2047-2048:45		2050-2100
	2111-2116		2115-2120
	2137-2143		2125-2135
	2238-2243		2145-2150
	2303-2307		2200-2210
18 Feb.	1436-1440	2 Mar.	1950-2005
	1441-1444		2015-2030
19 Feb.	2139-2149	8 Mar.	0625-0635
	2213-2225		0715-0722
			0731-0736
		14 Mar.	0955-1000
			1007-1011

PERIODS OF MAGNETIC TAPE RECORDINGS (Continued)

Over frozen ground, WRL, 1961

Date	Time (EST)	Date	Time (EST)
25 Jan.	2000-2010	14 Feb.	2002-2009
	2031-2046		2058-2105
	2108-2115		2138-2144
6 Feb.	1955-2000	30 Mar.	1357-1405
			1445-1450
8 Feb.	1429-1433		
	1531-1536		

Over ice, Ford Lake, 1961

Date	Time (EST)	Date	Time (EST)
20 Feb.	2015-2025		
	2049-2100		

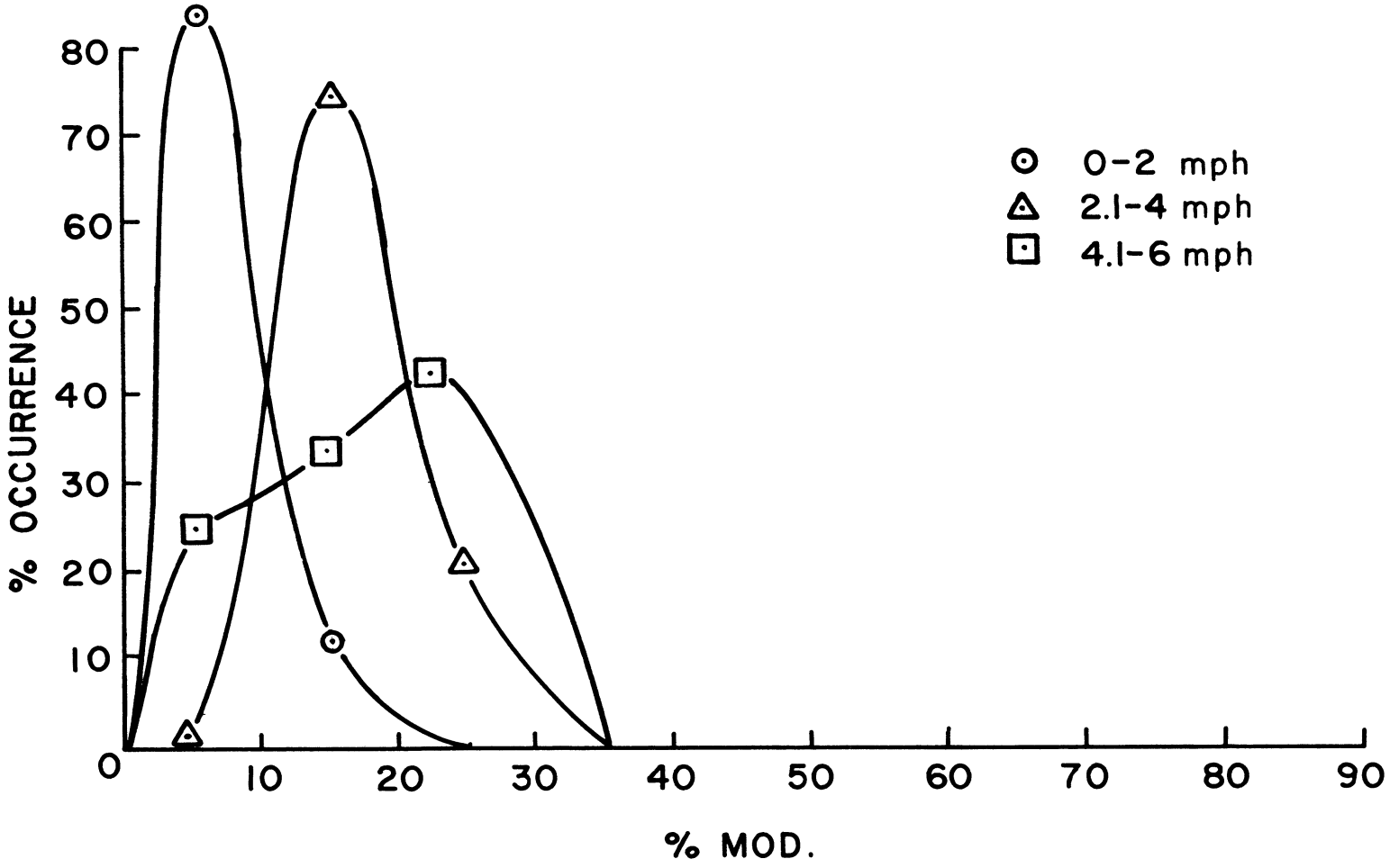

Figure 2. Percentage Frequency of Per Cent Modulation for Three Categories of Wind Speed During Overcast Skies at Night Over Snow.

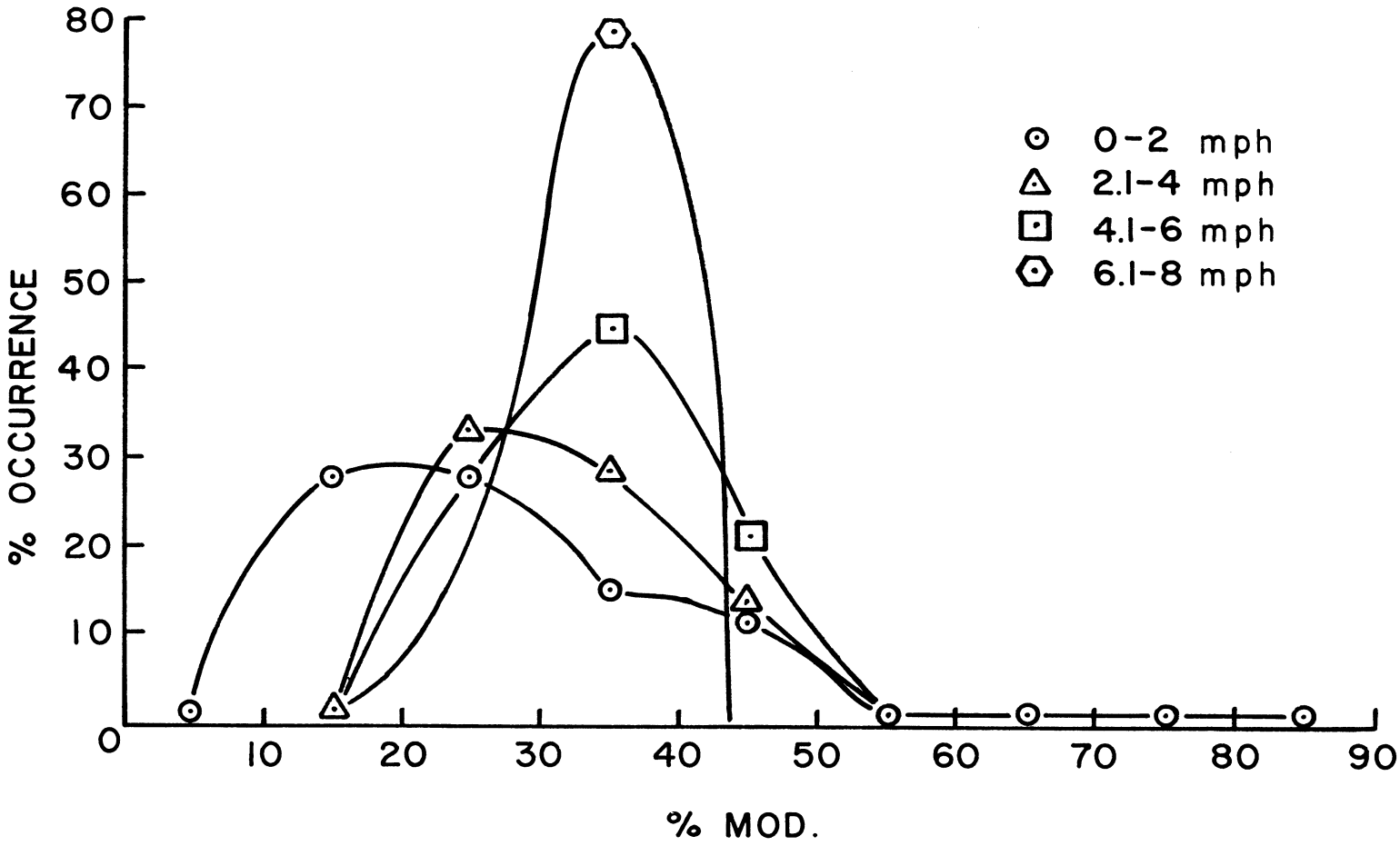

Figure 3. Percentage Frequency of Per Cent Modulation for Four Categories of Wind Speed During a Clear or Scattered (less than 0.6 cloudiness) Sky Condition at Night Over Snow.

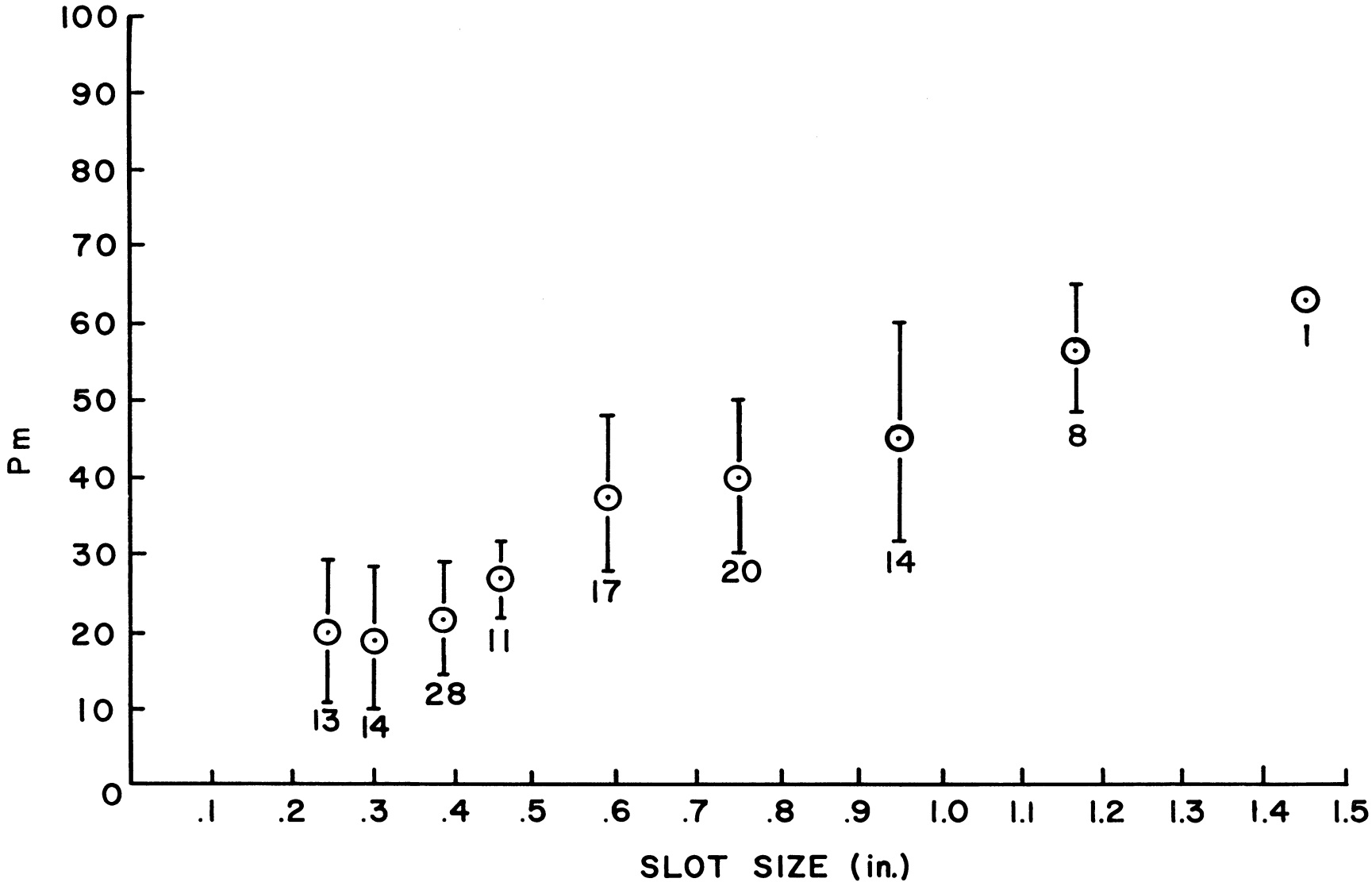

Figure 4. Per Cent Modulation vs Smallest Slot Size Discernible at Night Over Snow. The number of observations averaged for each point is shown and the standard deviation for each point is indicated by a vertical line segment.

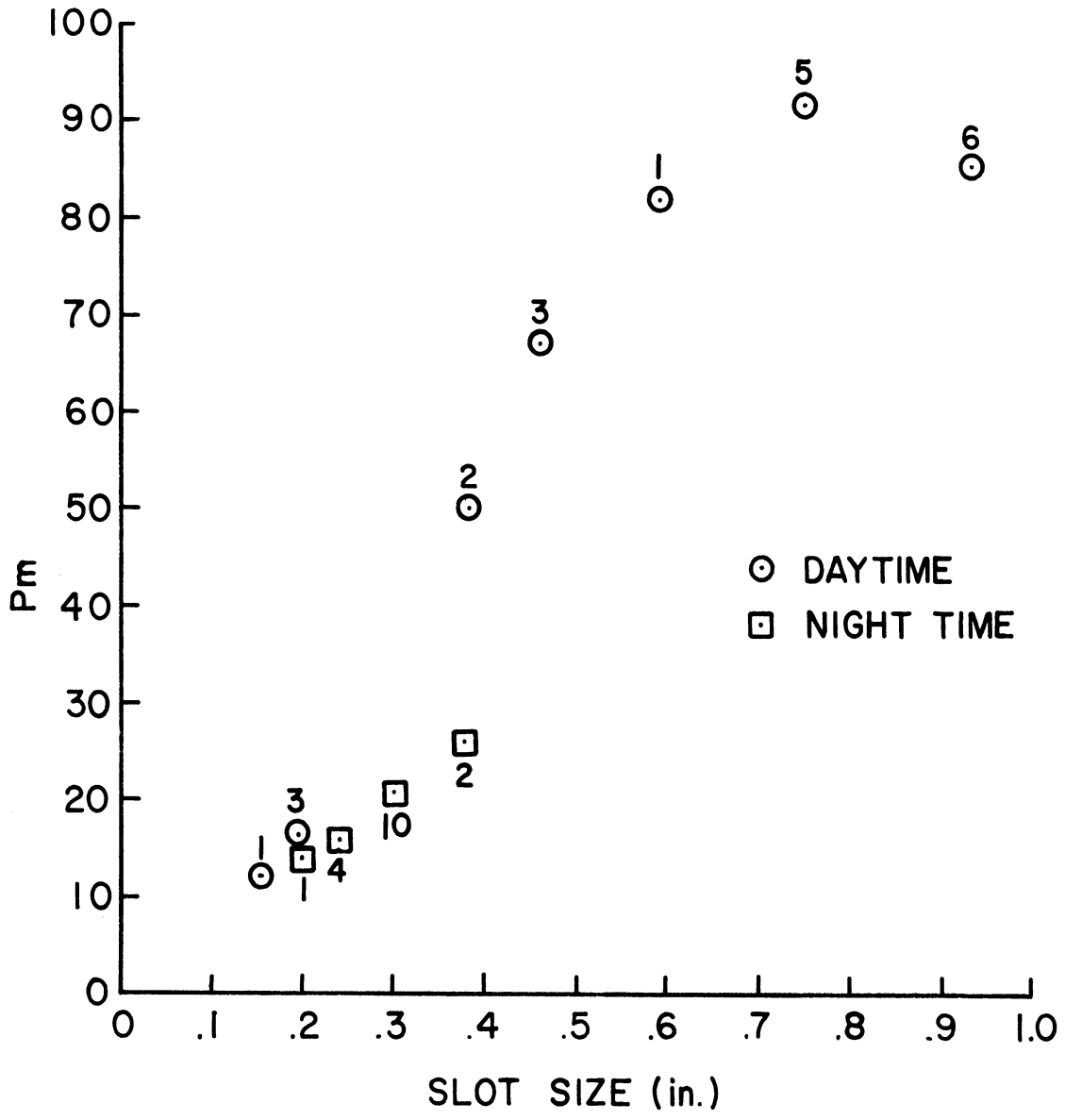

Figure 5. Per Cent Modulation vs Smallest Slot Size Discernible at Night and During Daytime over Frozen Ground. The number of observations averaged for each point is indicated.

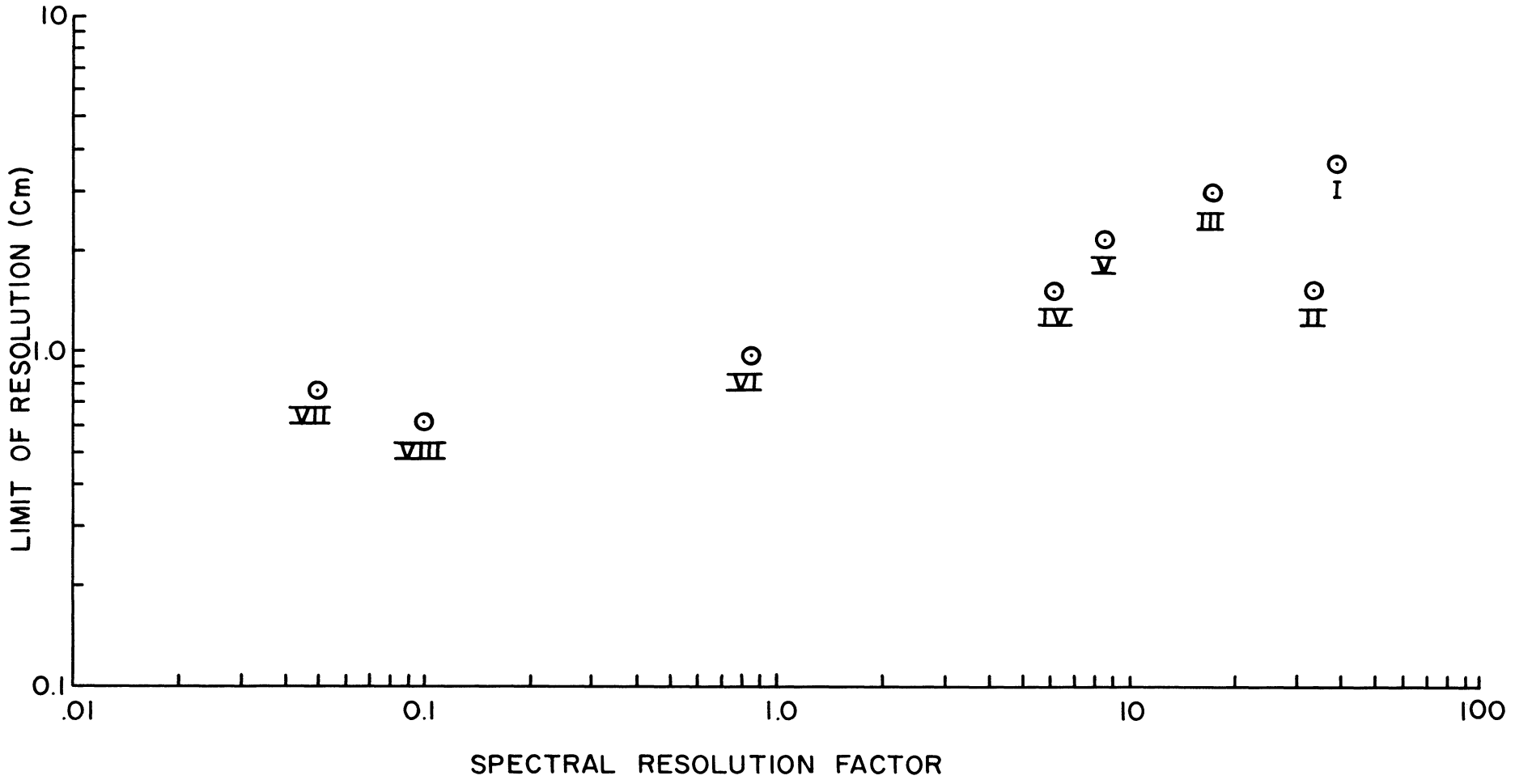

Figure 6. Spectral Resolution Factor vs Smallest Slot Size Discernible at Night over Snow for the Eight 2-minute Periods Identified in Table VI.

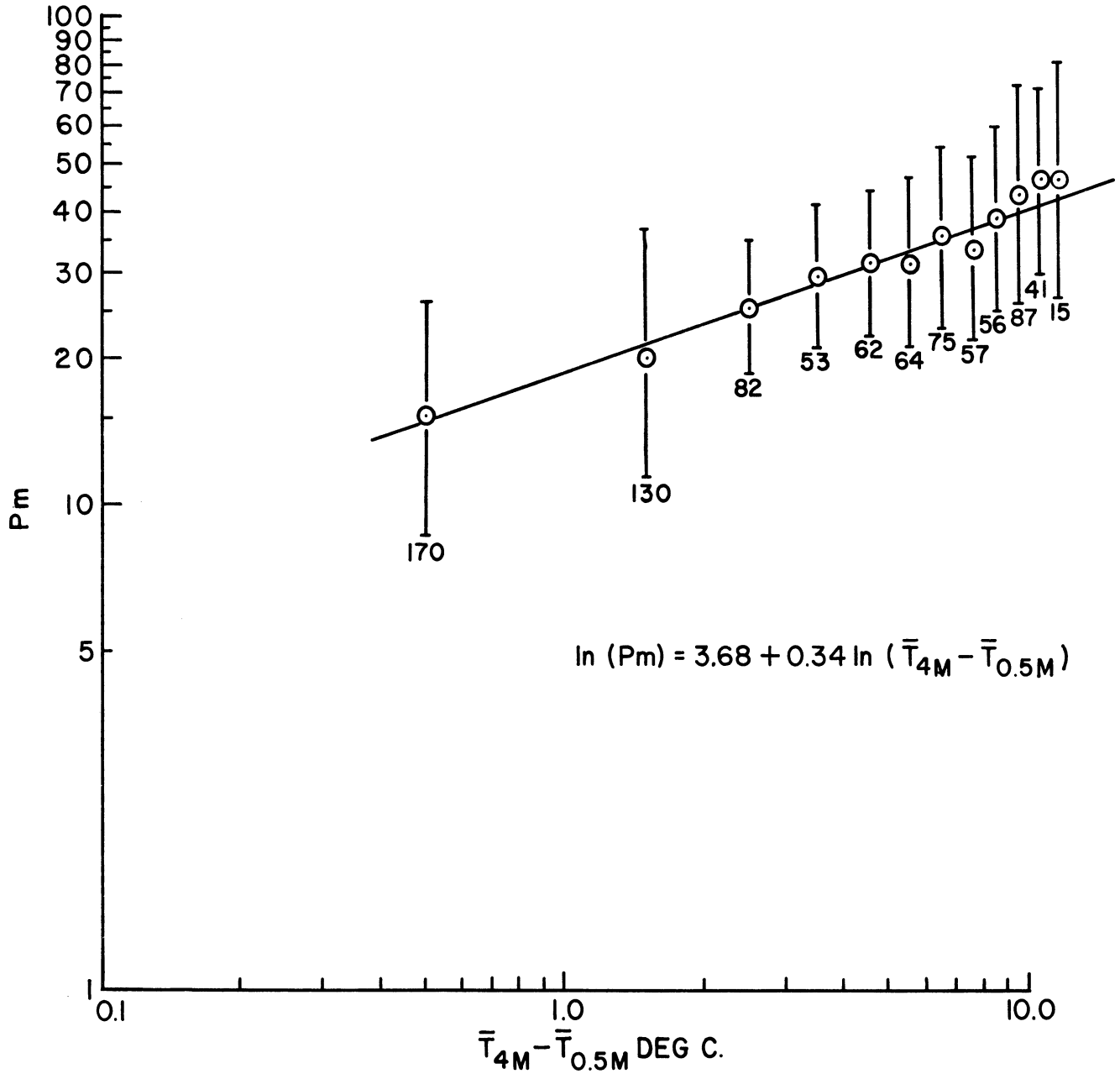

Figure 7. Per Cent Modulation vs Inversion Magnitude Between 4 and 0.5 Meters Over Snow in Logarithmic Coordinates. Each point is the average of all per cent modulation observations for each one degree temperature difference. The number of observations of per cent modulation averaged for each point is shown and the standard logarithmic deviation for each point is indicated by a vertical line segment.

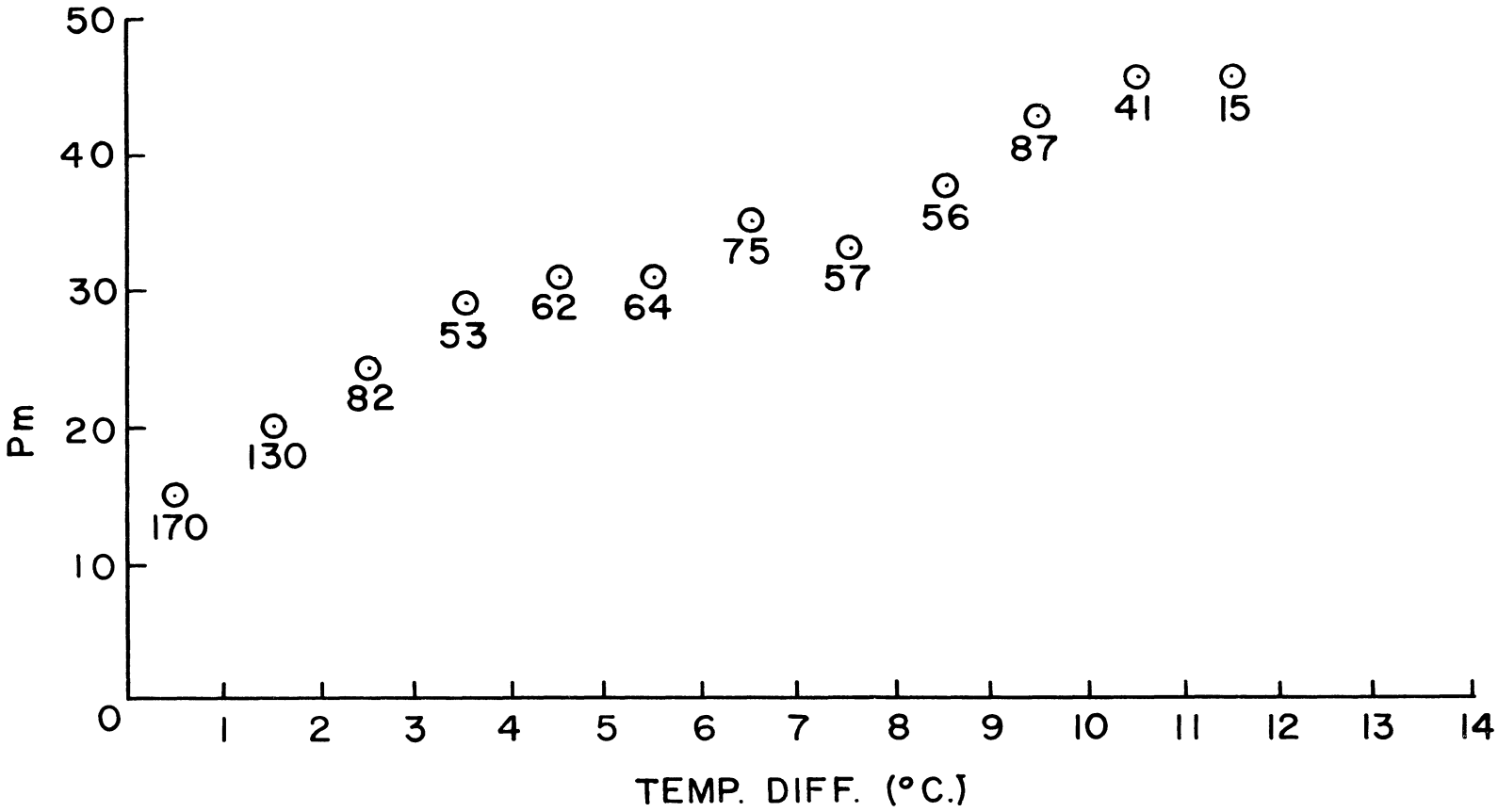

Figure 8. Per Cent Modulation vs Inversion Magnitude Between 4 and 0.5 Meters Over Snow in Linear Coordinates for the Same Data Shown in Figure 7.

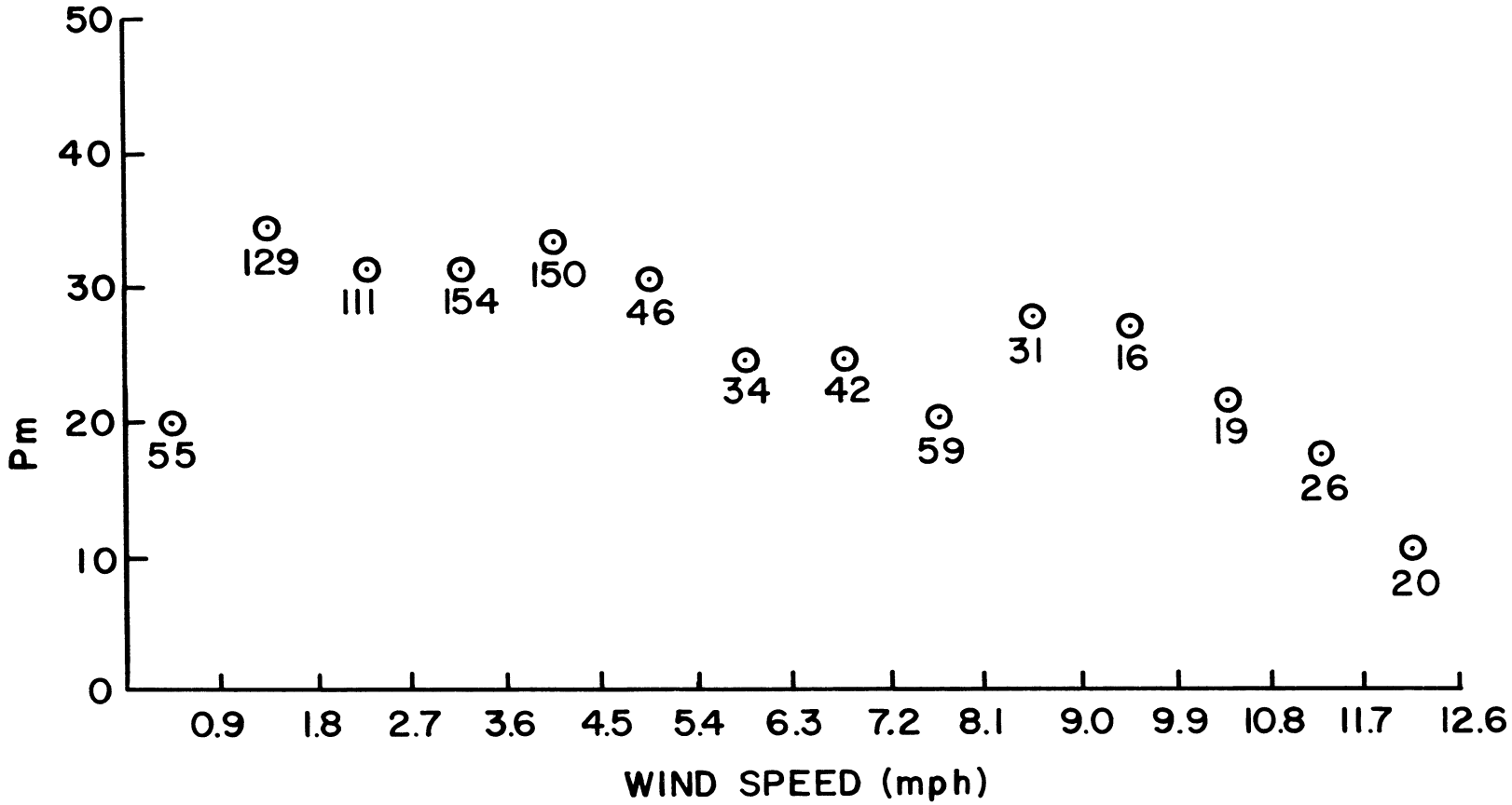

Figure 9. Per Cent Modulation vs Wind Speed at 2 Meters over Snow at Night. Each point is the average of all per cent modulation observations for each 0.9 mph wind speed interval. The number of observations of per cent modulation averaged for each point is indicated.

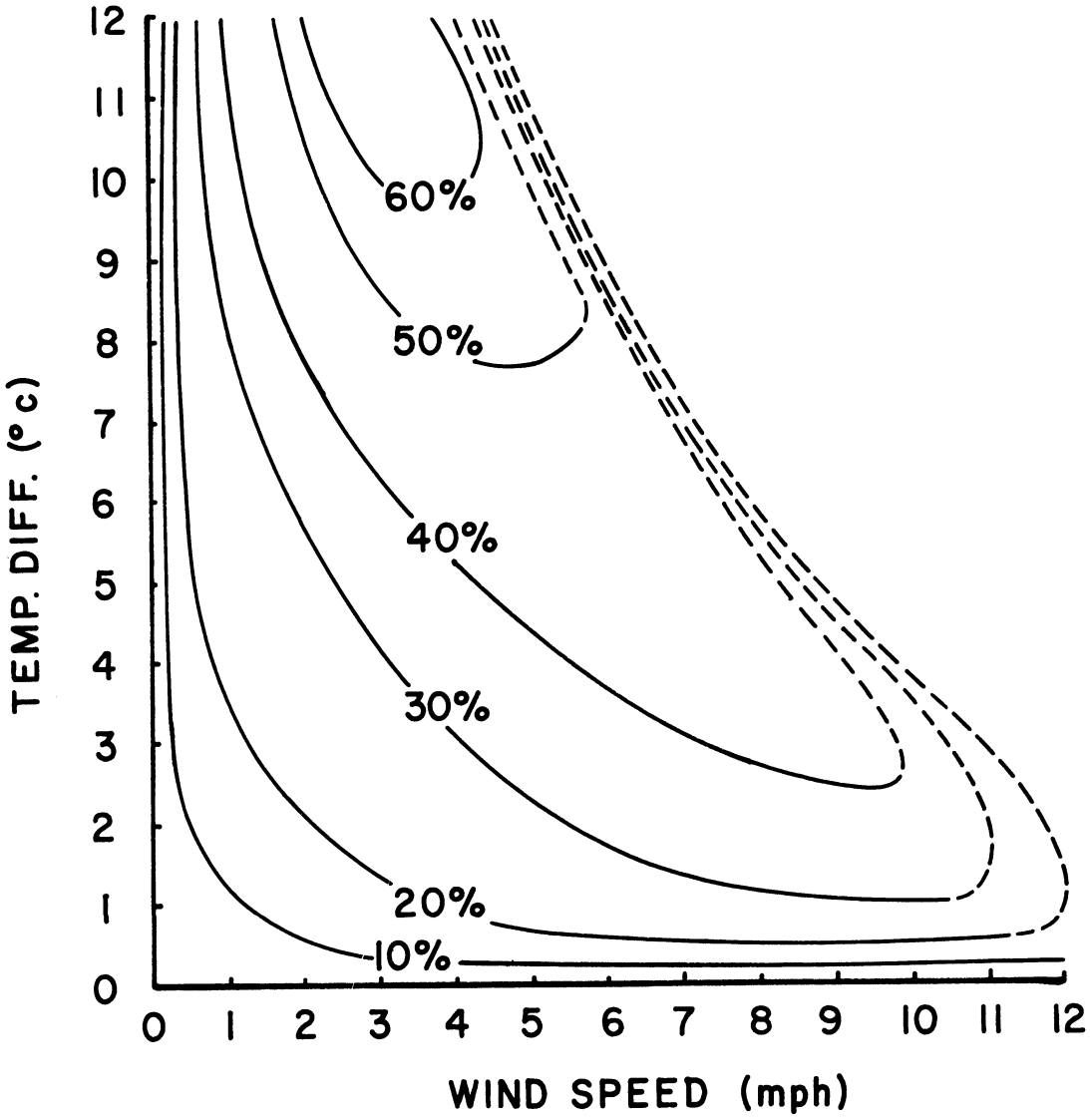

Figure 10. Relationship of Per Cent Modulation to Inversion Magnitude Between 4 and 0.5 Meters and Wind Speed at 2 Meters over Snow for all Nighttime Observations.

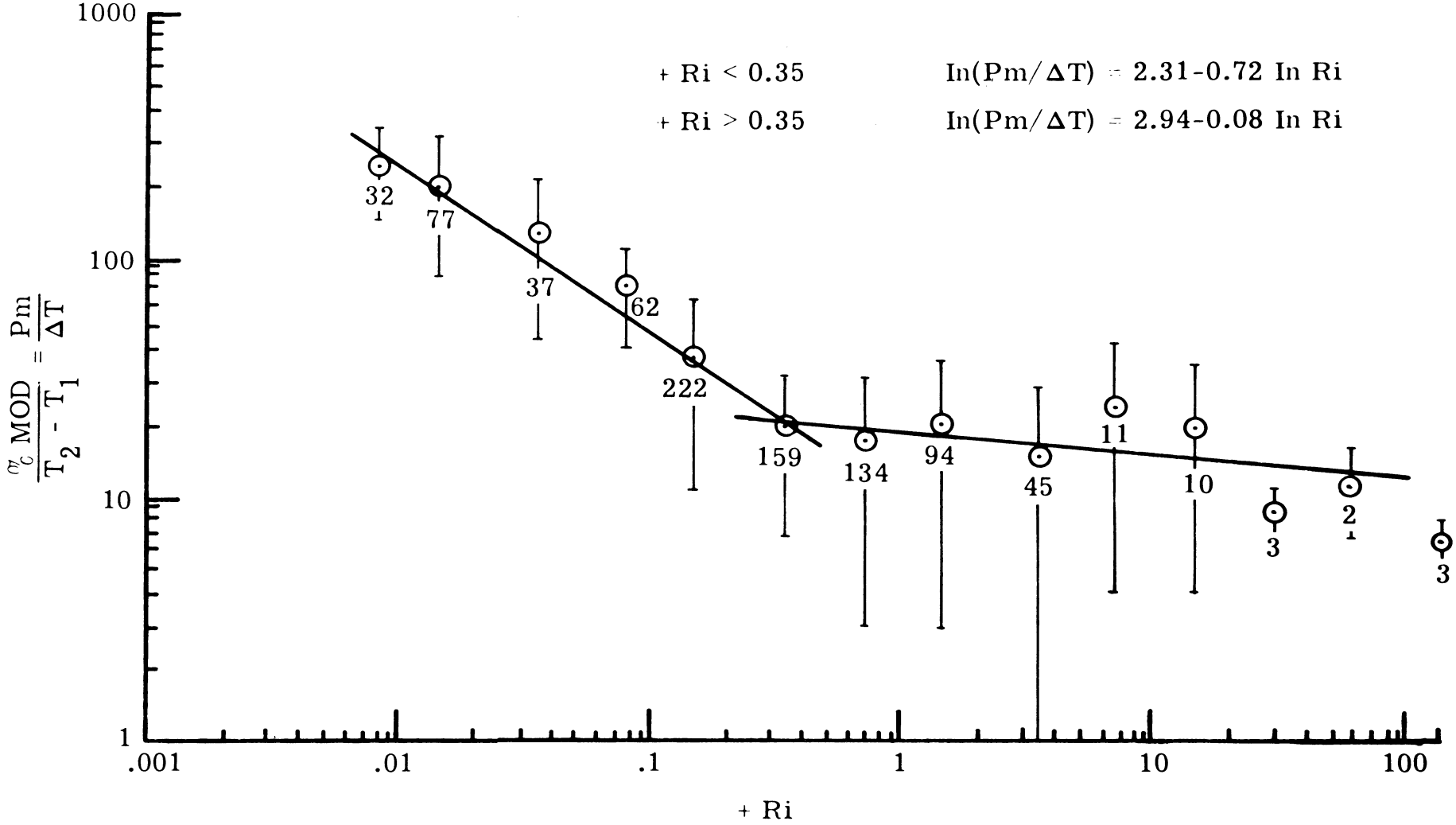

Figure 11. Per Cent Modulation per Unit Temperature Difference Between 1 and 2 Meters vs Richardson Number over Snow for all Daytime and Nighttime Observations. The number of observations of Pm/ΔT averaged for each point is shown and the standard linear deviation is indicated by a vertical line segment.

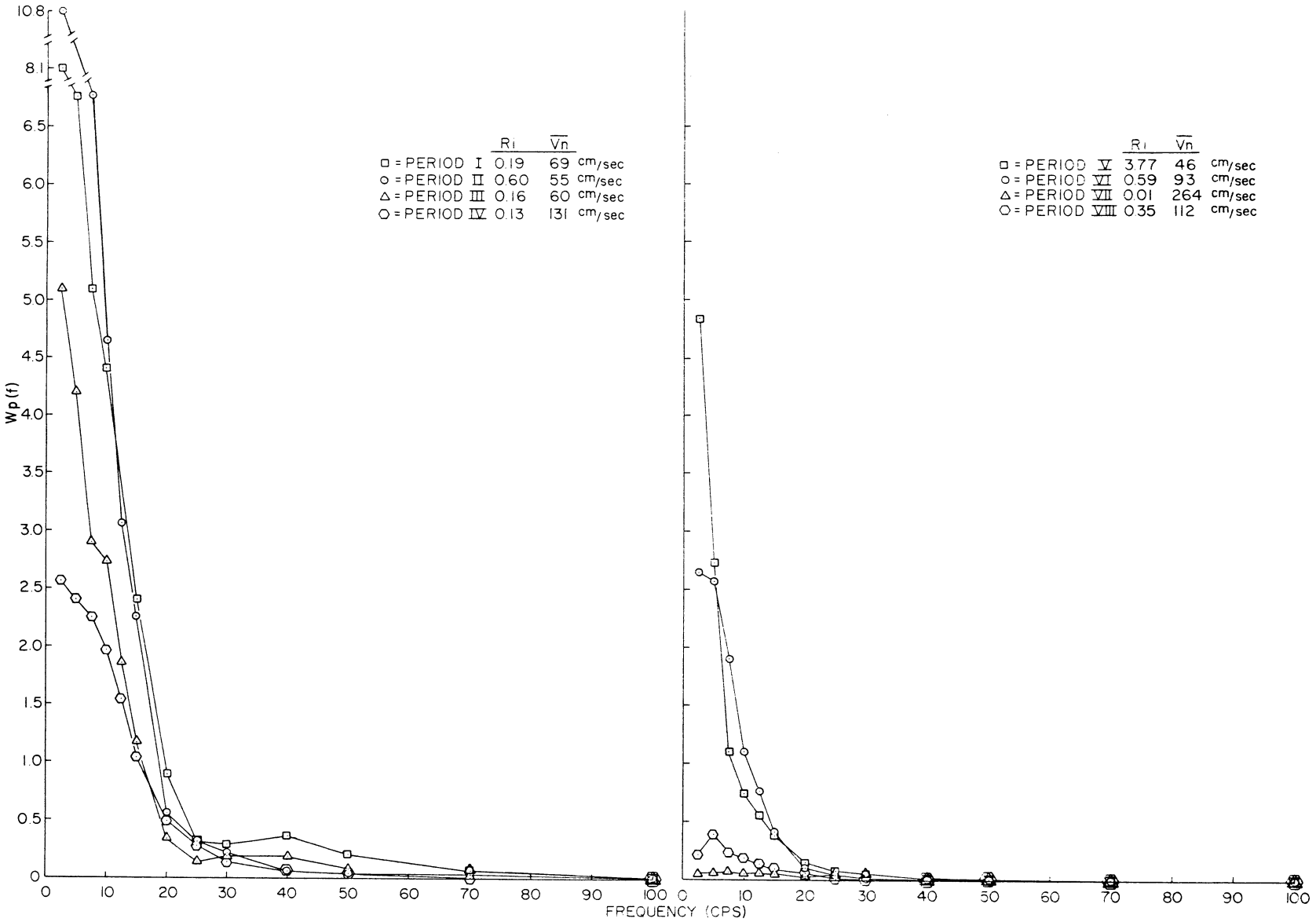

Figure 12. Power Spectra of Scintillation for Stable Conditions over Snow for Eight Periods Identified in Table VI.

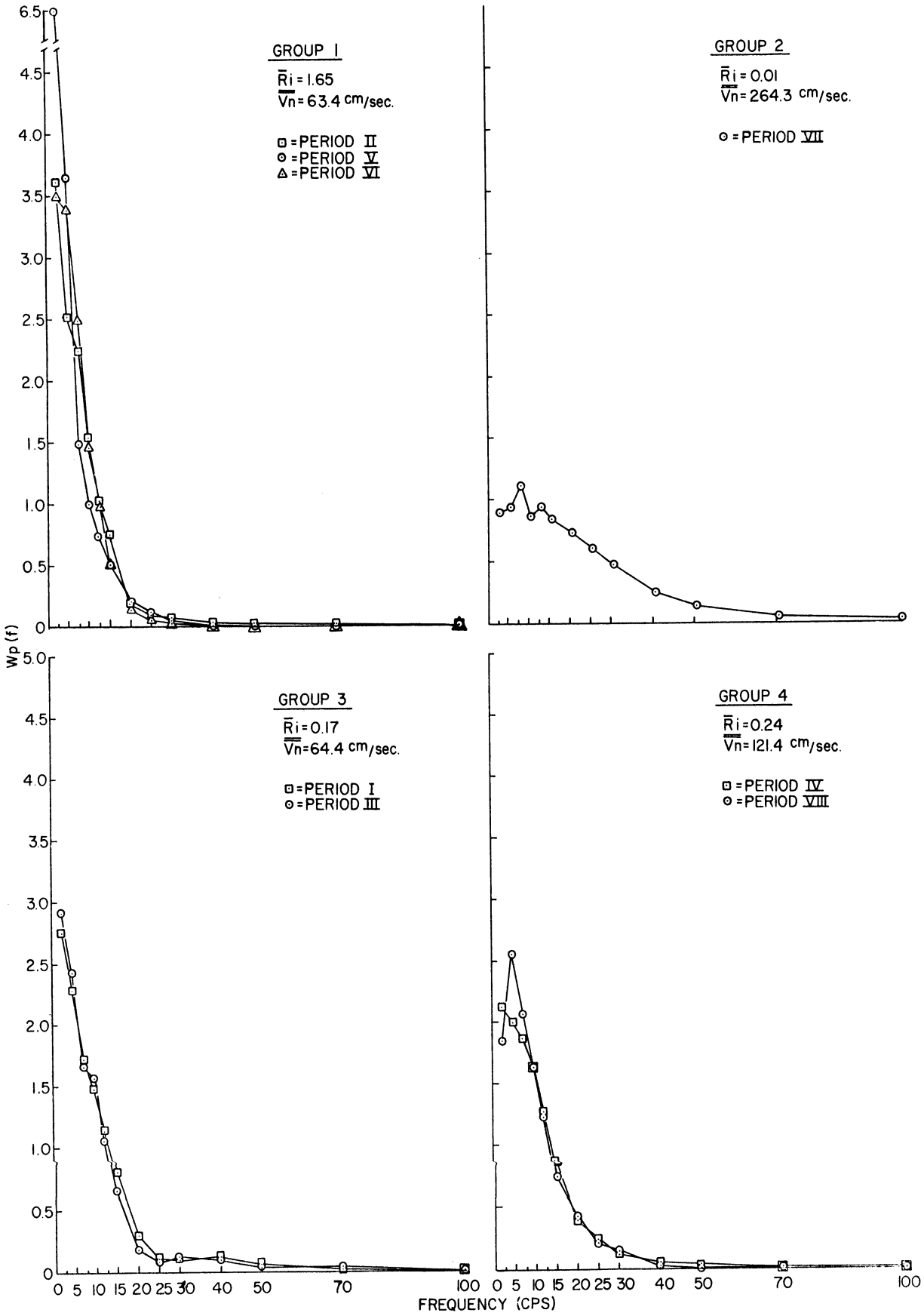

Figure 13. Normalized Power Spectra of Scintillation for Stable Conditions over Snow for Eight Periods Identified in Table VI.

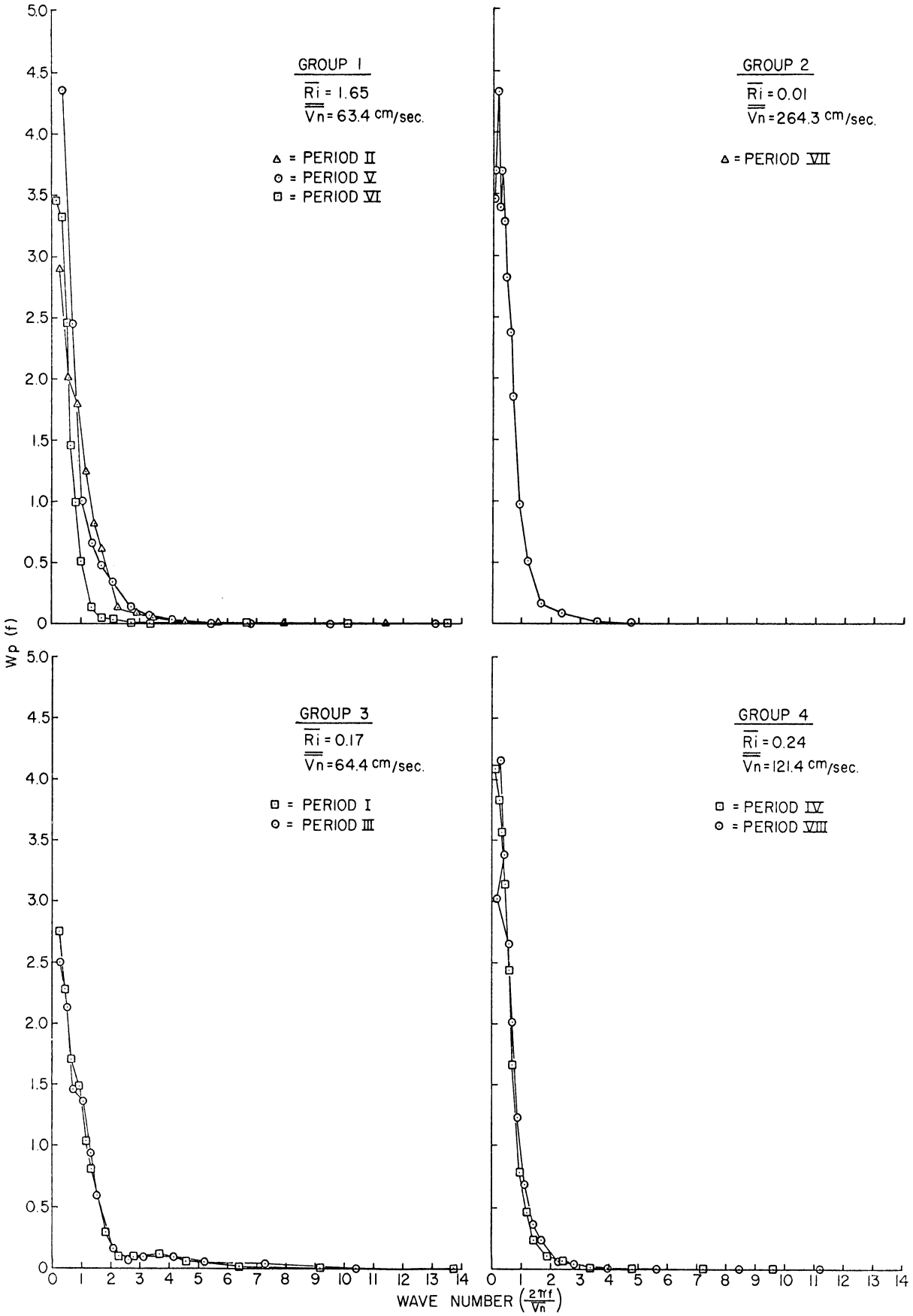

Figure 14. Normalized Power Spectra (Wave Number) of Scintillation for Stable Conditions over Snow for Eight Periods Identified in Table VI.

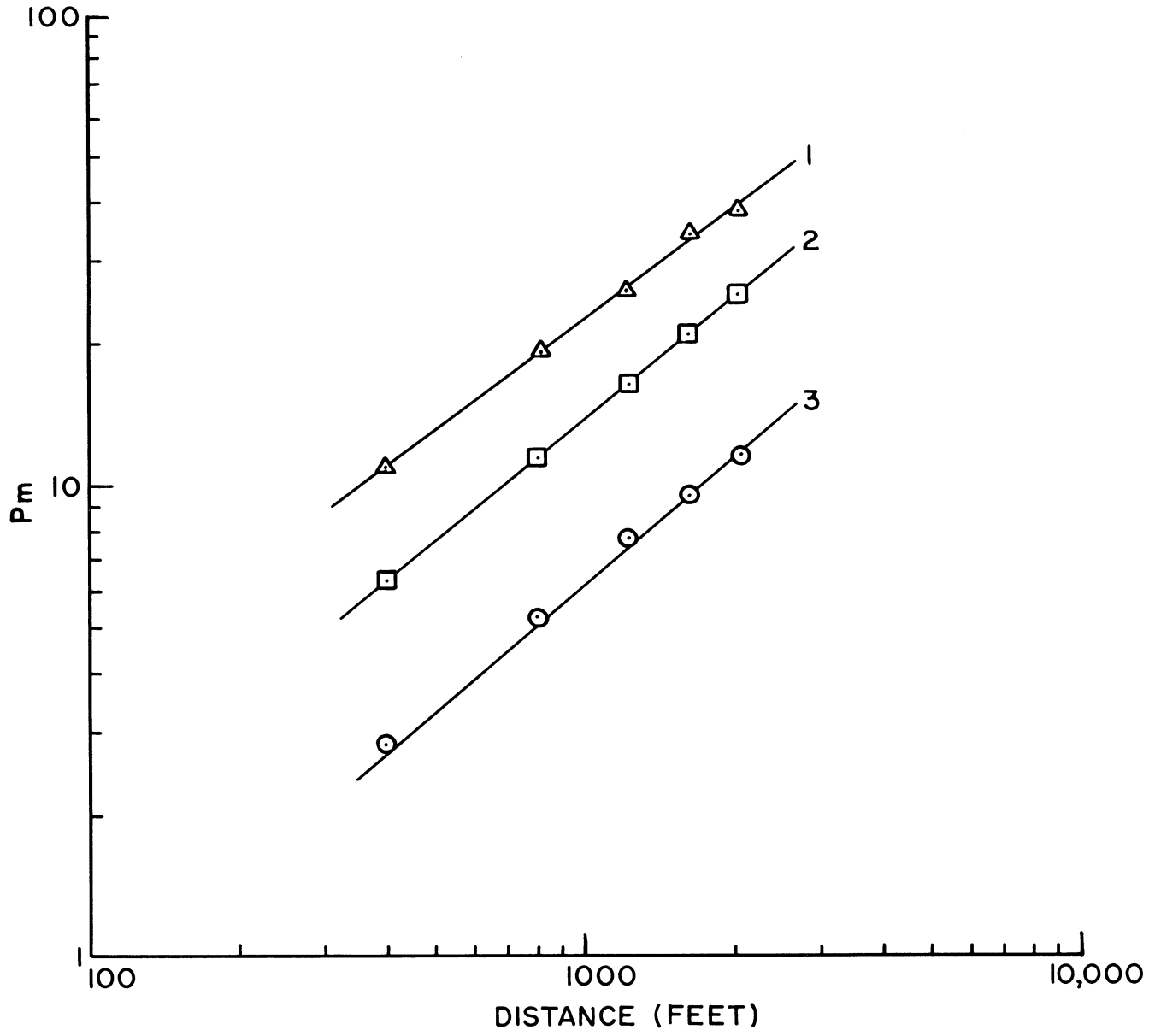

Figure 15. Per Cent Modulation vs Path Length

4. DISCUSSION

4.1 Scintillation and Micrometeorological Parameters

4.1.1 Index of Refraction Fluctuations--The dependence of visual resolution and scintillation on turbulence and thermal stratification arises basically from the fact that the speed of light varies with the density of the medium in which it propagates. Variations in density associated with turbulent mixing of thermally stratified layers create distortions in wave propagation which may be described as perturbations in both amplitude and phase. The effects of the perturbations appear as fluctuations in brightness of light from small objects and variations in shape and size for larger objects.

The relationship of the speed of light to the density of the medium through which it propagates is expressed by means of the index of refraction, n, which is the ratio of speed, c, in a vacuum to the speed, v, in the medium. Thus

$$n = c/v \tag{1}$$

and for air at pressures on the order of one atmosphere

$$n = 1 + A\rho \tag{2}$$

in which A is a constant and ρ is the density. To show the separate effects of temperature, pressure and water vapor the equation of state is introduced (Fleagle, 1950)

$$n = 1 + \frac{(p-e)\, A_1 + e\, \epsilon\, A_2}{RT} \tag{3}$$

in which p = atmospheric pressure (mb)
e = water vapor pressure (mb)
ϵ = ratio of molecular weights of water vapor and dry air = 0.622
R = gas constant for dry air = $2.876 \times 10^6 \text{cm}^2\ \text{sec}^{-2}\ \text{deg}^{-1}$
A_1 = 2.28
A_2 = 3.25

The relative significance of temperature and water vapor in index of refraction fluctuations may be determined by differentiating (partially) Equation (3):

$$\partial n / \partial T = \frac{-(p-e)\, A_1 - e\, \epsilon\, A_2}{RT^2}$$

and $$\partial n/\partial e = \frac{\leq A_2 - A_1}{RT}$$

Then $$\frac{\partial n/\partial e}{\partial n/\partial T} = \frac{-0.13T}{-1.14p + 0.13e} \qquad (4)$$

If extreme values of T, p and e are selected from the Appendix so as to maximize the ratio given by Equation (4), it is seen that the ratio for any of the experiments could not be as large as 0.04. Thus, a variation of humidity as large as 25mb would never be as significant as a temperature variation of 1°C. It is clear that the effects of humidity variations are entirely negligible when dealing with optical wave lengths.

Equation (3) may be reduced, therefore, to

$$n = 1 + \frac{A_1}{R}\frac{p}{T} \qquad (5)$$

Partial differentiation again, yields

$$\partial n/\partial T = -\frac{A_1}{R}\frac{p}{T^2} \qquad (6)$$

and $$\partial n/\partial p = \frac{A_1}{RT} \qquad (7)$$

Then $$\frac{\partial n/\partial p}{\partial n/\partial T} = -\frac{T}{p} \qquad (8)$$

For the data in the Appendix the maximum possible value of $\frac{T}{p}$ would be less than 1/3, showing that a pressure variation would have to be greater than 3mb to be equivalent to a 1°C temperature variation to cause equivalent changes in index of refraction. G. I. Taylor (1936) showed that the mean pressure variation $\sqrt{\overline{p^2}}$, in turbulent flow is of the same order as $1/2\ \rho\ (\overline{u^2} + \overline{v^2} + \overline{w^2})$. If $(\overline{u^2} + \overline{v^2} + \overline{w^2})$ is as large as 3.2×10^4 cm^2/sec^2*, then the pressure variation would amount to about 0.02mb. This would be equivalent to a temperature change of less than 0.007°C in its influence on the index of refraction. Clark (1953) has reported short period pressure fluctuation measurements obtained over a six-week period in winter.

*Take $\overline{u}$ = 6 mps and $\overline{u^2} \sim \overline{v^2} \sim 0.2\overline{u}$ and $\overline{w^2} \sim 1/2\ \overline{u^2}$ (cf. Sutton (1953) p. 250-254.)

Although he does not give complete information with which to apply his published calibration curve, the strongest fluctuation reported could not have been as large as 0.025 mb. An interesting feature of his results is that pressure fluctuations are considerably weaker with a surface layer inversion than without.

The significance of these values may be assessed in terms of temperature variations found in typical conditions in the atmospheric surface layer. Perepelkina (1957) found, for example, that for stable stratification the standard deviation of temperature measurements at a height of 1.7 meters could be expressed, for limited data, as:

$$\sigma_T = - 0.08 (T_1 - T_4)$$

in which T_1 and T_4 represent mean values of temperature at 1 meter and 4 meters respectively. Analysis of similar data published by Lettau and Davidson (1957) for the Great Plains Turbulence Field Program gives, on the other hand, a factor of at least twice that obtained by Perepelkina. In the Appendix it is seen that the range of $(T_1 - T_4)$ varies from zero to about -10°C so that temperature fluctuations for these data may be expected to vary from zero to as high as 1 or 1.5°C.

The foregoing discussion shows that, except for adiabatic and nearly adiabatic conditions, temperature fluctuations in turbulent flow are responsible for scintillation and the related deterioration in visual resolution. Equation (6) may be used, consequently, for relating temperature differences to index of refraction differences. For a given temperature differential, the index of refraction differential varies inversely as the square of the absolute temperature and directly as pressure. Thus, it can be expected that for given temperature fluctuations scintillation effects will be most severe in clear weather at sea level (high pressure) in high latitude (low temperature).

4.1.2 Scintillation and the Temperature Profile--The data analysis was directed toward relating scintillation and visual resolution to temperature and wind structure with the general assumption that fluctuations in pressure and water vapor content were negligible in comparison to those of temperature on their influence on index of refraction fluctuations. This led to the plan of relating statistics of scintillation to parameters related to thermal stratification and turbulence in the surface layer of the atmosphere. For a horizontal and statistically homogeneous surface, temperature fluctuations at a point may be thought of as the result of vertical motions which move parcels of air from their average mean position in a layer characterized by an average temperature height distribution. The model assumes that small motions are adiabatic. It is clear that for a given vertical displacement, the temperature deviation from the mean will be greater for greater average vertical temperature gradients. Perepelkina's findings quoted above support this idea as do the findings of other investigators. It follows, therefore, that in turbulent flow scintillation should

depend directly on the mean vertical temperature gradient. Perhaps the most striking evidence of this fact is the common observation that shimmer is absent, or at least at a minimum, when the temperature gradient vanishes near sunset, sunrise and during very windy and cloudy conditions.

Figure 7 shows the relationship of scintillation to inversion magnitude over snow. Each point is the mean of many two-minute averages of Pm within successive one-degree temperature difference increments. The temperature differences were obtained from the 4 and 0.5 meter heights. The number of samples in each point is indicated. Standard logarithmic deviations are shown by the vertical line segments for each point. The data were subjected to a weighted linear regression analysis which resulted in the line shown in the figure. Because the data are not categorized according to turbulence characteristics, pressure, or absolute temperature, each point represents an average for a large range of these conditions.

The systematic increase of scintillation with inversion magnitude is clearly evident. A flattening of the curve is indicated at the greatest temperature difference values, an expected condition for the onset of laminar motion. The slope of the line is 0.34, which compares to a slope of 0.35 given by Tatarski, et.al., (1958) for similar work conducted at night over grass in the steppe region of Russia. However, Tatarski, et.al., used the temperature difference between 8 and 2 meters in their relationship and their optical path was about 1 meter above the earth's surface. The results of both investigations confirm the significance of the vertical temperature gradient in controlling the intensity of scintillation. When combined with the results relating Pm to visual resolution (Figure 4), the figure gives basic information for estimating visual resolution from information on the most critical parameter relating visual resolution to weather conditions.

4.1.3 Scintillation and Average Wind Speed--The influence of wind speed on scintillation takes place directly through the effects of wind shear in creating vertical motions. For a given roughness and average temperature gradient, the wind shear at a given height is directly determined by wind speed. Thus, it may be expected that an increase in wind speed, other things being constant, would increase the intensity of vertical motions and hence scintillation. The same wind shear effects, on the other hand, tend to decrease the temperature gradient through a mixing action. The influence of wind speed on scintillation should depend strongly on the temperature gradient as well as on the roughness and, perhaps, on other dynamic influences such as its variability determined by external conditions.

In a general way, the data plotted in Figure 9 show that scintillation (Pm) at first gradually and then rapidly decreases with increase in wind speed, except for a region between zero and 2 mph where it increases with wind speed. It appears, therefore, that these data reflect the decrease in temperature gradient with increasing wind speed instead of an expected increase in Pm with increase in vertical motions. The exception is the zero to 2 mph region where,

because all data here represent stable stratification conditions, it can be expected that slight increases in wind disturb otherwise laminar or near-laminar flow in which scintillation would be at a minimum. Further discussion of this matter is given in Section 4.1.6.

There appears to be no obvious reason for the discontinuities in the curve between 6 and 9 mph. It is likely that these data represent different conditions than does the remainder of the data. In spite of the irregularities the results indicate that in stable stratification over snow, except for very low wind speed, scintillation decreases with increasing wind speed.

4.1.4 The Combined Effects of Wind Speed and Temperature Gradient--Figure 10 suggests that for a given temperature difference, Pm increases with increasing wind speed up to a maximum value--dependent on the temperature difference--and then decreases. The point of inflection on the wind speed scale is inversely related to the temperature difference. This may be explained by the fact that, while the wind speed and Pm are measured at about 2 and 1.5m, respectively, the temperature differences used here were those between 4 and 0.5 meters. Thus the actual gradient at the effective level of scintillation measurement may change with respect to $T_4 - T_{0.5}$ depending on the variation of wind speed with height. A more detailed analysis of wind and temperature data would presumably show a continued increase of Pm with wind speed for a given temperature gradient at the height of Pm measurement.

A similar effect is noted for increasing the inversion magnitude for a given wind speed in the region of 4 mph at very large inversions. This characteristic, shown specifically in the Pm = 60 line, is apparently related to the flattening observed at large inversion values in Figure 7, indicative of flow transitional between laminar and turbulent.

4.1.5 Scintillation and Surface Roughness--Insofar as surface roughness elements are responsible for vertical motion in an otherwise uniform field of horizontal motion, it may be expected that the aerodynamic roughness of a snow surface would exert some influence on scintillation and visual resolution independent of temperature gradient and wind shear effects. It is known, however, that the influence of roughness does not extend far in the vertical and that this extent is dependent upon the size and distribution of roughness elements, wind speed and thermal stratification. For relatively smooth surfaces and for stable thermal stratification the roughness effects are the smallest and extend the least distance in the vertical.

Aerodynamic roughness, z_o, were computed for five separate adiabatic periods for the KFS snow surface using Prandtl's logarithmic wind height relationship in which $\bar{u} \propto \ln z/z_o$ and the extrapolation method used by Davidson and Barad (1956) applied to the four heights of measurement.

Thus:

$$z_o = \ln^{-1} \frac{\ln z_i}{4} - \frac{\Delta \ln z}{4 \left(\frac{\Delta u}{R}\right)}$$

in which

$$R = \frac{(\bar{u}_4 - \bar{u}_{0.5}) + (\bar{u}_2 - \bar{u}_1)}{(\bar{u}_4 + \bar{u}_2 + \bar{u}_1 + \bar{u}_{0.5})}$$

$$\ln z_i = \ln z_4 + \ln z_2 + \ln z_1 + \ln z_{0.5}$$

$$\Delta \ln z = \ln z_4 + \ln z_2 - \ln z_1 - \ln z_{0.5}$$

The computed values of z_o for a snow surface ranged from 0.006 cm to 0.037 cm. Because of the small variation of z_o, its effects on scintillation could not be isolated from the effects of thermal stratification and wind. Furthermore, the effects of roughness differences between snow and ground surfaces on scintillation could not be isolated because identical micrometeorological conditions were not observed during the measurement programs over snow and frozen ground.

4.1.6 Scintillation and the Richardson Number--In studying the characteristics of scintillation it was convenient to look primarily for relationships between the degree of scintillation and the temperature profile and to regard the wind, roughness, and height as secondary factors affecting both the temperature profile and the turbulence. Wind speed, roughness, and height may be related through the wind speed shear, $\partial u / \partial z$. Thus, several parameters can be grouped conveniently in the non-dimensional Richardson number, Ri, defined by:

$$Ri = \frac{g}{T} \frac{\partial \theta / \partial z}{(\partial u / \partial z)^2}$$

This ratio describes the relative intensity of turbulence for shear flow with buoyancy effects Batchelor (1959, p. 2046) explains it as follows:

> "Think of a fluid parcel that migrates vertically a distance, ℓ, through a mean shear flow with an accompanying mean density gradient $\partial \rho / \partial z$. The buoyancy force acting on it is of the order of $\delta \rho g$, where $\delta \rho = \ell \partial \rho / \partial z$. The work done against this force is $\delta \rho g$. The difference in mean velocity at the two positions is δu. The kinetic energy released by the migration is thus of the order $\rho(\delta u)^2$. If the work done against buoyancy forces is much larger than the kinetic energy released the motion will extinguish itself; and if the work done against buoyancy forces is much less than the kinetic energy released, the buoyancy forces will have only a small effect on the motion. The ratio of the two energies may be put

in the form of Richardson number as usually quoted..."

If it is assumed that the Richardson number characterizes the intensity of turbulence and, therefore, the vertical motions, it should also characterize the amount of scintillation for a given mean temperature gradient. The reasoning follows from the idea that fluctuations in light intensity will be greater for greater density discontinuities between turbulent eddies and that these, in turn, will be greater, not only for greater mean gradients, but also for greater vertical motions.

The reasoning would appear to be valid for turbulent flow in either stable or unstable stratification. For stable stratification, however, a limit would be reached at a critical Richardson number since in laminar flow no scintillation would be expected. Because both turbulence and thermal stratification are required conditions for the existence of scintillation, it is clear that in stable stratification scintillation is limited on one end of the stability scale by the absence of thermal stratification and, on the other, by the absence of turbulence. Since the original hypothesis of Richardson (1920) that the critical value of Ri was unity for determining whether or not stably stratified flow would be turbulent, a number of investigators have attempted to determine whether or not a universal critical value existed, and if so, whether or not it is unity. The works of Ellison (1957), Townsend (1958) and Stewart (1959) may be cited as relatively recent contributions to the subject. It appears that if a critical value exists, it exists for only a given set of external flow conditions.

The transition between turbulent and laminar flow is not an abrupt one. It is characterized apparently by the occurrence of internal gravity waves which may, in effect, "break" in a random fashion. Long (1959) gives ample analytical and experimental evident in support of internal waves as a characteristic feature of stably stratified flow. Such waves are to be expected, therefore, in the highly stable flow observed occasionally during the KFS experiments. Evidence for their existence, furthermore, might be expected in both visual resolution and scintillation data. Specifically, visual resolution in the presence of gravity waves would be expected to be better than that in the presence of turbulence but poorer than that for pure laminar motion. In the last condition, for long optical paths, steady but vertically elongated images are observed. Superposition of internal waves would create image motion as well as variations in distortion, probably of a relatively large scale. Such image distortion and motion were, in fact, observed during experiments at KFS over snow for relatively brief periods of very strong inversion and very light wind. During such periods, furthermore, the scintillation minimum was similar to that observed during adiabatic periods. It was observed, furthermore, that small increases in wind speed often caused the situation to change abruptly to short intervals of very strong scintillation with the highest observed Pm values. The observations support the idea of the presence of internal gravity waves with frequent breaking to brief periods of turbulent flow. These conditions obviously represent a situation in which both visual resolution and scintillation oscillate between extreme values in relatively short time intervals.

In order to explore the relationships between scintillation and Ri for different conditions of stable flow, the ratio of Pm to mean temperature gradient, $T_2 - T_1$, was related to Ri for all data obtained over snow. The result is shown in Figure 11 presented in Section 3.2.2.

As expected from the foregoing reasoning, the ratio $Pm/\Delta T$ decreases systematically with increasing Ri. It is clear that a continuous curve could have represented the data as well as the two straight lines. The latter were chosen arbitrarily, however, with the thought that their intersection would specify a critical Ri for the conditions of the measurements. The lines shown were computed with linear regression and, as it turned out, the point of intersection at $Pm/\Delta T \simeq 20$, Ri = 0.35 fell at a data point, for which the number of observations was 159. This point was included only in the computations for the line representing conditions at Ri = 0.35.

The apparent change in slope at Ri = 0.35 may be taken as evidence in support of the idea of a change from turbulent flow to flow characterized mainly by gravity waves. The $Pm/\Delta T$, Ri line would have zero slope for pure laminar motion. Although it may be argued that the slope for $Ri > 0.35$ is not significantly different from zero, the mean value of $Pm/\Delta T$ for this region of the curve suggests that, on the average, the observed values of Pm were larger than those representing the "noise" level of the system as observed during adiabatic periods.

Insofar as the Richardson number may be considered a universal parameter to characterize turbulent and near-turbulent flow with thermal stratification, these results represent a fundamental relationship for estimating scintillation from wind and temperature information over a snow surface.

4.1.7 Scintillation Power Spectra--In addition to the correlation between the average intensity of scintillation (as measured by Pm) and visual resolution it is reasonable to expect that the spectral characteristics of scintillation would have an important relationship to one's ability to see a particular pattern. Specifically, for a given measured Pm, it may be expected that different limits of resolution may be found depending on whether the main variations in light intensity are of relatively high or low frequency. From another point of view, it may be reasoned that both the size and the speed of inhomogeneities in index of refraction would have an influence on the limit of resolution and that, insofar as these are measured by spectral characteristics of scintillation, the latter should reveal important information for relating visual resolution to meteorological conditions. The inadequacy of the average scintillation intensity, alone, as a parameter to specify visual resolution conditions is apparent in the scatter of the data shown in Figure 4.

Although several hours of data were recorded on magnetic tape for power spectral analysis, only eight two-minute periods could be analyzed. The results of the analysis are presented in Section 3.2.3 and in Figures 12, 13, and 14. (The method of analysis is described in Section 5.4.3 and the meteorological conditions for each spectrum are summarized in Table VI.) Each of the three

figures shows all eight spectra but each is a different representation to facilitate comparison of the spectra and to relate their characteristics to flow properties.

In the first of these, Figure 12, the spectra are shown as measured. Each spectrum represents an independent observation insofar as all except periods I and III were obtained on separate days. Periods I and III were obtained on the same day but were more than 30 minutes apart. There are large variations in relative power for frequencies between 2.5 and 20 cps, but perhaps the greatest differences are in the total areas represented by

$$\int_{2.5}^{200} W_p(f)\, df$$

for each spectrum. The areas should be proportional to the Pm values measured for the periods. A comparison shows good agreement for all spectra except those for periods VII and VIII. The discrepancies may be accredited to possible frequency dependency of the A. C. recording circuit. This question is being investigated.

To make more direct comparison possible, the spectra were normalized, as explained in Section 3.2.3, by a factor to give a constant value to the area under each curve. Figure 13 shows the normalized spectra grouped into four categories according to similarities in their shapes. Shown also are the appropriate average Richardson numbers and wind components normal to the optical path.

The spectra in the first group represent periods during which Ri is greater than 0.35, the critical value suggested by Figure 11. The high values of relative power for low frequencies in comparison to the spectra in group 3 (lower, left), which represents periods of comparable cross-wind, for example, support the idea that internal gravity waves were responsible for much of the scintillation observed here. The effect of cross wind speed should be seen by comparing groups 3 and 4 which have comparable Richardson numbers but cross-wind speeds which differ by a factor of 2. One would expect a relative increase in power for the higher frequencies for the higher cross wind. This is not evident here although the expected opposite effect at the lower frequencies is suggested. The spectrum in the upper right represents a period of small Ri and relatively high cross-wind. An expected decrease in power for the lower frequencies is clearly evident.

Theoretical and experimental work by Tatarski indicates that the frequency spectrum of the fluctuations of light intensity depends on $f(\sqrt{\lambda L}/\bar{V}_n)$ according to the relationship,

$$\frac{f\, W(f)}{\int_0^{\infty} W(f)\, df} = F\left(\frac{f\sqrt{\lambda L}}{\bar{V}_n}\right)$$

where L is the optical path length, λ is the wave length of light, and other terms have their usual meanings. If this relationship is valid, the normal component of the wind should explain differences in individual spectra.

If the frequency spectra are reduced in terms of wave number a normalization for wind speed is accomplished. Figure 14 shows the same eight spectra in terms of $W_p(f)$ vs k where $k = \frac{2\pi f}{V_n}$. While some of the differences among spectra are accounted for by the cross-path wind component, it can be seen that a large amount of variance is yet unexplained.

It is probable that some of the observed differences are due to the inadequacies in measurement of the wind components. However, the theoretical derivation by Tatarski is based upon assumptions that permit applications to atmospheric conditions not greatly different from adiabatic. It also cannot hold for the condition where the wind is parallel to the light path. Thus it is not surprising that differences in spectra remain even after normalization for movement of the total field of view. It is hoped that analysis of more spectra will permit isolation of the remaining influences.

4.1.8 Scintillation and Path Length--The increase of scintillation and other optical effects of turbulence with increase in length of optical path is a commonly observed phenomenon. On a bright day, for example, the more distant an object, the more it appears to move and to be distorted. The distance effect is also easily observed in the case of stellar scintillation, which, for a given star, has been found to increase as its position changes from near zenith to near the horizon, increasing the length of the atmospheric path.* Apparently the first systematic observations of the variation of scintillation with length of path near the ground were made by Siedentopf and Wisshak (1948). They found that the relationship between Pm and length of path had the characteristics of a saturation curve that nearly reached its limiting value at a path length of 1200 meters. A more detailed analysis shows that their data may be represented by three straight lines for different path lengths, L, as follows:

$$80m < L < 400m \qquad Pm \propto L^{1.3}$$

$$400m < L < 1000m \qquad Pm \propto L^{0.75}$$

$$1000m < L < 1600m \qquad Pm \propto L^{0.10}$$

Gurvich, Tatarski and Cvang (1958), however, have presented both theory and experimental results that correspond to $Pm \propto L^{.91}$ for $100m < L < 2000m$. Their results are based on the theory of wave propagation in an isotropic

*The change in angle between the optical path and atmospheric density gradients may have an influence on the observed scintillation increase, also, although this effect apparently has not been recognized by the astronomers.

turbulent field in which the index of refraction may be regarded as a conservative passive additive. It is assumed that the correlation between index of refraction values at two points in space is proportional to the 2/3 power of the distance between them in accordance with the Kolmogorov equilibrium range for isotropic turbulence. An additional restriction for the specific result cited here is that

$$\ell_o \ll \lambda L \ll L_o$$

in which ℓ_o is the internal, or micro, scale of turbulence ($\approx$ 1 cm.), λ is the wave length of light, L_o is the external, or macro, scale of turbulence ($\approx$ 10 to 100 m) and L is the length of optical path. This means that the theory should apply to path lengths greater than 200 meters if the other conditions are met.

Their experimental results were obtained by moving a light source to different positions corresponding to L = 250, 500, 1000 and 2000m. Both theoretical and experimental results are given in terms of a quantity,

$$\sigma^2 = \overline{(\ln I - \overline{\ln I})^2}$$

in which I is the apparent intensity of the light source. It can be shown that σ is related to Pm by a constant factor, for Pm significantly less than 100.

The results of experiments at the Willow Run field station, as shown in Figure 15 are in close agreement with the findings of Gurvich, et. al. for small temperature gradients, both for lapse and for inversion conditions. The set of data for $T_{2m} - T_{1m} = +0.8°C$ suggests that Pm increases less rapidly with path length for stable stratification. Unfortunately neither Siedentopf and Wisshak nor Gurvich, et. al., report their findings in terms of temperature gradients so that additional experimental results are needed to explore the validity of these ideas.

4.2 Visual Resolution and Scintillation

4.2.1 Over Snow at Night--The relationship between scintillation and visual resolution shown in Figure 4 includes 126 observations obtained over snow at night. The standard deviations and the number of observations of Pm for each slot size at the limit of resolution are shown. A systematic decrease in resolution capability with increasing Pm is clearly evident except for low scintillation, high resolution conditions. The small change of Pm with slot size for these conditions indicates the limitation imposed on the method of observation by the observer's ocular qualities, the magnifying power of the telescope, the illumination of the resolution chart, and other factors which are less obvious, but possibly as important. (See Section 5.1 for a description of the equipment and procedures used for visual resolution determination.)

The scatter of individual observations, as indicated by the standard deviations, may be explained by a number of factors. Perhaps one of the most important for conditions of poor resolution was the time variability of scintillation. This was particularly pronounced during periods of extreme thermal stratification and very light wind. The variability influenced the measurements because of the time required to establish the limit of resolution. As a result, the final slot size accepted as the resolution limit in some cases may not have been a good measure of the average conditions for a two-minute interval.

An appreciation of the observational problem may be gained from the observer's comments recorded during a period of strong and variable scintillation. The following statements were made during a period when the limit of resolution was determined to be a relatively large slot size of 0.93 inches.

> "The vertical gradient in shimmer (object motion) is very high. The lower two charts on the turntable (about 0.75 meters above snow) are distorting to diffuse elliptical shapes which are dancing up and down. At times the lower portions appear fused with the snow surface. The uppermost charts (about 1.8 meters above snow) are much more distinct and circular. The legs of the tripod (standing on the snow near the chart) appear curved and the tripod appears to have been lifted. The shed which houses the telephotometer also appears to have shrunk in width and expanded vertically. It appears as if water were flowing near the snow surface nearly obliterating the bottom of the shed."

Spatial variations in image distortion were clearly evident in such conditions. At times a well-defined layer of maximum distortion was observed to move upward as high as the uppermost rings on the chart, distorting each target as it moved. Above the upper, and beneath the lower, limits of the layer no distortion was present and the resolution was good. When the wind speed exceeded about 8 mph, however, the distortion was not great and was uniformly distributed with height.

The foregoing comments suggest that under many conditions the parameter Pm is not likely to be well correlated with resolution limit. If the AC component measurement systems respond equally well to all frequencies of scintillation, Pm is a measure only of the intensity of distortions and gives no information on their size or speed. It may be reasoned, therefore, that the scatter indicated in Figure 4 may be reduced by a consideration of spectral characteristics of scintillation. Thus, the power spectra for the eight two-minute periods listed in Table VI were selected for a preliminary analysis of their relationship to visual resolution. As the data in the table reveal, the eight periods represent a large range of resolution and scintillation conditions as well as some periods for which the general relationship shown in Figure 4 is clearly not represented. Analysis of spectral characteristics of these periods might be expected, therefore, to suggest relationships that would have less scatter than those involving only per cent modulation.

Figure 6 represents a relationship between visual resolution and spectral characteristics of scintillation in terms of a "spectral resolution factor" for the eight periods. The spectral resolution factor was derived with the assumption that size, speed and local, small-scale gradients associated with index of refraction discontinuities would all contribute to the limit of visual resolution. It was reasoned, in addition, that the major influences determining a given resolution limit would be those associated with discontinuities having characteristic lengths equal to or less than the slot size dimension. Effects of larger discontinuities would tend to displace the total image rather than to distort and to confuse its boundaries. A measure of these effects may be obtained from a scintillation frequency spectrum if it is transformed to a wave number spectrum by the relationship

$$k = \frac{2\pi f}{\overline{V}_n}$$

in which k = wave number, cycles/cm
f = frequency, cycles/sec
$\overline{V}_n$ = average wind speed normal to the optical path.

The total scintillation "power", then, due to discontinuity effects equal to and smaller than the slot size, s, representing the limit of resolution, is

$$\int_{1/s}^{\infty} W_p(k)\, dk$$

The effect of speed may be included simply by multiplying by $\overline{V}_n$, so that a spectral resolution factor may be defined as

$$F = \overline{V}_n \int_{1/s}^{\infty} W_p(k)\, dk$$

which transforms to

$$F = 2\pi \int_{\overline{V}_n/2\pi s}^{\infty} W_p(F)\, df$$

for direct computation from frequency spectra.

The transformation involved in this development requires the entire field of index of refraction discontinuities to have a uniform velocity normal to the optical path and the field itself not to change in time. The effect of the telephotometer aperture integration, furthermore, has been neglected so that spectral characteristics for wave lengths of the order of the diameter of

the aperture and less do not bear direct relationships to the index of refraction discontinuities as do spectral characteristics for larger wave lengths.

In spite of these approximations, the spectral resolution factor appears to have a close relationship to the limit of resolution. Because of the very few data used in the analysis, however, the results must be regarded as highly tentative.

Another factor that may be responsible for part of the scatter of the basic data used in preparing Figure 4 is that the observations were made by two observers. One observer made all observations before 29 February 1960; the other all observations over a snow surface after that date. It is worth noting in this connection that visual resolution estimates for the eight periods selected for spectral analysis were made by the first observer, except for that of period II. This may account for the apparently anomolous position of the point for period II in Figure 6.

Finally, it should be mentioned that unavoidable variations in both physiological and psychological responses of any one observer may have an important influence on all observations of this nature. In view of this fact and of the variability of atmospheric influences on visual resolution, future work should include both photographic measurements of resolution and scintillation spectral characteristics.

4.2.2 Over Snow in Daylight--The relatively few observations of visual resolution made over snow in daylight correspond in a general way with results for the data obtained at night. The resolution was relatively good and the Pm was low for most of the observations as would be expected from the fact that all temperature differences measured for the daytime observation periods were relatively small. The data are too few to isolate a possible effect of daylight on the observer's performance.

4.2.3 Over Frozen Ground at Night--Visual resolution determinations made over frozen ground at night are shown in Figure 5. Although the number of observations was limited, the relationship and behavior with respect to scintillation were very similar to those observed over snow at night.

4.2.4 Over Frozen Ground in Daylight--Visual resolution measurements made over frozen ground in daylight are also shown in Figure 5. Although there are relatively few observations it is clear that, in comparison to nighttime data for both snow and frozen ground, the changes in Pm for a given resolution increment are significantly larger for these data. Although part of the difference may be the result of natural effects, there are at least two aspects of the measurement method that must be considered. First, there is the possibility that illumination of the resolution chart by daylight had an important influence on the observer's ability to see the targets. It can be argued that this would influence the findings in the direction observed.

A second, and perhaps more significant factor, was that for these observations the telephotometer was equipped with an internal aperture to reduce the influence of daylight on the phototube response. Following the observations, it was learned that the internal aperture had the effect of increasing the Pm values by an amount that increased with increase in intensity of scintillation. However, the aperture was required only on very bright days. Additional experimentation is considered necessary to establish corrections in order to make direct comparisons between measurements obtained with and without the internal aperture.

Although direct comparisons are not possible with these data, it was the experience of the observer that visual resolution in daylight over frozen ground responded to temperature structure and general meteorological conditions in a way quite similar to that observed at night.

4.2.5 Over Ice--Because a shorter optical path (1600 feet) was necessary over ice and because suitable weather conditions were not experienced, the few visual resolution determinations are not considered comparable to those made over snow and frozen ground.

5. EQUIPMENT AND PROCEDURES

5.1 Visual Resolution Equipment and Measurement Procedures

A Landolt broken-ring resolution chart was used to determine an observer's visual resolution capabilities for different scintillation conditions. Figure 16 shows the chart as it appeared during measurements over ice. The visual targets were black broken rings (C-shaped figures) photographically reproduced and dry-mounted on 20-inch white cardboard disks. The contrast between each black ring and the white background was 0.96. At any one time, six disks with rings of different sizes were attached peripherally to a larger disk that could be rotated to permit any ring to appear in the viewing position at the height of 1.5 meters. Once in the viewing position, each broken ring could also be rotated to any desired orientation. For nighttime operation, the chart was uniformly illuminated by an intense flood light.

Twenty-one broken rings having outside diameters from 0.20 to 17.76 inches were available. The slot sizes, or gap widths, of the broken rings equaled the ring thicknesses and ranged from 0.04 to 3.55 inches. Each broken ring was 1.25 times as large as the previous one in the series. The ratio 1.25, selected on the basis of experimental results obtained by Fritz (1928), was used by Gordon (1959) in tests to evaluate the optical design of night binoculars.

The resolution chart was located near the telephotometer and operated by a person in telephone communication with an observer stationed near the light source. The latter viewed the chart with a 24-power telescope and reported his estimate of the orientation of each broken ring brought into viewing position by the chart operator. Progressively smaller broken rings, with arbitrary orientations, were moved into position until the observer, in the judgment of the chart operator, could no longer discern the correct orientation. The recorded limit of visual resolution was the slot size of the smallest broken ring whose orientation could be correctly identified. The times of the determinations were noted in order to relate the resolution limits to corresponding measurements of scintillation. Except for three periods of observation over snow, after 27 February 1960, all resolution determinations were made by the same observer.

5.2 Scintillation Equipment and Measurement Procedures

5.2.1 General--A block diagram of the instrumentation used to measure scintillation is shown in Figure 18. A 5-inch diameter, 12 volt, sealed beam lamp was directed to a 3-inch refracting telescope-photometer system located about 1780 feet away. The telescope, a Warner and Swasey, Model No. 667 azimuth instrument, is shown with the photometer in Figure 19. The photometer alone, with a side removed, is shown in Figure 20. A DuMont type 6467 multiplier phototube, located at the focus of the interior lens system, provided an electrical analog of the luminous flux at the telescope objective.

A schematic circuit diagram of the scintillation measurement system is shown in Figure 21. The photometer output (proportional to average apparent

brightness of the source) is indicated by a microammeter galvanometer damped to prevent response to rapid fluctuations. A convenient average brightness level is maintained by inserting neutral density filters in the photometer. The average meter reading is controlled, in addition, by adjustment of the gain of the multiplier phototube. The average brightness is termed "DC level" for purposes of evaluation and is calibrated in units of millivolts with reference to ground potential.

To obtain a measure of the mean magnitude of the fluctuations in brightness the electrical output of the multiplier phototube is amplified by a low frequency amplifier, rectified and then integrated. The system is calibrated in terms of equivalent sine-wave peak-to-peak voltage. The observed magnitude is termed the "AC level" and, since this value is also related to the "DC level," scintillation is finally evaluated as a ratio of AC to DC levels and termed "per cent modulation." In this way scintillation measurement is independent of slow changes in source brightness due to attenuation variations or battery and lamp aging.

The electrical output of the multiplier phototube contains all information necessary for analysis of the frequency spectra of the scintillation. Since analysis in the field in "real time" is difficult to accomplish, the data are recorded on magnetic tape by means of frequency modulation of a constant-frequency carrier signal. The recorded data are retained for subsequent analysis in the laboratory by techniques described in Section 5.4.3.

Detailed descriptions of the measuring circuits are given in the following three sub-sections.

5.2.2 DC Component Indicating System--The "DC level" is indicated by a 0-25 microammeter in the cathode circuit of the cathode follower. The meter is adjusted to "zero out" the dark current of the multiplier phototube or background light level and is damped to the extent that it does not respond to rapid fluctuations in the phototube current resulting from the light scintillation.

The "DC level" is calibrated in terms of the voltage at the grid of the cathode follower tube. A potentiometer measurement is used as a reference standard. The sensitivity is adjustable to a chosen calibration by means of the cathode load resistor, $R_{(5)}$, (Figure 21). Figure 22 shows the linear response of the DC indicating system. The DC reading is directly proportional to the average light intensity incident upon the phototube although no calibration in terms of luminous flux density has been made.

5.2.3 AC Component Indicating System--The phototube signal is capacitor-coupled to a three-stage amplifier resulting in elimination of the average or "DC" component. The amplified signal is rectified by the crystal diodes $V_{(4)}$ and $V_{(5)}$. Capacitor $C_{(10)}$ and resistor $R_{(24)}$ form a rapid charge, low leakage circuit which smooths the peaks of the applied voltage. The charge on capacitor $C_{(10)}$ determines the bias on the balanced amplifier $V_{(3)}$. The difference in

plate current of the two triodes is determined by the charge on capacitor $C_{(10)}$ and, therefore, is a function of the amplitude of the charging voltage.

The AC measuring system is calibrated in terms of an AC voltage applied at the grid of the cathode follower tube, $V_{(2)}$. A Ballantine, Model 316, Infrasonic, peak-to-peak voltmeter was employed as a standard. Since the gain of the amplifier is adjustable, sensitivity of the system is variable over a certain range. A typical calibration curve is shown in Figure 23. The response of the meter is approximately linear down to a level of about 50 millivolts, below which the calibration approaches the noise level. The cathode follower $V_{(2)}$ has a limited linear range of response and, therefore, the gain is a function of the DC bias. Separate AC calibrations are necessary for each of the DC levels of operation.

The output of the AC meter is recorded on an Esterline Angus 0-1 milliampere recorder. The "AC level" is evaluated in terms of equivalent sine-wave peak-to-peak amplitude. For input signals other than constant amplitude sine waves, the output could differ by an unknown amount from the true mean peak amplitude. The frequency response curve is shown in Figure 24. Response falls off below about 4 cps due to the discharge rate of the storage circuit. Also, the linear amplifier response is limited to frequencies below about 400 cps. All calibration was accomplished at 30 cps.

Final evaluation of scintillation is accomplished as a ratio of AC to DC level. This gives a measure of scintillation that is independent of the gain of the multiplier phototube and avoids the necessity of calibration of the system in terms of luminous flux density. Precise definition of the ratio, termed per cent modulation, is known only in terms of equivalent sine wave modulation since the AC meter does not indicate true amplitude of the actual noise signal. For a sine wave input of constant amplitude,

$$\% \text{ Modulation} = \frac{\text{AC}}{\text{DC}} \times 100 = \frac{2.828 \text{ RMS Voltage}}{\text{DC Voltage}} \times 100$$

5.2.4 Magnetic Tape Recording System--The electrical analog of scintillation is recorded directly with a magnetic tape system similar to that described by McLaughlin and Prout (1959). The major component is a modified Ampex Model 601 dual-channel tape recorder one channel of which is used for data and the other for voice announcements. A photograph of the recording system is shown in Figure 25.

The multiplier phototube signal is taken directly from the load resistor of the cathode follower stage and supplied to the input of a low frequency pre-amplifier. A schematic diagram of the pre-amplifier is shown in Figure 26. A curve of the amplifier frequency response is shown in Figure 27. The gain is nearly constant between 1 and 300 cps with the -3Db points at 0.6 and 600 cps.

The output from the low frequency amplifier is fed through a step attenuator to a frequency modulation module similar in electrical design to that of the Ampex FR-100 recording system. The circuit diagram is shown in Figure No. 28. The carrier frequency is determined by a standard Ampex center-frequency plug-in unit. The low frequency amplifier, f-m module combination provides a means of recording directly the analog signal of scintillation in the frequency range from 0.6 to 600 cps at a tape speed of 7 1/2 inches per second.

5.3 Meteorological Measurement System

Wind and temperature profiles and wind direction were measured continuously throughout all periods of scintillation measurement. The profiles were measured with sensors at nominal heights of 0.5, 1.0, 2.0 and 4.0 meters and the wind direction at about 4 meters.

5.3.1 Temperature Sensing and Recording Equipment--The temperature sensors were 36 B and S gauge copper-constantan thermocouple junctions supported in flat-plate radiation shields similar to those described by Portman (1953). The shields were supported at the end of 24 inch arms on an aluminum mast as shown in Figure 29. The mast was oriented with the arms normal to the mean wind direction when possible. In this way the influence of the mast on measurements of both temperature and wind was reduced to a minimum.

Similar thermocouple radiation shields have been tested for radiation error (Portman, 1960). The tests show that an error of significant magnitude in the measurement of air temperature may result under certain conditions. The error becomes most serious under conditions of low sun angle and low wind speed. Since most of the measurements during this program were made at night, it is believed that errors due to radiation effect were small.

For measurements over snow the thermocouple circuit was arranged to yield temperature differences for the three height intervals: 0.5 to 1, 0.5 to 2, and 0.5 to 4 meters. For measurements over frozen ground and ice, the intervals were 1 to 2 and 1 to 4 meters and, in addition, the absolute temperature at 1 meter was recorded. These were recorded in sequence for one third minute intervals on a Leeds and Northrup Speedomax Model S, AZAR recorder. A Leeds and Northrup DC amplifier was employed to provide the desired sensitivity of about 0.1°C per chart scale division. Periodically, an absolute air temperature at the 0.5 meter level was measured with an Assman or a standard sling psychrometer.

5.3.2 Wind Sensing and Recording Equipment--Wind speed was measured with Beckman and Whitley Model 170-34 anemometers. They were supported on the same mast as that used for the thermocouple radiation shields as shown in Figure 29. The anemometers were adjusted so that the cups were at the same level as the radiation shields to provide a measure of wind and temperature at identical heights above the surface.

Wind speeds were recorded with a four-channel pulse counting system. A schematic diagram of the system is shown in Figure 30. Each revolution of the anemometer cups produces a single pulse which is amplified and indicated on the Veeder Root Decade counter. The counters provide decade outputs which are recorded on an Esterline Angus 20-pen operation recorder. A permanent record of each revolution of the anemometer cups is thus obtained.

The anemometers were compared for similarity of calibration by exposure on a horizontal bar as shown in Figure 31. The bar was oriented normal to the wind in an area of uniform terrain. Several comparisons made throughout the program indicated that less than a 1% difference in calibration existed among the four sensors employed.

A continuous record of wind direction was obtained with a military version of the Bendix "aerovane," Wind Measuring Set AN/GMQ-11, and Wind Speed and Direction Recorder RO-2/GMQ. Records were not reliable for periods of low wind due to the rather high response threshold (2 to 3 knots) of this equipment. A chart speed of 6" per hour was employed to permit an estimation of the mean wind direction for each 2 minute period of the record.

5.4 Data Reduction, Processing and Analysis Methods

All data recorded continuously on strip-charts, viz., wind speed and direction, temperature and the AC component of scintillation, were reduced and processed to obtain averages for two-minute intervals. The visual resolution and DC component of scintillation were logged manually for the appropriate intervals and needed no processing prior to tabulation. The spectral analysis was made for two-minute intervals to correspond with other data analysis.

Details of the methods used are described in the following sub-sections.

5.4.1 Temperature--Two-minute averages were determined by estimating visually the average ordinate for the continuous trace with the aid of a transparent overlay. Because of the sampling rate, each two minute interval contained two separate one-third minute records. The resulting average voltages were converted to temperature difference.

5.4.2 Wind--Wind speeds were determined by counting total revolutions for each two minute interval as indicated on the operations recorder chart. The two-minute sum was converted to wind speed according to calibration information supplied by the manufacturer. Average wind direction was determined from the continuous record in a way similar to that used for temperature.

5.4.3 Scintillation Per Cent Modulation--Two-minute average values of the AC component were obtained from the continuous recording in a way similar to that used for temperature. After conversion from ordinate values to millivolts according to calibration information, the average value was divided by the DC value logged for the corresponding time interval to obtain the per cent modulation.

5.4.4 Scintillation Power Spectra--The spectral information presented in this report was obtained by the method of time compression with a magnetic tape-loop machine and subsequent frequency analysis with a harmonic wave analyzer. The tape-loop machine was capable of four speeds ranging from 7 1/2 ips to 60 ips and could use a loop up to 75 ft in length. The wave analyzer, a Hewlett-Packard Model 300A, was used with an Esterline Angus recording milliammeter. The method used was similar to that described by Parks (1960).

For each spectrum, two minutes of data originally recorded on magnetic tape at 7 1/2 ips with a f-m carrier of 6.75 kc, were transferred to a 75 foot tape loop (at 7 1/2 ips). The loop was then played back at 60 ips (shifting the carrier frequency to 54 kc), the signal was demodulated, and the analog output was fed into the wave analyzer. The wave analyzer gives an rms value of the amplitude for the frequency components in any 10 cps band over the range of 20 cps to 20 kc. The factor-of-eight time compression obtained by rapid play-back of the loop machine permitted analysis of the scintillation data for the rms amplitude in any 1.25 cps band over the range of 2.5 cps to 2500 cps. The rms amplitude of the frequency component was squared for display as power spectra.

The above technique was selected after a comparison of three methods of wave analysis to evaluate the most efficient procedure in terms of time and accuracy. These methods were: (1) measurement of the output of tuned passive filters (bandwidth a fixed percentage of the center frequency), (2) harmonic wave analysis with an analog computer (analysis carried out in real time, bandwidth a fixed percentage of the center frequency), and (3) time compression by means of a tape loop with harmonic analysis by means of an audio frequency wave analyzer. The time compression obtained by rapid playback of a magnetic tape loop significantly reduces the time required for data analysis.

A particular two-minute segment from the data obtained on 8 March 1960 was subjected to three methods of analysis. In Figure 32 are compared the results obtained with a digital computer, and two loop-analyzer systems. The digital, and one analog analysis were done by personnel of the Boeing Aircraft Corporation. The analog systems employed at Boeing automatically scans the frequency range while the system employed in this laboratory required manual scanning of the desired frequency range. These results demonstrate the accuracy of the present system.

5.5 Experiment Site Description

5.5.1 Keweenaw Field Station--The measurements over snow were made at the U. S. Army Cold Region Research and Engineering Laboratory's Keweenaw Field Station at the Houghton, Michigan, municipal airport. The station is 1090 feet above sea level and about 500 feet above the level of Lake Superior, six miles to the northwest.

Figure 33 is an aerial view of the field station. The telephotometer was housed in a small "skid shack" and the indicating and recording equipment for both the telephotometer and the micrometeorological sensors was located in

a van near it. The light source was 1780 feet from the telephotometer in a direction 30 deg from north. It was west of, and parallel to, the vehicle tracks shown in the photograph (Figure 33).

The mast supporting anemometers and thermocouples was located near the optical path, 170 feet from the telephotometer. The aerovane was 80 feet north of the telephotometer.

A uniform snow cover, about 0.5 meters deep, covered the entire field for all observation periods.

5.5.2 Willow Run Airport--The measurements over frozen ground were made at the University of Michigan Micrometeorological Field Station located at the Willow Run Airport. The experimental area is enclosed within the dashed line shown in Figure 34. The 1780 foot optical path was oriented in a north-south direction along the east edge of the airfield. Observations were made only with winds which had a westerly component so that the air passed over a level and uniform surface for several thousand feet before it moved through the optical path. The area of the field station was covered uniformly with mixed grasses mowed to a height of about 10 cm.

5.5.3 Ford Lake--The measurements over ice were made on a section of Ford Lake, approximately five miles from Willow Run Airport. The selection of the site was based on a suitable fetch across smooth ice with westerly winds. However, the optical path length was limited to 1600 feet because of the size of the lake. Very smooth, nearly transparent ice 15 inches thick existed during both periods of measurement.

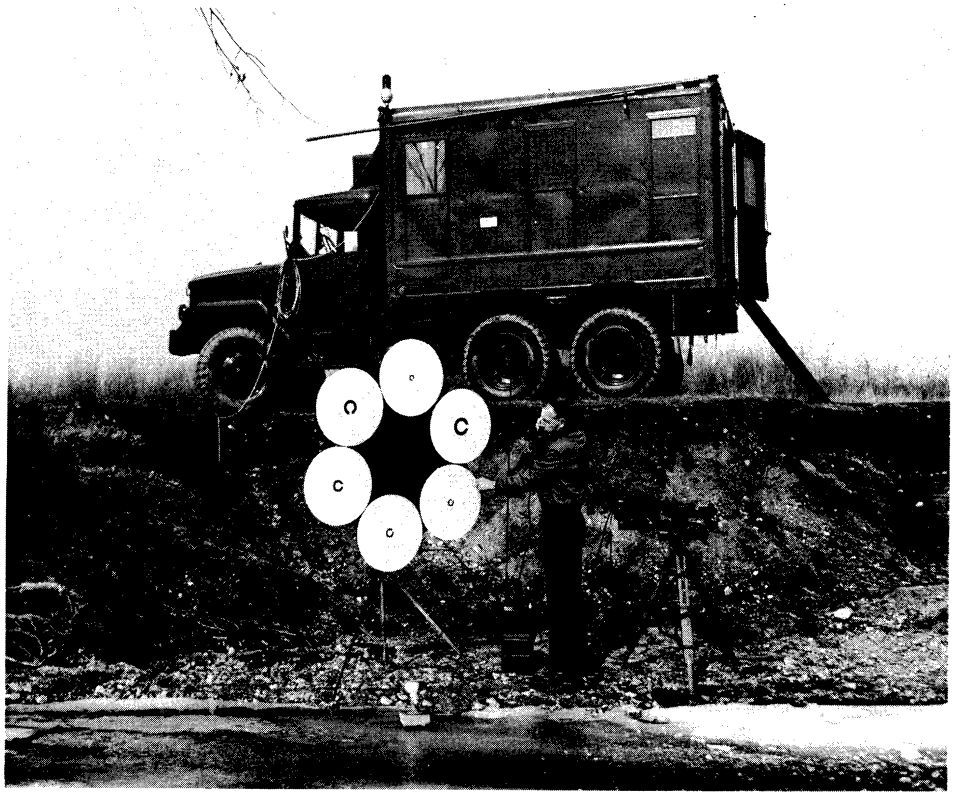

Figure 16. Landolt Broken-ring Chart, Telephotometer and Communications System.

Figure 17. Observer, Telescope, D. C. Light Source, and Communications System.

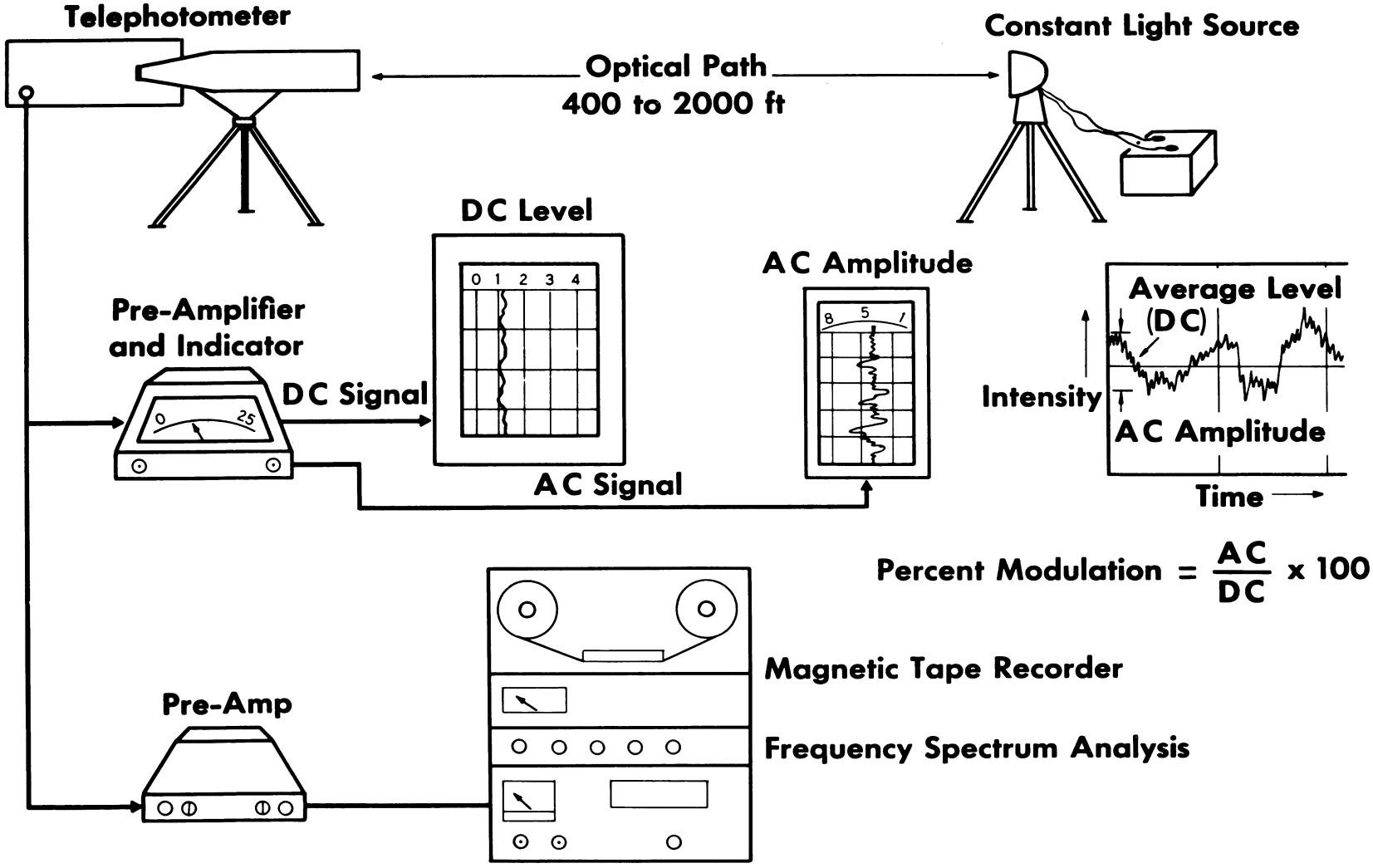

Figure 18. Block Diagram of Scintillation Measurement System.

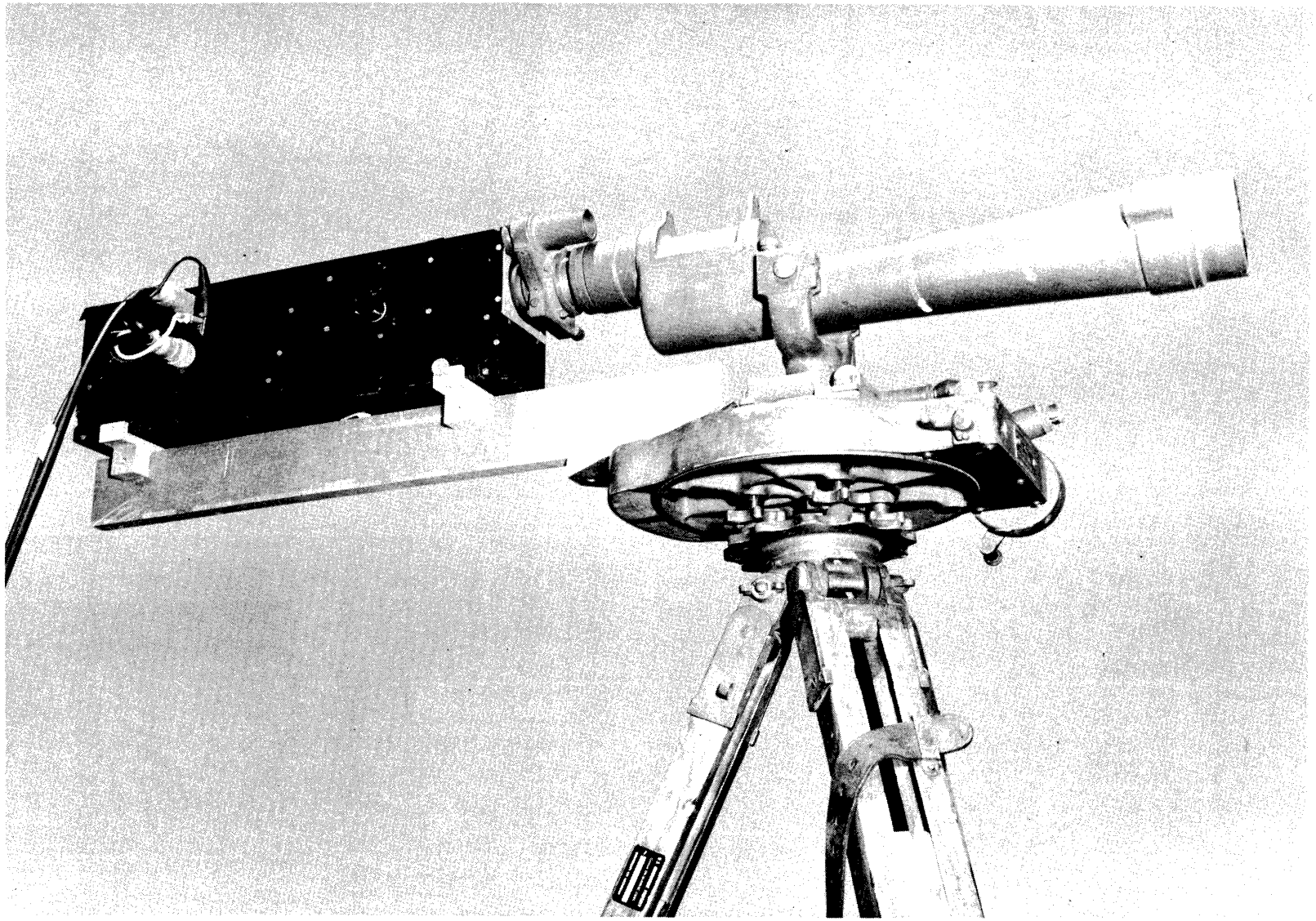

Figure 19. Three-inch Refracting Telescope with Attached Photometer.

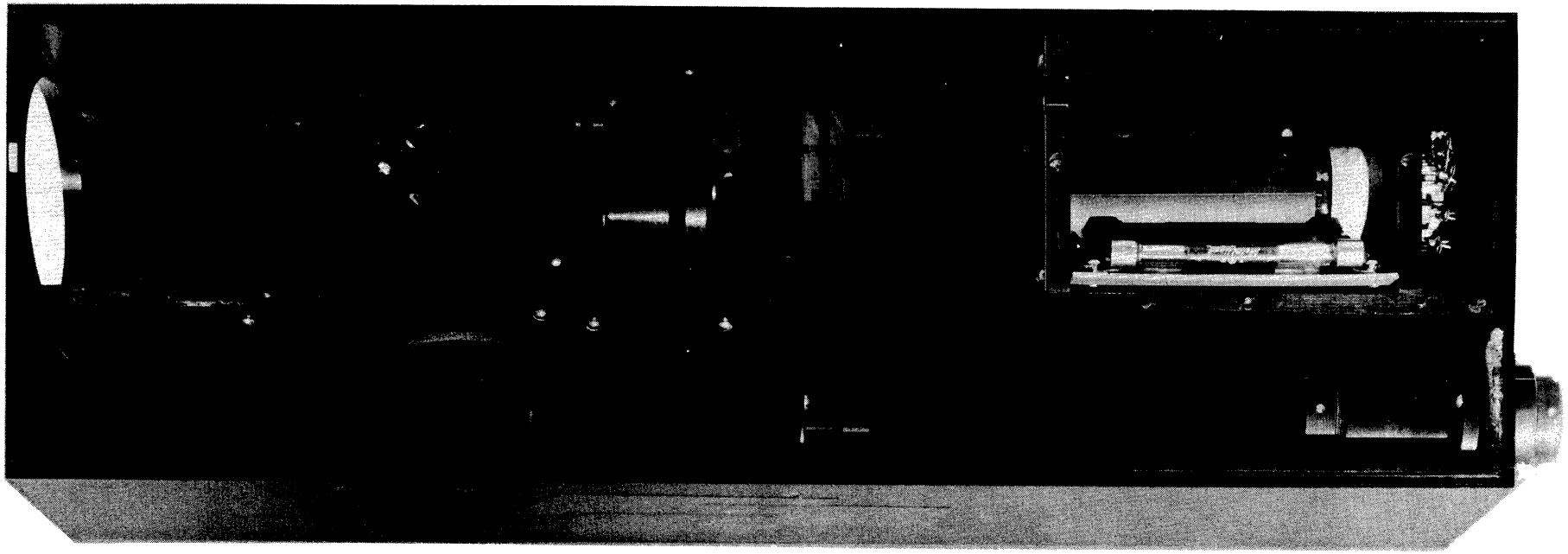

Figure 20. Interior of Photometer with Lens System and Multiplier Phototube at Focus of Lens System.

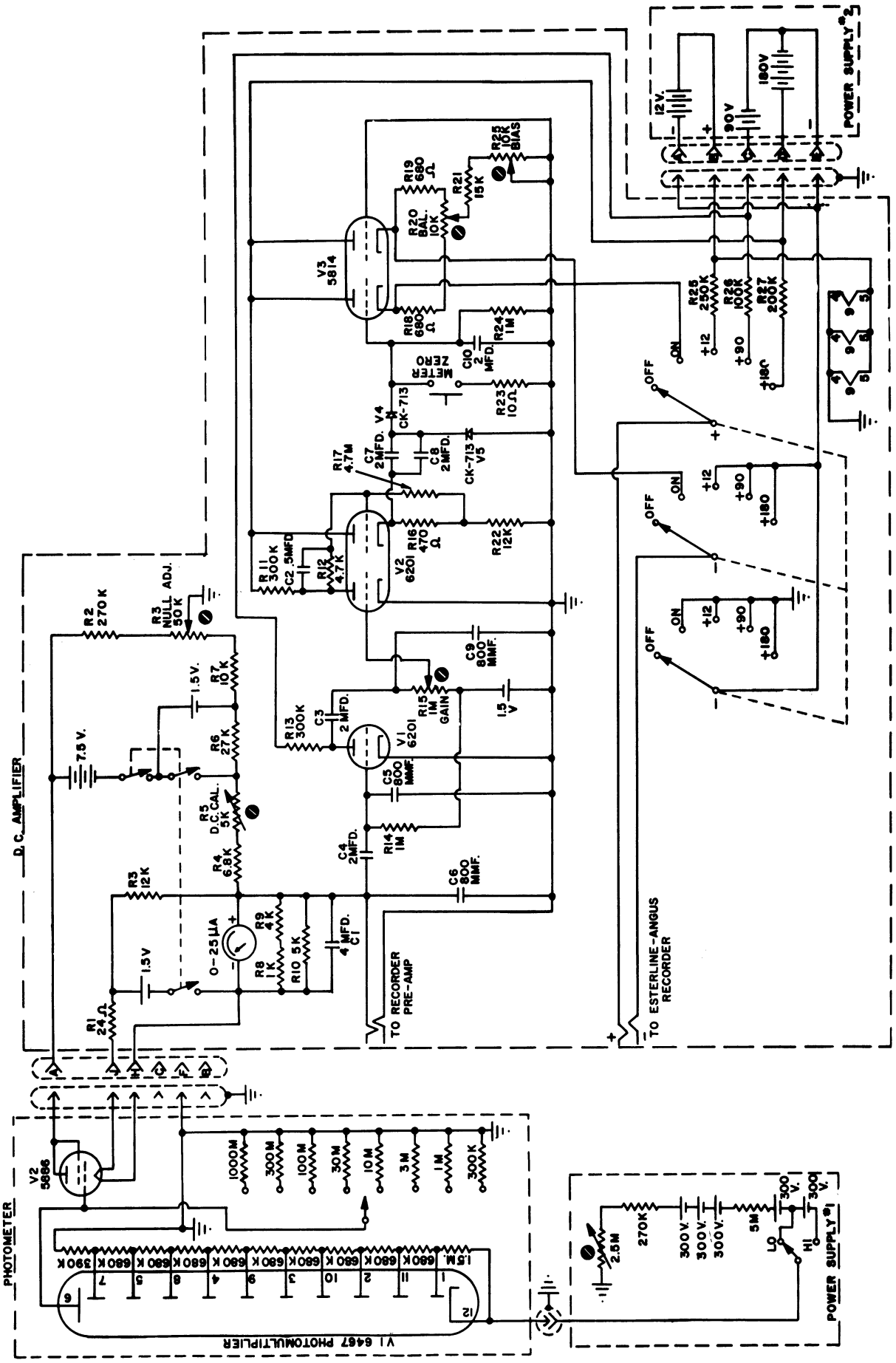

Figure 21. Schematic Circuit Diagram of Scintillation Measurement System.

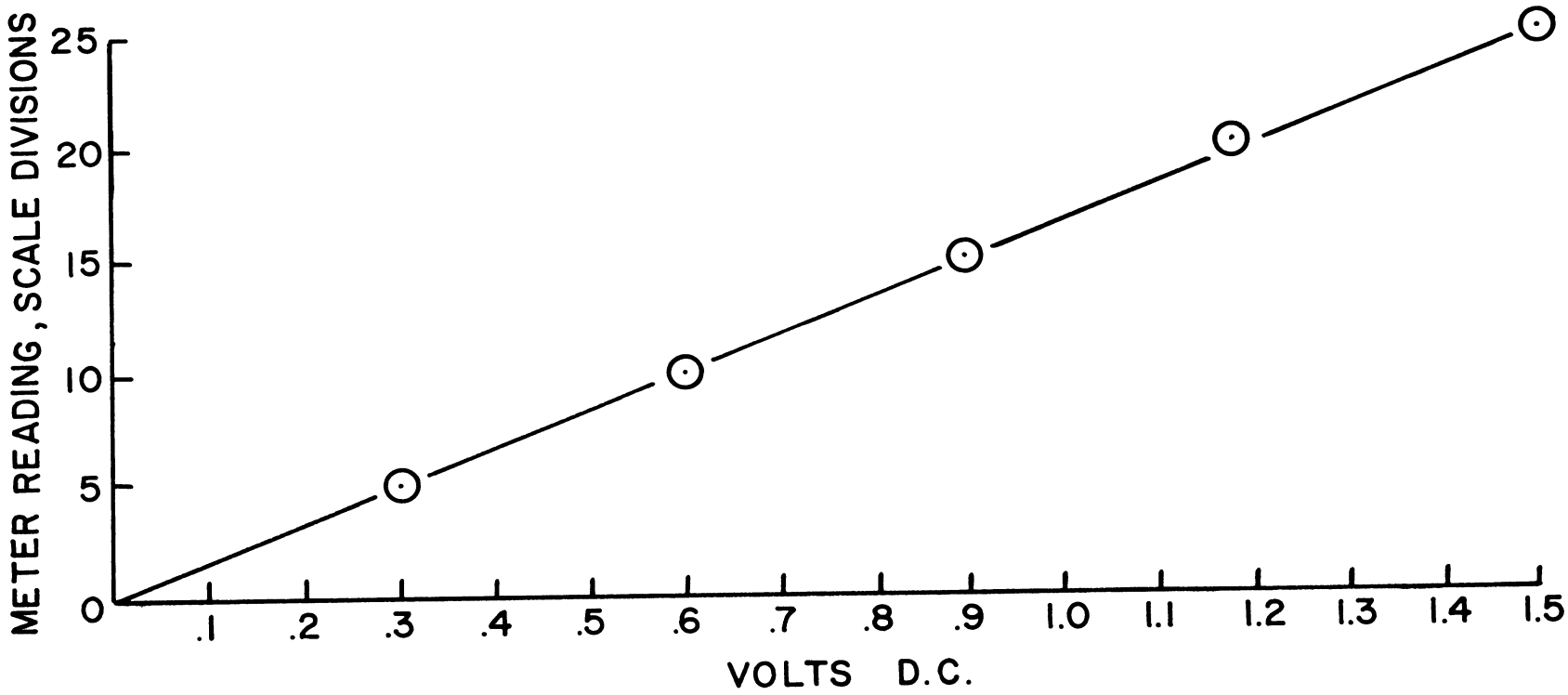

Figure 22. Calibration Curve for the D. C. Meter Reading (Scale Divisions) vs D. C. Level (Volts).

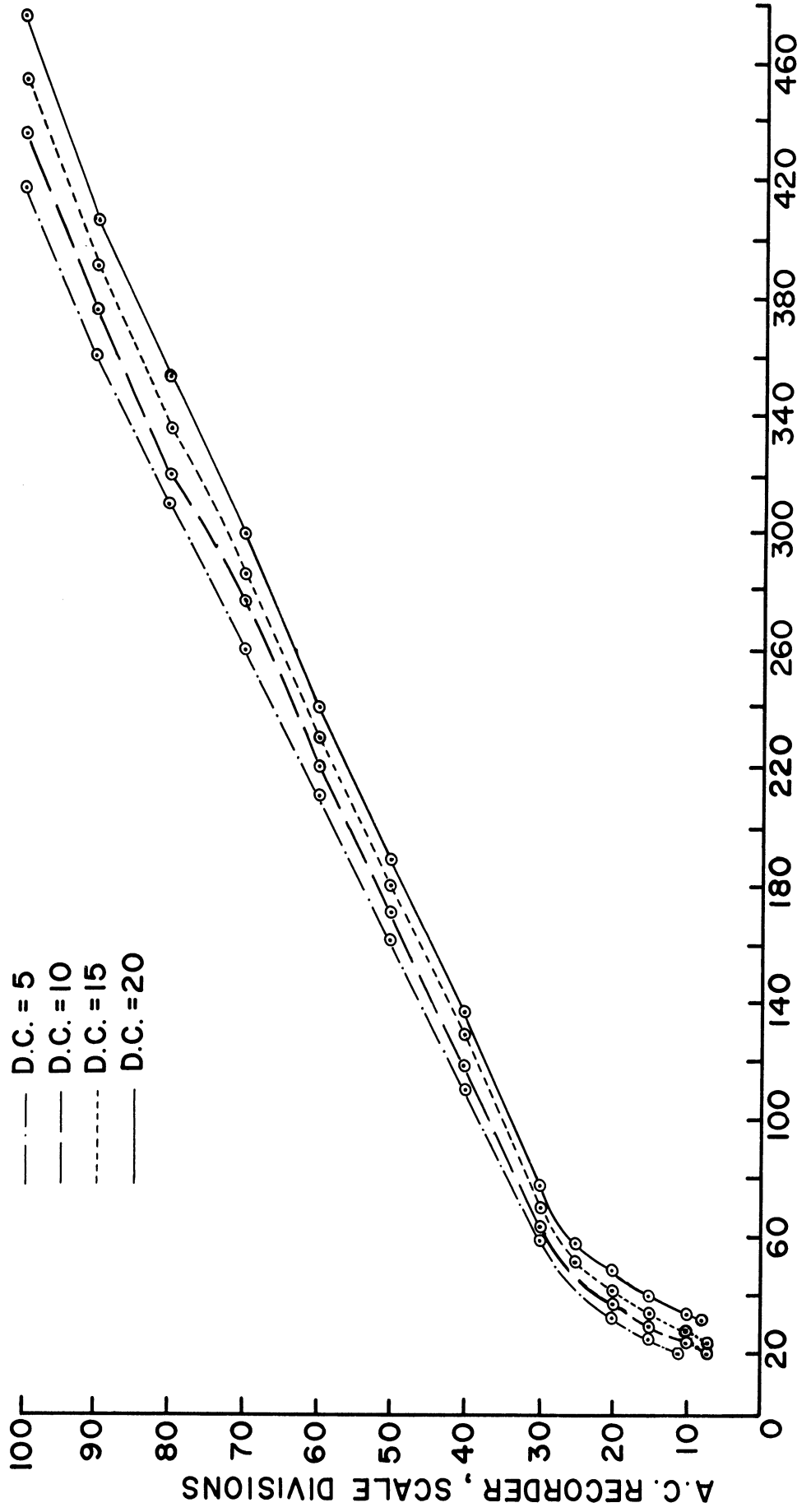

Figure 23. Calibration Curve for the A. C. Recorder Reading (Scale Divisions) vs A. C. Level (Millivolts).

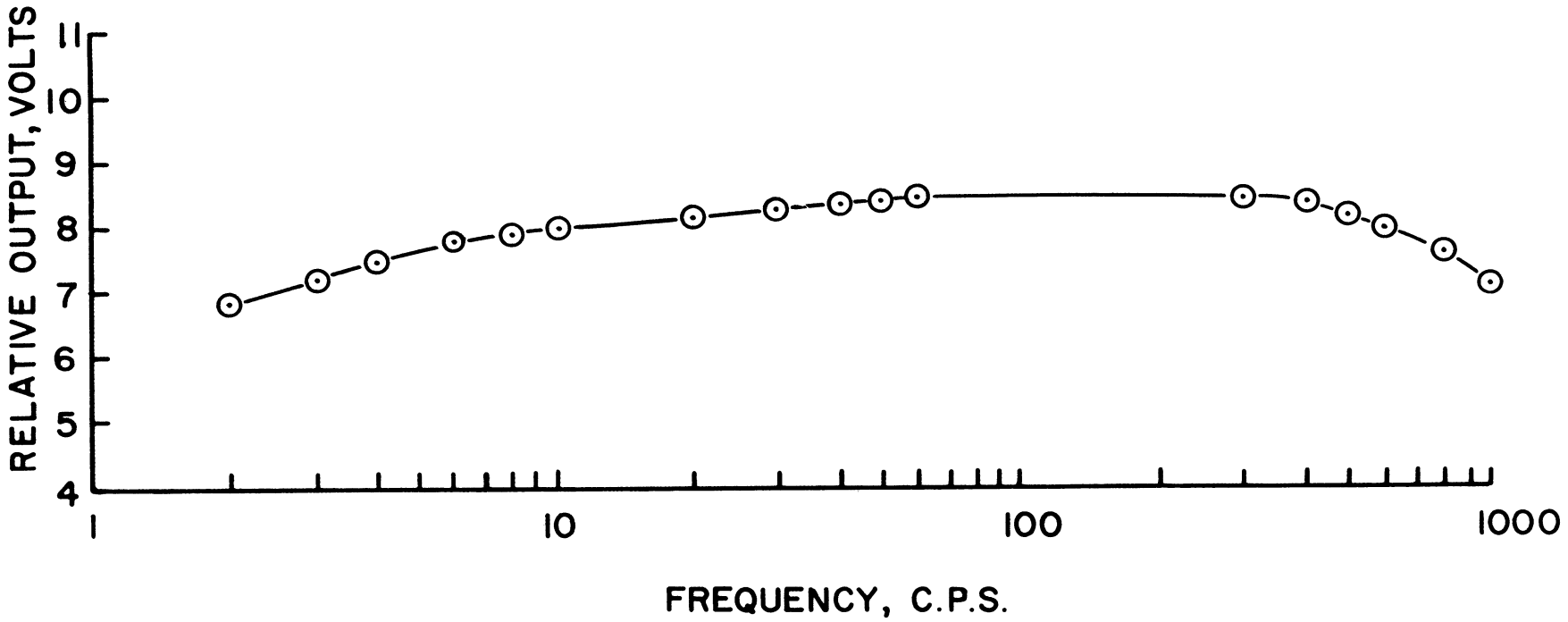

Figure 24. Frequency Response Curve for the A. C. Amplifier for Various D. C. Levels.

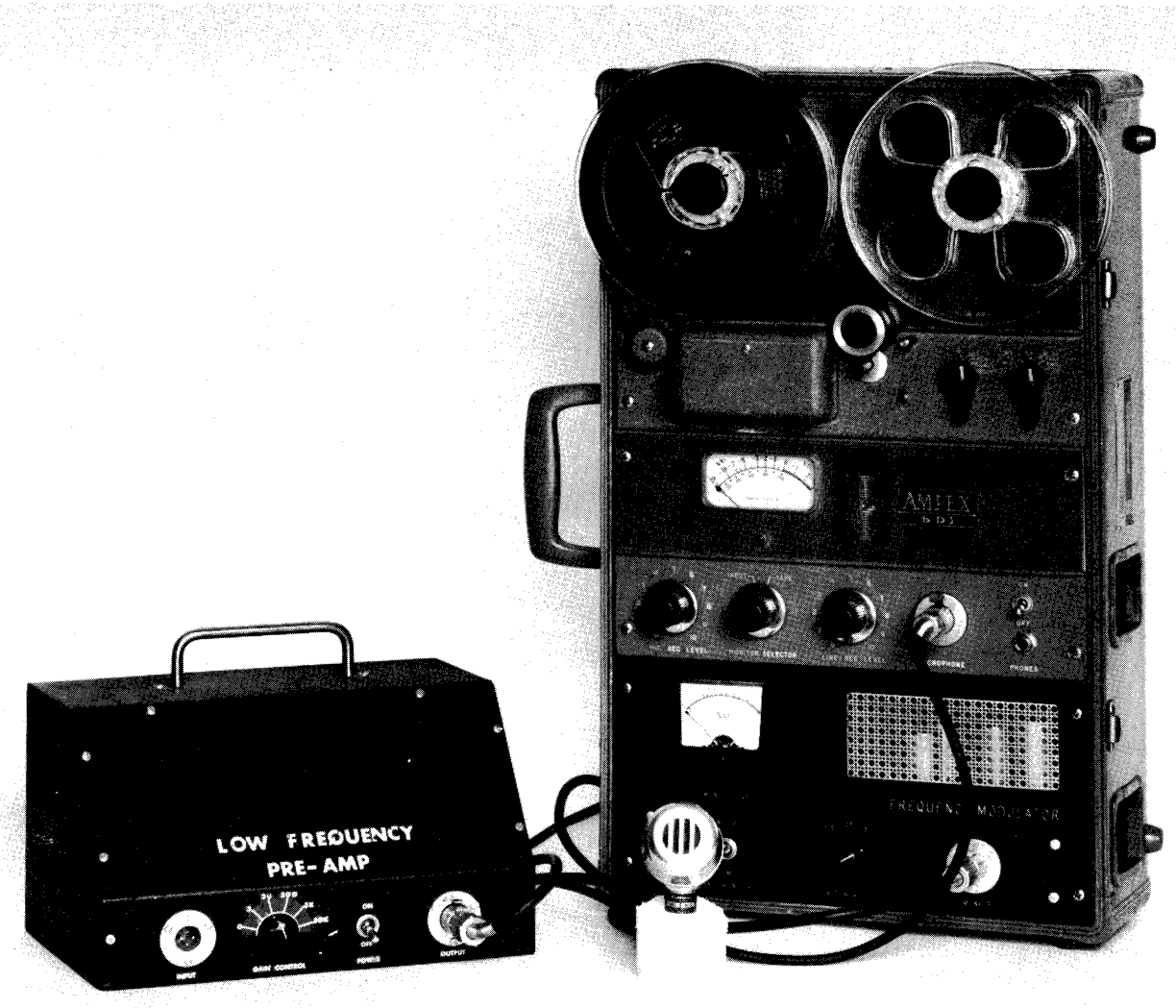

Figure 25. Frequency Modulation Ampex 601 Tape Recorder and Low-frequency Pre-amplifier.

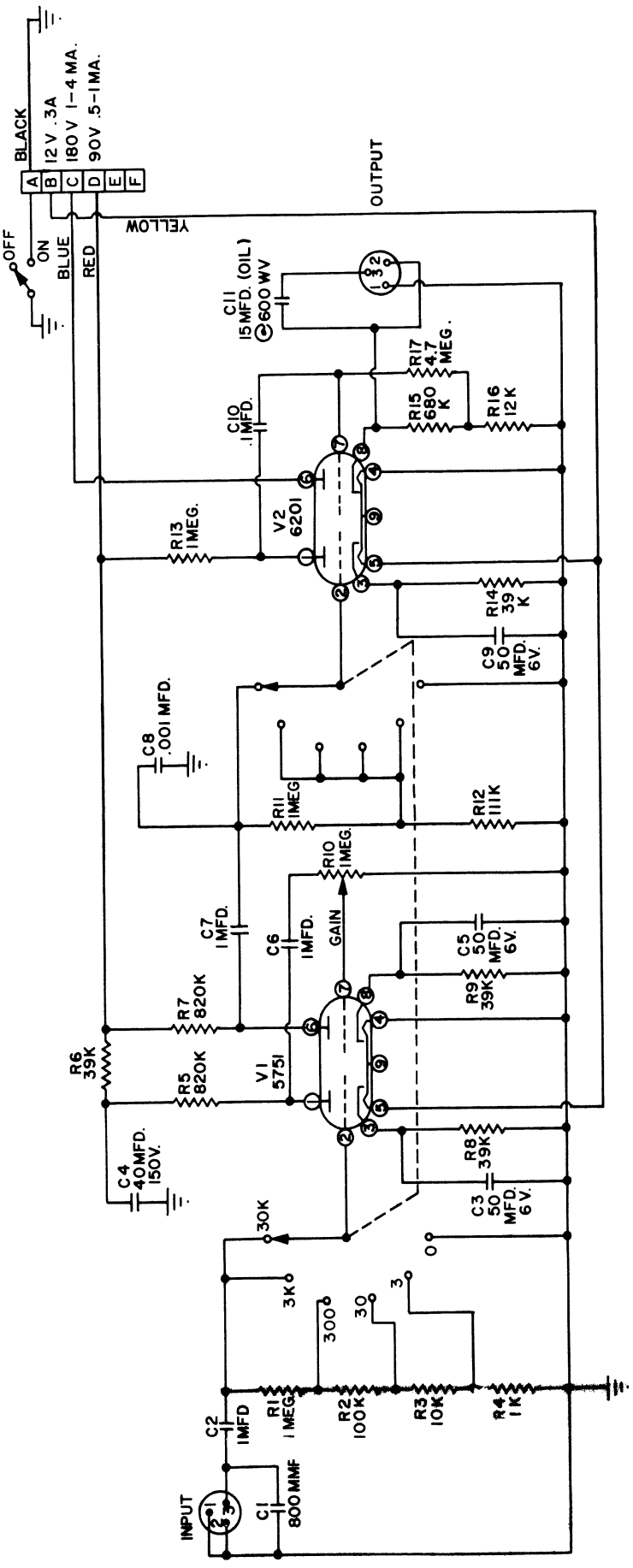

Figure 26. Schematic Circuit Diagram of Low-frequency Pre-amplifier for Ampex 601 Magnetic Tape Recorder.

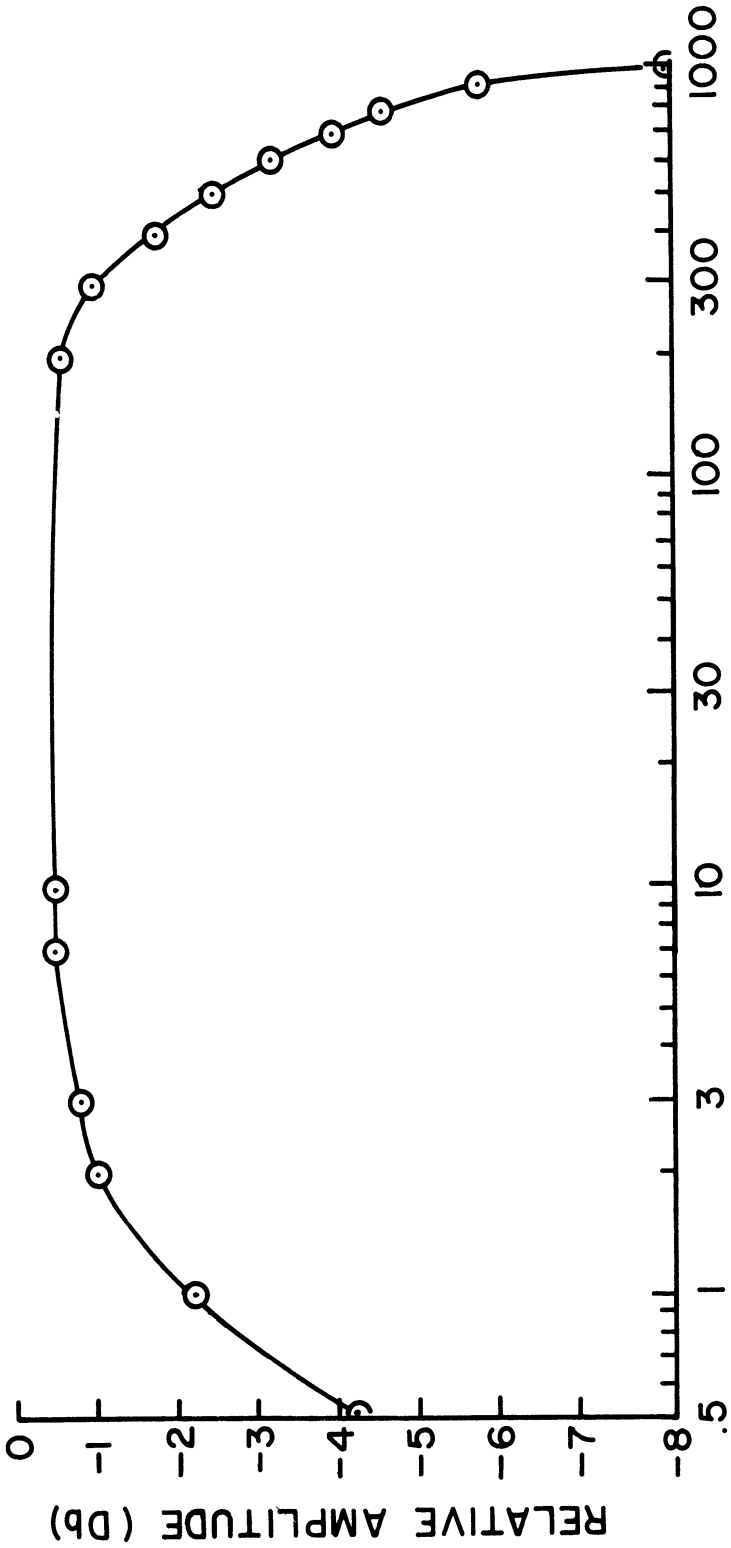

Figure 27. Frequency Response Curve for the Low-frequency Pre-amplifier.

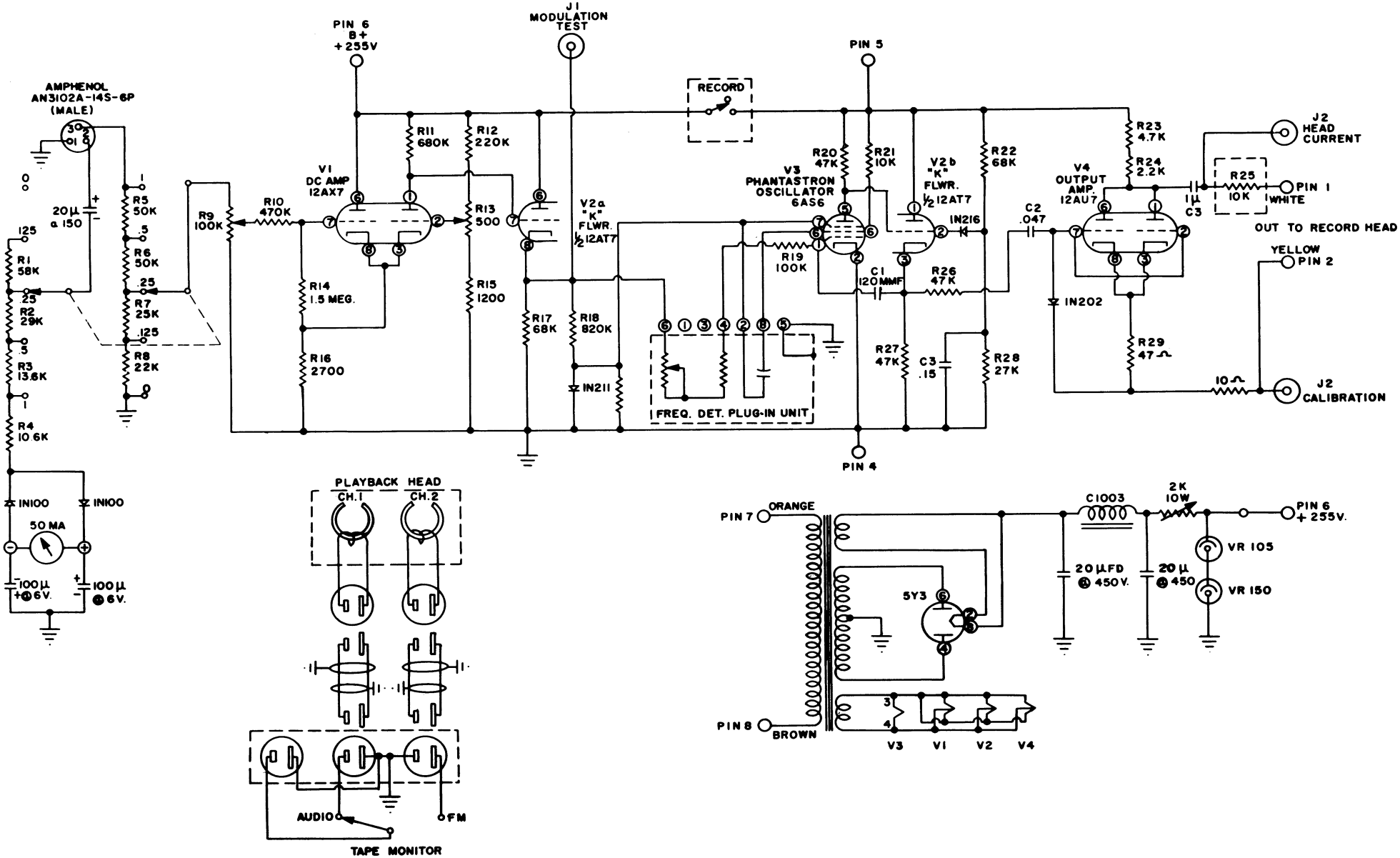

Figure 28. Schematic Circuit Diagram of the F-M Record Module for the Ampex 601 Magnetic Tape Recorder.

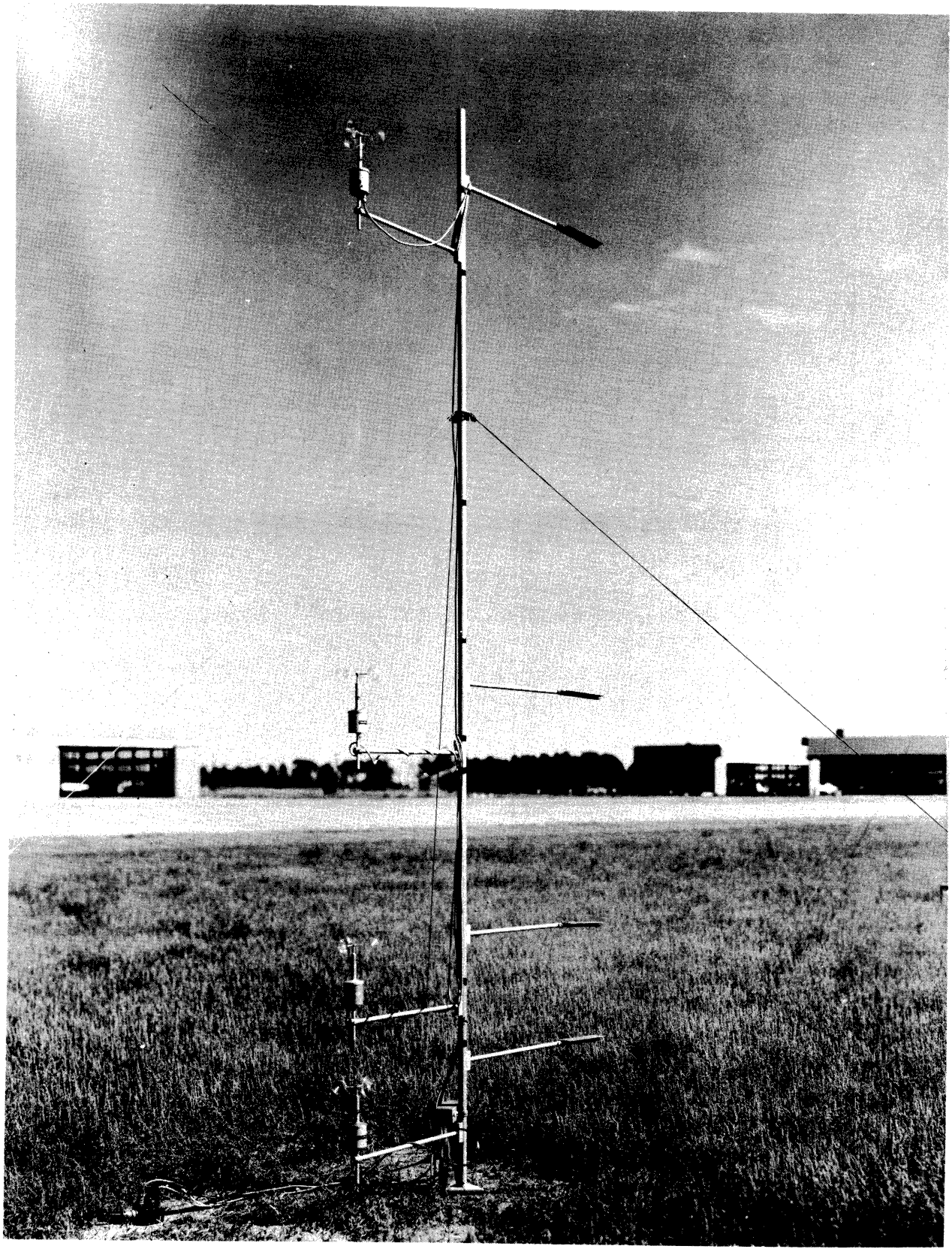

Figure 29. Micrometeorological Profile Mast with Anemometers and Shielded Thermocouples at Four Levels.

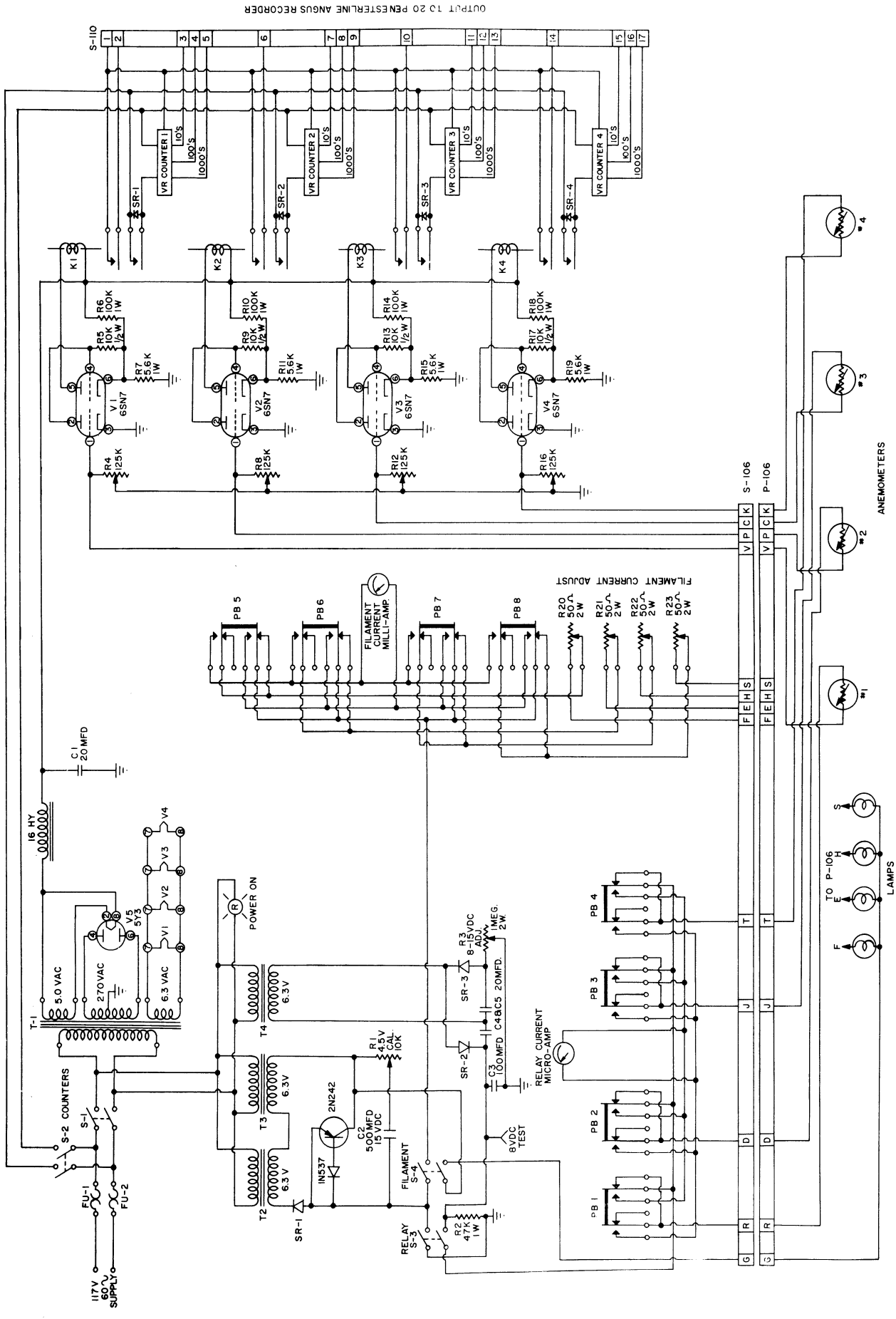

Figure 30. Schematic Circuit Diagram of Wind Profile Recording System.

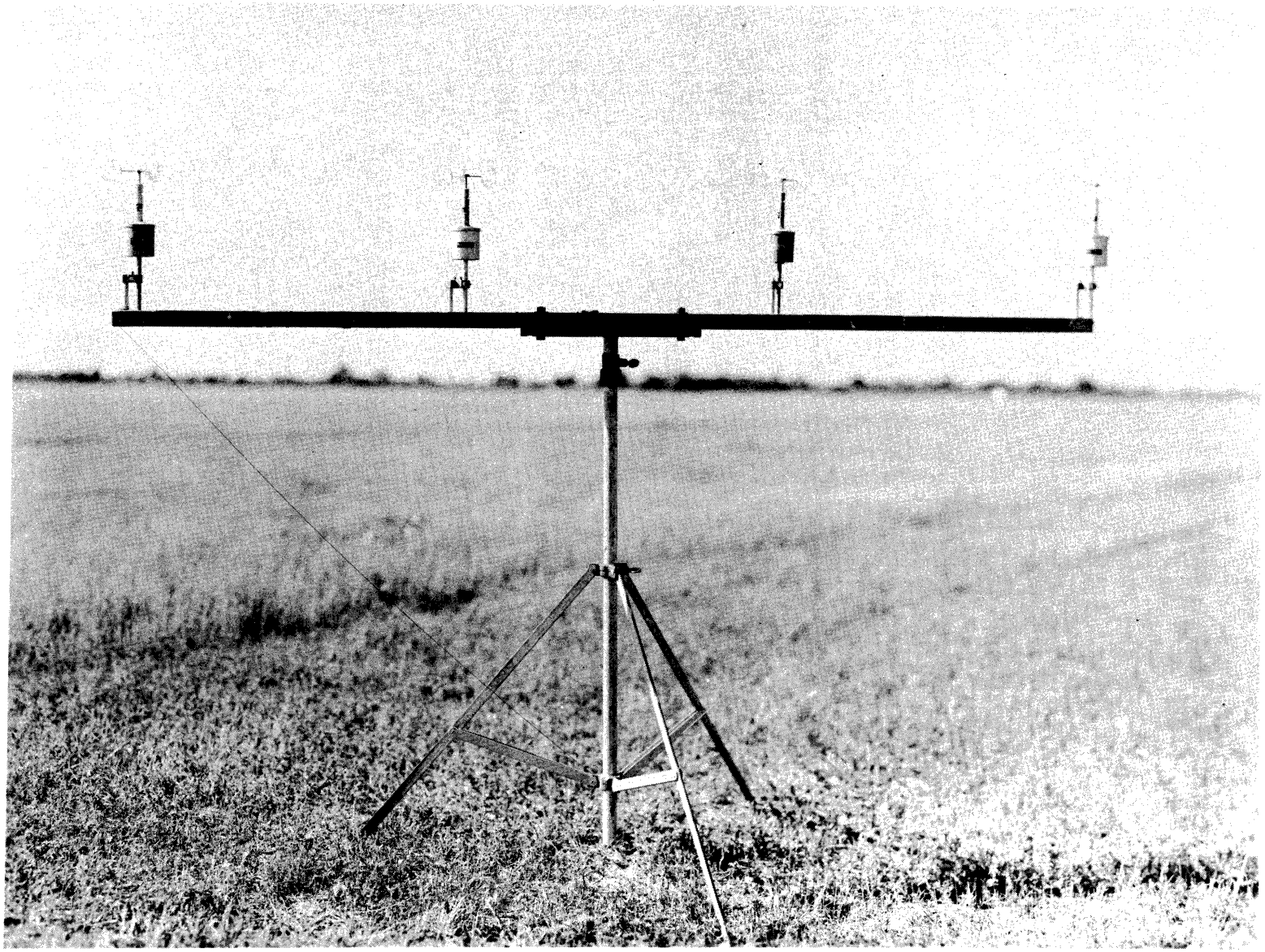

Figure 31. Anemometer Comparison Technique.

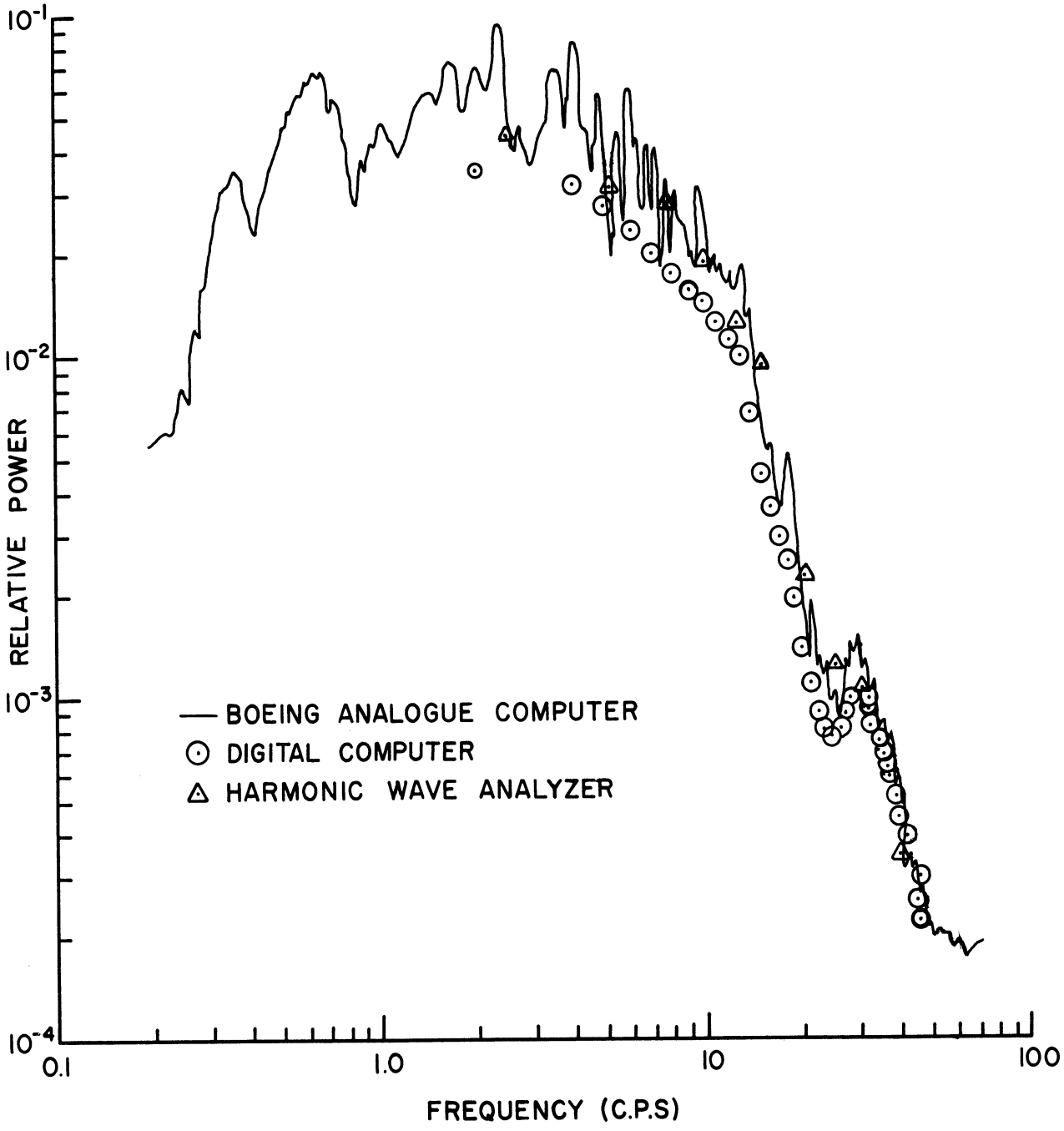

Figure 32. Results of Three Methods of Spectral Analysis.

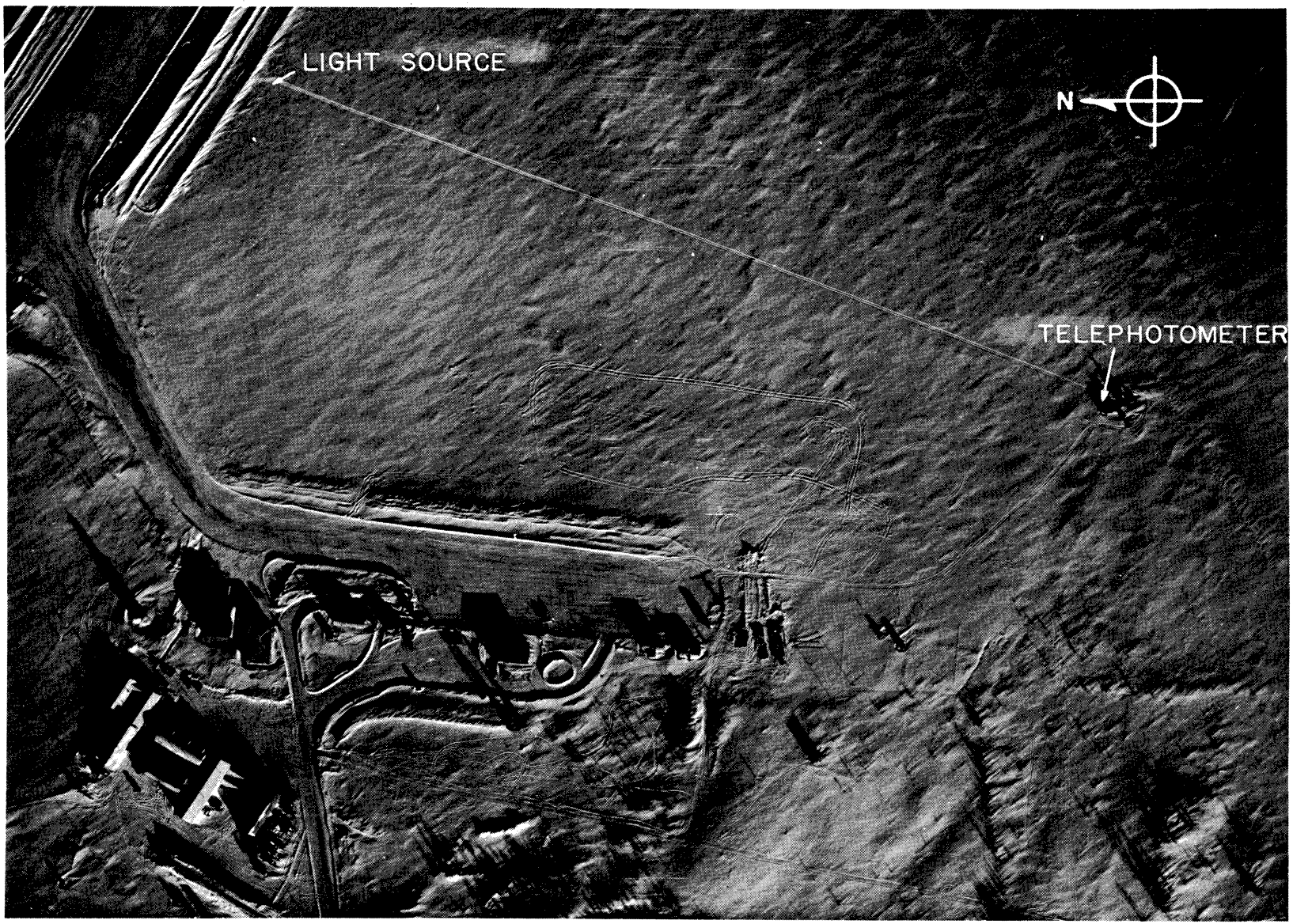

Figure 33. Keweenaw Field Station Experiment Site.

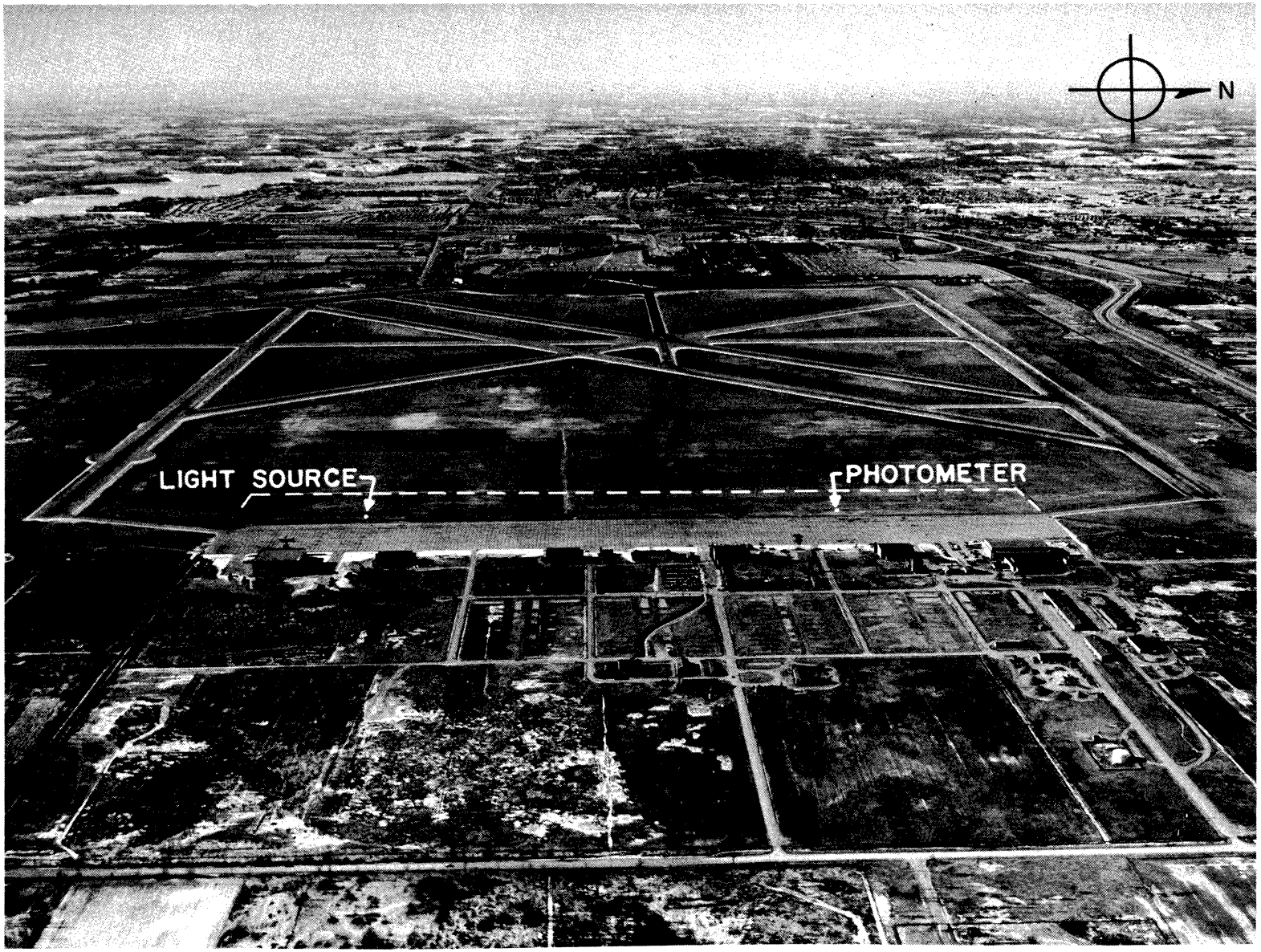

Figure 34. Willow Run Airport Experiment Site.

REFERENCES

Batchelor, G. K., 1959: Discussion of Paper, J. Geophys. Res., 64(3), p. 2046.

Clark, R. D. M., 1953: "An Investigation of Certain Short-period Atmospheric Micro-oscillations," J. Meteor., 10, 179-186.

Davidson, B., and M. L. Barad, 1956: "Some Comments on the Deacon Wind Profile," Trans. Am. Geophys. Union, 37, 168-175.

Ellison, T. H., 1957: "Turbulent Transport of Heat and Momentum from an Infinite Rough Plane," J. Fluid Mech., 2(5), 456-466.

Fleagle, R. G., 1950: "The Optical Measurement of Lapse Rate," Bull. Am. Met. Soc., 31, 2, 51-55.

Fritz, N. A., 1928-30: "Essai de determination experimentale de la progression a donner a l'echelle d'acuite visuelle," Bul. Soc. Belge. Opthal., 60, 58-66.

Gordon, D. A., 1959: "The Optical Design of Night Binoculars," Unpubl. Rpt., Univ. of Mich. WRL Labs.

Gurvich, A. S., V. I. Tatarski, and L. P. Cvang, 1958: "An Experimental Research on the Statistical Characteristics of Scintillation of a Light Source at Ground Level," (Translation by E. R. Hope), Dok. Akad. Nauk, SSSR, 123(4), 655-658.

Lettau, H. H., 1957: "Computation of Richardson numbers, Classification of Wind Profiles, and Determination of Roughness Parameters," Exp. the Atmos. First Mile, New York, Pergamon Press, Inc., 1, 157-167.

Long, R. R., 1959: "The Motion of Fluids with Density Stratification," J. Geophys. Res., 64(3), 2151-2163.

McLaughlin, R. and J. Prout, 1959: "A Portable Seismic Magnetic Tape Recorder," Earthquake Notes, 30, 26-33.

Mikesell, A. H., H. A. Hoag, and J. S. Hall, 1951: "The Scintillation of Starlight," J. Opt. Soc. America, 41(10), 689-695.

Parks, J. K., 1960: "A Comparison of Power Spectra of Ocean Waves Obtained by an Analog and a Digital Method," J. Geophys. Res., 65(5), 1557-1563.

Perepelkina, A. V., 1957: "Some Results of the Investigation of Turbulent Fluctuations of Temperature and the Vertical Component of Wind Velocity," (Translation by A. Nurklik), J. Acad. Sci., Geophys. Ser., 6, 765-778.

Portman, D. J., 1957: "Shielded Thermocouples," Exp. the Atmos. First Mile, New York, Pergamon Press, Inc., 1, 157-167.

_____, Some Heat Transfer Characteristics of Two Thermocouple Probes, Univ. of Mich., O. R. A. Rpt. in prep.

Richardson, L. F., 1920: "The Supply of Energy from and to Atmospheric Eddies," Proc. Roy. Soc. London, A, 97, 354-373.

Siedentopf, von H., and F. Wisshak, 1948: "Die Szintillation der Strahlung Terrestrischer Lichtquellen und ihr Gang mit der Tageszeit," Optik, 3(5/6), 430-433.

Stewart, R. W., 1959: "The Natural Occurrence of Turbulence," J. Geophys. Res., 64(3), 2112-2115.

Sutton, O. G., 1953: Micrometeorology, New York, McGraw-Hill.

Tatarski, V. I., A. S. Gurvich, M. A. Kallistratova, and L. V. Terenteva, 1958: "The Influence of Meteorological Conditions on the Intensity of Light Scintillation Near the Earth's Surface," J. Soviet Astron., 2, 578-581.

Tatarski, V. I., 1961: Wave Propagation in a Turbulent Medium, (Translation by R. A. Silverman), New York, McGraw-Hill.

Taylor, G. I., 1936: "The Mean Value of the Fluctuation of Pressure and Pressure Gradient in a Turbulent Fluid," Proc. Cambridge Phil. Soc., 32, 380-384.

Townsend, A. A., 1958: "Turbulent Flow in a Stably Stratified Atmosphere," J. Fluid Mech., 3, 361-372.

MICROMETEOROLOGICAL AND SCINTILLATION DATA

February 3, 1960

Time, EST	Anemometer Revolutions				Temperature Difference, °C			Wind Dir. Degrees	% Mod.
2 min. period, ending	0.5m	1m	2m	4m	1m-0.5m	2m-0.5m	4m-0.5m		
2128	MSG	MSG	MSG	MSG	.5	1.0	1.8	185	40
2130	252	285	320	"	.4	1.0	1.5	"	41
2132	232	262	295	"	.6	.8	1.7	"	39
2134	269	298	324	"	.5	.6	1.2	"	38
2136	235	266	301	"	.4	1.0	1.3	"	36
2138	242	270	301	"	.4	.7	1.3	"	37
2140	223	250	290	"	.4	.8	1.7	"	36
2142	220	249	291	"	.4	.8	1.2	"	36
2144	MSG	MSG	MSG	"	.4	1.0	1.4	"	36
2146	212	239	272	"	.5	.7	1.4	195	36
2148	203	230	269	"	.4	1.0	1.3	"	37
2150	229	251	291	"	.4	.6	1.0	"	35
2152	237	258	300	"	.4	.7	1.0	"	35
2154	213	233	270	"	.4	.7	1.2	"	34
2156	186	210	250	"	.4	.7	1.3	"	34
2158	224	248	291	"	.4	.7	.8	"	35
2200	215	235	274	"	.2	.6	1.1	"	34
2202	MSG	MSG	MSG	"	.4	.6	1.2	"	35
2204	"	"	"	"	.2	.7	1.0	"	36
2206	"	"	"	"	.4	.8	1.0	"	33
2208	"	"	"	"	.4	.6	1.0	"	35
2210	258	286	330	"	.4	.6	1.1	"	35
2212	263	288	327	"	.2	.6	1.0	"	34
2214	250	276	313	"	.4	.7	1.1	"	33
2216	219	241	281	"	.4	.8	.8	"	35
2218	244	261	296	"	.2	.6	1.0	"	33
2220	227	248	291	"	.2	.6	1.1	"	33
2222	260	284	328	"	.2	.5	1.0	"	32
2224	257	285	334	"	.2	.6	.8	"	33
2226	243	267	317	"	.4	.6	.8	"	34
2228	260	292	339	"	.4	.5	1.0	"	33
2230	226	256	300	"	.4	.6	1.0	"	35
2232	234	265	297	"	.2	.5	1.0	"	34
2234	226	259	300	"	.2	.6	.8	"	34
2236	218	239	275	"	.2	.5	1.1	200	34
2238	228	255	298	"	.2	.6	1.0	"	33
2240	224	254	300	"	.2	.5	.8	"	33
2242	237	271	311	"	.2	.5	.6	"	30
2244	209	238	272	"	.2	.5	.7	"	28
2246	204	243	281	"	.1	.5	.6	"	28
2248	218	256	298	"	.2	.5	.7	"	28
2250	272	312	358	"	.2	.4	.6	"	28
2252	237	278	323	"	.2	.5	.6	"	27

February 3, 1960 (Continued)

Time, EST	Anemometer Revolutions				Temperature Difference, °C			Wind Dir. Degrees	% Mod.
2 min. period, ending	0.5m	1m	2m	4m	1m-0.5m	2m-0.5m	4m-0.5m		
2254	263	302	340	MSG	.2	.4	.7	200	27
2256	292	329	376	"	.2	.5	.5	"	27
2258	249	286	324	"	.2	.4	.5	"	27
2300	267	297	338	"	.2	.4	.7	"	27
2302	262	306	353	"	.2	.5	.5	"	27
2304	270	311	356	"	.2	.5	.5	"	26
2306	260	302	344	"	.1	.2	.5	"	25
2308	279	320	367	"	.2	.4	.6	"	25
2310	279	327	362	"	.2	.4	.6	"	26
2312	262	307	350	"	.2	.5	.6	"	26
2314	281	327	379	"	.1	.4	.5	"	26
2316	280	326	368	"	.1	.4	.5	"	25
2318	281	322	379	"	.2	.5	.6	"	25
2320	299	339	384	"	.2	.5	.6	"	25
2322	274	311	366	"	.2	.4	.6	"	26
2324	292	328	379	"	.2	.5	.7	"	26
2326	MSG	MSG	MSG	"	.1	.5	.6	"	28

February 4, 1960

1546	146	171	208	MSG	.4	1.0	1.5	090	43
1548	155	185	230	"	.5	1.1	1.3	090	47
1550	148	176	216	"	.5	1.0	1.9	090	45
1552	158	183	230	"	.5	1.1	1.7	085	45
1554	146	175	218	"	.5	1.2	1.9	085	48
1556	131	156	193	"	.5	1.1	1.5	090	43
1558	136	163	201	"	.5	1.1	1.5	090	41
1600	127	151	186	"	.6	1.2	1.8	095	38
1602	118	145	181	"	.6	1.2	2.0	090	41
1604	124	151	191	"	.6	1.3	2.1	095	41
1606	117	140	173	"	.7	1.2	1.8	100	41
1608	105	130	167	"	.6	1.3	2.0	100	38
1610	127	152	187	"	.5	1.2	2.0	095	44
1612	128	154	185	"	.6	1.1	1.5	095	42
1614	131	156	193	"	.5	1.0	1.7	100	44
1616	125	149	181	"	.7	1.1	1.7	100	42
1618	125	146	181	"	.6	1.0	1.7	095	42
1620	119	142	180	"	.6	1.2	1.9	095	42
1622	117	140	180	"	.6	1.4	1.9	090	44
1624	131	162	199	"	.6	1.0	1.9	090	44
1626	147	175	217	"	.5	1.1	1.8	090	45
1628	147	175	215	"	.6	1.3	2.0	090	45
1630	121	150	190	"	.6	1.3	2.1	090	42

February 4, 1960 (Continued)

Time, EST	Anemometer Revolutions				Temperature Difference, °C			Wind Dir. Degrees	% Mod.
2 min. period, ending	0.5m	1m	2m	4m	1m-0.5m	2m-0.5m	4m-0.5m		
1632	106	132	175	MSG	.7	1.3	2.2	090	36
1634	107	136	177	"	.7	1.4	2.2	085	38
1636	111	137	184	"	.7	1.4	2.4	085	35
1638	118	145	185	"	.7	1.7	2.4	085	35
1640	101	131	171	"	.8	1.8	2.6	085	35
1642	89	120	160	"	1.0	1.9	2.7	095	33
1644	91	122	162	"	.8	2.1	2.7	095	33
1646	98	134	175	"	1.1	2.1	2.5	090	38
1648	89	122	166	"	1.1	2.5	2.9	090	40
1650	68	101	162	"	1.3	2.9	3.7	090	38
1652	68	96	148	"	1.1	2.5	3.3	090	45
1654	72	103	147	"	1.1	1.8	3.4	085	45
1656	108	136	174	"	1.0	2.2	2.6	085	31
1658	81	113	157	"	1.1	2.4	3.3	085	35
1700	69	95	130	"	1.1	2.1	2.9	085	33
1702	47	71	110	"	.6	1.3	2.8	080	31
1704	38	68	120	"	1.0	1.9	3.1	090	31
1706	39	58	98	"	.6	1.1	2.8	090	29
1708	40	61	97	"	.8	1.8	3.4	095	35
1710	46	65	113	"	1.0	2.5	3.4	090	33
1712	40	65	109	"	1.2	2.4	3.1	090	27
1714	10	40	85	"	.1	1.1	2.4	095	25
1716	20	50	98	"	1.1	2.5	3.3	100	24
1718	51	89	126	"	1.7	2.8	3.4	"	29
1720	51	76	112	"	1.7	3.4	3.6	"	31
1722	53	73	115	"	1.1	2.8	4.0	"	33
1724	61	87	130	"	1.7	3.3	3.9	"	38
1726	75	102	147	"	1.3	3.6	4.6	"	47
1728	73	108	165	"	1.5	4.2	4.8	"	55
1730	65	97	155	"	1.4	3.4	5.4	095	51
1732	70	97	140	"	1.2	2.7	4.7	085	49
1734	55	82	117	"	1.0	2.2	3.9	085	40
1736	43	74	126	"	1.2	2.1	4.3	095	35
1738	71	102	151	"	1.2	2.6	3.6	100	40
1740	88	120	161	"	1.3	2.5	3.4	100	29
1742	75	103	141	"	1.2	2.4	3.4	095	39
1744	75	108	149	"	1.4	2.4	3.1	090	39
1746	84	118	162	"	1.2	2.2	3.1	"	34
1748	95	122	168	"	1.0	2.2	3.1	"	40
1750	82	112	156	"	1.0	2.0	3.3	"	42
1752	84	110	148	"	1.0	2.0	2.8	"	43
1754	94	122	159	"	.7	1.8	2.6	095	47
1756	98	124	167	"	.6	1.5	2.6	095	44
1758	106	131	172	"	.7	1.7	2.7	095	44

February 4, 1960 (Continued)

Time, EST	Anemometer Revolutions				Temperature Difference, °C			Wind Dir. Degrees	% Mod.
2 min. period, ending	0.5m	1m	2m	4m	1m-0.5m	2m-0.5m	4m-0.5m		
1800	101	130	170	MSG	.7	1.7	2.6	095	43
1802	107	134	178	"	.7	1.8	2.9	100	45
1804	115	143	182	"	.7	1.5	2.5	100	45
2132	MSG	MSG	MSG	MSG	.1	.2	.2	090	13
2134	"	"	"	"	.1	.2	.2	090	14
2136	"	"	"	"	.1	.2	.4	095	13
2138	"	"	"	"	.1	.2	.2	095	14
2140	"	"	"	"	.1	.2	.4	095	14
2142	"	"	"	"	.1	.2	.2	090	13
2144	"	"	"	"	.1	.2	.4	085	14
2146	"	"	"	"	.1	.2	.4	"	15
2148	"	"	"	"	.1	.4	.4	"	16
2150	"	"	"	"	.1	.5	.4	"	18
2152	"	"	"	"	.2	.4	.5	"	18
2154	"	"	"	"	.2	.4	.5	"	20
2156	"	"	"	"	.2	.5	.6	"	20
2158	"	"	"	"	.2	.4	.6	090	20
2200	"	"	"	"	.1	.4	.7	095	21
2202	"	"	"	"	.1	.4	.6	"	20
2204	"	"	"	"	.1	.4	.5	"	20
2206	"	"	"	"	.1	.4	.7	"	MSG
2208	"	"	"	"	.1	.4	.6	"	"
2210	"	"	"	"	.2	.4	.5	"	"
2212	"	"	"	"	.2	.2	.6	"	"
2214	"	"	"	"	.2	.5	.6	090	20
2216	"	"	"	"	.2	.4	.6	085	20
2218	"	"	"	"	.2	.5	.7	085	20
2220	"	"	"	"	.1	.4	.6	085	20
2222	"	"	"	"	.1	.4	.6	095	19
2224	"	"	"	"	.1	.2	.5	095	21
2226	"	"	"	"	.1	.2	.4	095	19
2228	"	"	"	"	.1	.2	.4	105	18
2230	"	"	"	"	.1	.2	.2	110	18
2232	"	"	"	"	.1	.2	.4	110	16
2234	"	"	"	"	.1	.2	.2	105	15
2236	"	"	"	"	.1	.2	.2	105	15
2238	"	"	"	"	.1	.2	.2	100	13
2240	"	"	"	"	.1	.2	.4	095	12
2242	"	"	"	"	.1	.2	.4	100	13
2244	"	"	"	"	.1	.2	.4	105	13
2246	"	"	"	"	.1	.2	.4	100	14

MICROMETEOROLOGICAL AND SCINTILLATION DATA

February 4, 1960 (Continued)

Time, EST	Anemometer Revolutions				Temperature Difference, °C			Wind Dir. Degrees	% Mod.
2 min. period, ending	0.5m	1m	2m	4m	1m-0.5m	2m-0.5m	4m-0.5m		
2248	MSG	MSG	MSG	MSG	.2	.2	.5	100	15
2250	"	"	"	"	.1	.5	.5	100	16
2252	"	"	"	"	.1	.4	.6	105	19
2254	"	"	"	"	.1	.2	.5	105	20
2256	"	"	"	"	.1	.2	.4	105	17
2258	"	"	"	"	.1	.2	.5	105	16
2300	"	"	"	"	.1	.4	.4	105	16

February 5, 1960

1528	MSG	MSG	MSG	MSG	0	0	0	320	3
1530	"	"	"	"	"	"	"	325	"
1532	"	"	"	"	"	"	"	320	"
1534	"	"	"	"	"	"	"	320	"
1536	"	"	"	"	"	"	"	320	"
1538	"	"	"	"	"	"	"	315	"
1540	140	150	164	176	"	"	"	315	"
1542	127	137	147	155	"	"	"	310	"
1544	139	152	162	173	"	"	"	310	"
1546	126	137	148	154	"	"	"	305	"
1548	131	145	161	174	"	"	"	310	"
1550	131	142	155	169	"	"	"	315	4
1552	137	153	165	175	"	"	"	310	3
1554	148	164	177	194	-0.1	"	-0.1	310	4
1556	150	164	177	195	0	"	0	320	"
1558	138	*154	164	MSG	-0.1	"	"	315	"
1600	133	*148	163	"	0	"	"	310	"
1602	126	*139	154	"	"	"	"	315	"
1604	142	*150	165	"	"	"	"	325	"
1606	148	*159	172	"	"	"	"	325	"
1608	162	*177	191	"	"	"	"	325	MSG
1610	139	*150	158	"	"	"	"	315	4
1612	124	*135	153	"	"	"	"	320	"
1614	144	*160	174	"	"	"	"	315	"
1616	129	*140	152	"	"	"	"	325	"
1618	149	*169	185	"	-0.1	"	"	320	"
1620	146	*162	174	"	0	"	"	320	"
1622	196	*212	231	"	"	"	"	325	"
1624	171	*190	208	"	"	"	"	320	"
1626	173	*188	202	"	"	0.1	"	320	"

*Interpolated during near adiabatic conditions

February 5, 1960 (Continued)

Time, EST	Anemometer Revolutions				Temperature Difference, °C			Wind Dir. Degrees	% Mod.
2 min. period, ending	0.5m	1m	2m	4m	1m-0.5m	2m-0.5m	4m-0.5m		
1628	196	*213	229	MSG	0	0.1	0	310	4
1630	159	*172	184	"	"	0	"	305	"
1632	128	*140	152	"	"	"	"	305	"
1634	121	*131	142	"	"	"	"	310	"
1636	133	*148	156	"	"	"	"	305	"
1638	125	*136	147	"	"	0.1	0.1	310	"
1640	149	*162	174	"	"	0	0	310	"
1642	157	*171	184	"	"	0.1	0	315	5

*Interpolated during near adiabatic conditions.

February 9, 1960

1118	310	341	369	400	-.03	-.05	-.1	015	5
1120	283	311	333	358	-.05	-.03	-.05	360	"
1122	270	298	318	340	0	0	-.05	005	"
1124	295	324	345	364	0	-.03	-.05	015	"
1126	271	299	325	345	0	-.03	-.08	005	"
1128	266	290	308	330	0	0	-.08	010	"
1130	285	314	340	358	0	-.03	-.05	010	"
1132	342	376	403	431	-.03	-.05	-.1	025	"
1134	348	385	414	437	-.05	-.05	-.1	020	"
1136	276	299	315	328	-.05	-.03	-.05	355	"
1138	267	296	318	327	0	0	-.05	015	"
1140	267	307	320	MSG	-.03	-.05	-.1	020	MSG
1142	248	272	290	"	-.03	-.03	-.15	020	5
1144	280	310	333	"	-.05	-.05	-.1	025	4
1146	294	327	352	"	0	-.03	-.08	015	4
1148	287	314	337	"	0	-.03	-.08	010	5
1150	309	341	362	"	0	.03	-.03	360	5
2122	173	192	209	225	0	.05	.05	045	5
2124	170	189	207	226	"	.05	.05	045	5
2126	186	210	230	262	"	.05	.05	050	5
2128	192	213	234	261	"	.05	.05	050	6
2130	155	176	195	219	"	.05	.05	055	6
2132	175	199	223	248	"	.05	.05	045	7
2134	170	193	213	242	"	.03	.03	050	7
2136	181	202	222	255	"	.03	.03	050	8
2138	209	236	259	284	"	.05	.05	055	8
2140	194	221	246	274	"	.05	.05	055	8

February 9, 1960 (Continued)

Time, EST	Anemometer Revolutions				Temperature Difference, °C			Wind Dir. Degrees	% Mod.
2 min. period, ending	0.5m	1m	2m	4m	1m-0.5m	2m-0.5m	4m-0.5m		
2142	173	194	219	241	0	.03	.03	055	7
2144	182	203	231	255	"	.05	.05	055	7
2146	173	195	220	241	"	.05	.05	060	6
2148	180	205	222	238	"	.05	.05	060	6
2150	162	182	200	212	"	.03	.05	065	6
2152	152	173	203	229	"	.03	.03	060	6
2154	193	220	244	264	"	.05	.05	065	6
2156	268	299	326	354	"	.05	.03	055	5
2158	258	286	317	348	"	.05	.05	055	5
2200	290	326	361	398	"	.05	.05	055	6
2202	243	269	294	320	"	.05	.05	050	5
2204	241	275	310	347	"	.05	.05	040	5
2206	341	377	409	450	"	.05	.08	040	5
2208	359	400	440	487	"	.05	.08	040	5
2210	313	348	375	416	"	.05	.05	035	5
2212	314	348	378	417	"	.03	.08	035	5
2214	323	361	400	440	"	.05	.05	035	6
2216	362	403	447	494	"	.05	.05	040	6
2218	363	404	431	472	"	.05	.05	045	6
2220	336	373	408	448	"	.05	.05	050	6
2222	302	335	362	398	"	.05	.05	055	6
2224	272	305	341	378	"	.05	.05	055	7
2226	251	281	311	342	"	.05	.05	065	6
2228	200	230	258	283	"	.05	.05	065	6
2230	209	232	261	283	"	.05	.05	070	6

February 12, 1960

1916	221	245	264	290	.1	.2	.2	300	MSG
1918	189	206	230	256	.1	.2	.3	295	12
1920	179	200	225	256	.1	.3	.4	295	13
1922	178	198	218	235	.1	.3	.3	295	14
1924	167	182	203	MSG	.2	.3	.5	315	17
1926	205	228	245	"	.1	.3	.4	335	19
1928	191	212	235	"	.2	.2	.6	330	20
1930	171	188	204	"	.2	.4	.6	315	21
1932	103	120	139	"	.2	.6	.7	310	21
1934	99	113	130	144	.5	.6	.8	310	20
1936	77	91	110	119	.4	.8	1.0	320	19
1938	56	68	81	93	.5	.6	.9	320	18
1940	70	82	92	108	.2	.8	.7	335	19
1942	MSG	MSG	MSG	MSG	.5	.7	.9	335	20
1944	42	54	60	76	.7	1.1	1.5	335	18

February 12, 1960 (Continued)

Time, EST	Anemometer Revolutions				Temperature Difference, °C			Wind Dir. Degrees	% Mod.
2 min. period, ending	0.5m	1m	2m	4m	1m-0.5m	2m-0.5m	4m-0.5m		
1946	36	49	64	76	.8	1.1	.9	330	17
1948	47	62	77	88	1.0	1.0	1.4	330	15
1950	48	61	72	85	.1	1.2	1.4	340	15
1952	61	75	88	102	.7	1.0	1.4	340	21
1954	62	78	96	115	.6	1.3	1.0	335	25
1956	88	103	114	128	.7	1.1	1.5	330	25
1958	70	88	103	124	1.2	1.1	2.0	315	26
2000	74	90	113	134	.8	1.4	2.0	315	26
2002	58	77	99	120	.7	1.9	2.4	320	24
2004	56	77	94	114	1.3	1.9	1.9	325	25
2006	73	94	113	135	1.3	1.7	2.3	320	26
2008	77	97	112	132	1.1	1.7	2.1	305	28
2010	73	96	115	135	1.0	2.1	2.6	300	31
2012	69	83	102	123	1.0	1.4	1.7	300	30
2014	67	79	92	104	.8	1.3	2.0	270	24
2016	67	79	102	115	1.0	1.5	3.0	245	22
2018	83	90	110	121	.8	2.2	3.4	245	25
2020	54	72	92	122	.7	1.7	2.9	230	22
2022	61	74	97	145	.7	1.5	2.8	225	21
2024	51	64	91	128	.6	1.5	2.8	220	20
2026	28	41	61	99	.7	1.9	2.8	215	18
2028	37	39	60	103	.5	1.9	2.9	220	23
2030	48	52	77	112	.8	3.0	4.2	225	23
2032	62	75	89	135	1.1	2.4	4.6	230	19
2034	49	66	98	132	1.1	2.6	5.3	235	22
2036	60	73	103	136	1.1	3.9	4.8	240	24
2038	53	75	99	160	1.2	2.6	5.1	240	20
2040	50	78	125	MSG	1.0	3.6	6.1	245	28
2042	73	103	174	"	.7	3.5	6.0	250	36
2044	137	173	232	"	1.0	5.0	5.1	245	35
2046	141	177	237	"	.8	4.6	5.2	250	37
2048	148	184	245	"	1.0	3.8	4.6	250	36
2050	149	176	226	"	.5	1.9	3.7	245	29
2052	138	162	206	275	.5	1.3	3.3	250	26
2054	116	151	192	243	.5	1.8	2.7	260	25
2056	91	111	149	200	.7	1.4	2.8	270	25
2058	78	106	139	187	1.0	2.1	3.5	275	22
2100	76	101	135	183	1.4	2.7	3.8	285	24
2102	77	106	150	200	1.2	2.5	3.6	285	24
2104	83	109	153	201	.8	2.1	2.9	285	21
2106	88	114	148	191	1.0	2.8	3 1	290	20
2108	76	103	139	178	1.2	2.0	2.6	300	20
2110	98	124	162	194	1.5	2.1	2.5	300	21

February 12, 1960 (Continued)

Time, EST	Anemometer Revolutions				Temperature Difference, °C			Wind Dir. Degrees	% Mod.
2 min. period, ending	0.5m	1m	2m	4m	1m-0.5	2m-0.5	4m-0.5m		
2112	93	116	147	176	.8	1.9	2.4	305	22
2114	95	119	152	187	1.0	1.7	2.1	305	MSG
2116	87	113	139	167	.8	1.7	2.5	300	"
2118	83	105	132	159	1.0	1.9	2.3	310	"
2120	68	92	121	143	1.2	2.2	2.9	300	"
2122	59	77	101	126	1.1	2.1	3.1	300	"
2124	57	75	106	131	1.1	2.9	3.7	300	"
2126	60	85	107	139	1.6	2.7	3.0	295	"
2128	60	87	113	141	1.8	2.1	3.1	290	"
2130	43	73	100	133	2.5	3.3	4.0	290	"
2132	49	67	101	134	1.4	3.3	4.3	295	"
2134	51	70	98	133	1.2	2.8	3.4	295	"
2136	53	64	79	110	1.3	1.4	3.6	300	"
2138	50	70	86	111	1.7	1.8	3.1	295	"
2140	49	71	91	109	2.0	3.0	4.2	290	25
2142	78	98	134	160	1.4	4.0	4.7	275	28
2144	79	106	162	195	.8	3.6	5.3	265	36
2146	66	84	128	179	1.2	2.8	4.8	275	34
2148	54	79	125	164	2.0	4.0	6.0	275	MSG
2218	33	83	123	148	3.1	5.5	6.2	320	29
2220	80	95	122	134	1.8	5.1	5.6	295	32
2222	92	108	130	169	1.0	2.1	3.9	275	29
2224	80	92	113	154	.6	1.4	2.9	280	23
2226	67	93	102	144	1.4	1.7	4.3	290	26
2228	66	103	133	165	2.2	3.1	4.7	285	26
2230	51	71	104	151	1.8	3.7	4.7	305	24
2232	39	49	80	121	1.2	3.6	5.1	310	25
2234	61	74	104	149	1.9	3.0	4.4	305	29
2236	64	91	119	156	2.8	3.6	5.8	300	29
2238	29	56	103	144	1.1	4.4	7.0	295	32
2240	57	94	132	169	2.1	5.4	6.7	290	32
2242	78	109	152	183	1.8	4.3	5.5	280	MSG
2244	85	111	147	183	1.2	3.6	5.8	285	34
2246	61	88	128	186	1.2	3.6	6.5	290	33
2248	75	106	143	180	2.2	3.9	5.4	310	38
2250	84	118	156	194	1.7	3.8	4.6	320	37
2252	98	128	158	190	1.7	2.7	3.4	315	37
2254	98	130	157	181	1.7	3.1	3.1	315	39
2256	95	124	153	185	1.7	2.2	3.1	310	43
2258	98	125	152	185	1.3	2.7	3.5	310	41
2300	90	120	148	178	1.9	2.8	3.6	305	39

February 12, 1960 (Continued)

Time, EST	Anemometer Revolutions				Temperature Difference, °C			Wind Dir. Degrees	% Mod.
2 min. period, ending	0.5m	1m	2m	4m	1m-0.5m	2m-0.5m	4m-0.5m		
2302	87	111	134	168	1.4	3.0	4.4	295	40
2304	86	114	144	168	1.5	4.4	5.8	290	40
2306	86	116	149	177	1.5	4.2	6.0	285	41
2308	101	128	165	192	1.0	3.0	4.8	280	39
2310	74	97	123	178	1.1	2.4	6.2	285	39
2312	55	90	135	169	1.9	4.6	6.7	300	30
2314	57	88	116	147	2.8	3.9	5.9	310	34
2316	50	98	132	157	2.9	6.0	6.3	315	38
2318	49	98	138	165	3.0	5.6	6.7	320	39
2320	76	114	149	176	2.8	4.8	4.8	320	36
2322	81	105	150	182	1.4	3.7	5.6	315	39
2324	60	89	132	165	2.8	5.4	7.1	310	38
2326	57	92	137	166	2.9	5.1	6.3	310	34
2328	72	105	132	164	2.4	4.3	4.5	315	37
2330	88	122	158	192	2.0	3.1	3.7	315	37
2332	88	109	147	180	2.0	3.9	4.7	305	35
2334	84	102	121	138	2.0	4.5	4.5	285	32
2336	95	123	146	187	1.1	2.5	4.4	275	29
2338	42	64	88	137	1.2	2.7	5.5	285	29
2340	26	51	83	116	1.2	2.5	6.0	295	29
2342	29	57	86	115	2.1	3.7	5.1	305	25
2344	19	45	66	84	2.2	4.3	5.3	310	21
2346	24	40	65	95	1.5	4.2	5.5	300	20
2348	13	41	71	111	2.2	5.0	6.0	305	23
2350	27	45	55	72	3.3	5.4	6.3	320	23
2352	10	33	47	56	3.1	5.8	6.8	320	18
2354	17	33	47	57	3 0	5.5	7.3	325	9
2356	27	28	52	64	1.3	5.2	6.1	305	12
2358	31	49	63	74	1.7	4.7	6.6	280	18
0000	13	29	77	125	1.1	3.5	7.0	280	31
0002	25	40	95	129	1.3	6.1	7.6	285	41
0004	39	63	92	113	1.4	4.5	6.2	300	38
0006	34	60	94	108	1.7	5.3	6.5	305	22
0008	84	99	112	116	2.0	4.0	6.0	325	16
0010	74	102	117	122	3.7	4.7	5.5	340	16
0012	36	78	103	119	2.9	5.6	6.2	330	12
0014	32	82	104	121	3.0	6.8	7.8	320	13
0016	MSG	MSG	MSG	MSG	3.9	6.0	6.3	325	15
0018	"	"	"	"	3.0	5 3	6.1	335	24
0020	"	"	"	"	2.9	5.4	6.5	335	19
0022	"	"	"	"	2.0	5.5	7.3	325	16
0024	103	132	141	143	1.0	2.0	5.6	315	23
0026	87	120	135	140	2.7	5.2	6.5	300	25
0028	78	111	127	140	2.2	5.4	6.1	300	28

February 12, 1960 (Continued)

Time, EST	Anemometer Revolutions				Temperature Difference, °C			Wind Dir. Degrees	% Mod.
2 min. period, ending	0.5m	1m	2m	4m	1m-0.5m	2m-0.5m	4m-0.5m		
0030	70	99	121	125	1.2	6.3	7.0	300	29
0032	59	94	120	136	1.8	5.8	7.3	300	22
0034	73	108	125	164	2.9	5.6	6.8	295	29
0036	83	121	131	167	2.7	4.7	6.7	300	29
0038	71	108	132	165	2.1	5.8	7.1	300	36
0040	61	92	124	160	1.9	6.0	7.9	300	39
0042	56	90	131	150	1.3	5.3	7.7	300	34
0044	80	119	138	154	2.6	5.0	7.5	300	33
0046	82	111	134	MSG	.8	5.2	7.9	305	34
0048	78	112	136	"	1.3	2.8	6.1	310	34
0050	79	116	147	128	1.9	4.0	6.5	320	24
0052	86	123	146	136	2.6	4.5	6.1	330	23
February 13, 1960									
1920	21	36	39	68	1.5	3.7	7.1	360	25
1922	33	36	29	51	1.0	1.8	5.3	360	33
1924	52	40	21	46	.8	1.8	4.6	355	37
1926	38	47	15	24	1.2	1.8	3.7	355	29
1928	12	14	2	15	1.2	2.2	3.8	355	26
1930	2	1	3	14	1.3	2.8	3.9	355	23
1932	6	5	1	15	.6	2.0	3.0	355	24
1934	31	25	3	12	1.7	.8	2.8	360	26
1936	29	25	10	19	1.7	2.2	3.7	005	27
1938	22	18	7	42	1.1	2.5	4.5	015	29
1940	21	22	47	91	1.0	2.9	6.2	015	33
1942	48	56	55	77	1.1	3.5	5.2	290	39
1944	55	64	48	55	2.0	3.1	5.0	290	39
1946	62	74	64	65	1.9	2.6	4.8	290	43
1948	83	90	92	80	2.0	2.4	3.5	300	35
1950	65	92	95	75	2.6	2.4	4.3	305	28
1952	63	86	94	96	1.5	3.3	4.2	310	26
1954	74	96	93	91	2.2	2 8	4.7	305	22
1956	46	76	80	72	1.3	3.7	5.3	305	32
1958	42	66	80	58	1.1	2.9	4 6	310	36
2000	50	61	89	69	.8	3.3	5.4	315	37
2002	32	49	83	71	.8	3.5	6.1	320	28
2004	33	66	81	57	1.5	3.7	6.9	320	21
2006	17	45	78	54	1.1	5.2	7.5	320	19
2008	29	52	85	50	1.2	5.2	7.1	320	27
2010	28	57	82	57	1.1	4.0	6.6	320	26
2012	43	73	73	43	.7	3.4	5.3	320	23
2014	70	97	81	31	1.0	4.0	5.8	320	26

February 13, 1960 (Continued)

Time, EST	Anemometer Revolutions				Temperature Difference, °C			Wind Dir.	%
2 min. period, ending	0.5m	1m	2m	4m	1m-0.5m	2m-0.5m	4m-0.5m	Degrees	Mod.
2016	53	78	104	40	1.3	3.1	5.8	320	35
2018	35	63	95	54	.8	2.1	6.0	330	43
2020	40	59	99	70	.4	1.3	5.8	340	39
2022	43	70	119	83	.5	1.5	5.9	335	47
2024	80	108	123	74	.7	2.9	5.6	335	46
2026	85	112	129	77	.8	3.5	5.6	340	34
2028	72	99	127	78	.8	3.8	6.3	340	36
2030	72	100	128	85	1.3	3.5	6.8	340	39
2032	52	76	118	92	.7	3.0	6.9	345	39
2034	34	57	98	91	.5	1.8	6.6	340	39
2036	14	40	93	89	.6	2.0	6.7	335	36
2038	45	74	95	90	.8	2.1	6.0	335	36
2040	53	61	66	96	1.0	1.7	4.0	335	39
2042	44	50	60	100	.5	1.1	3.9	345	45
2044	35	41	57	112	.5	1.3	4.7	350	51
2046	18	28	49	99	6	1.2	4.8	350	52
2048	6	22	42	86	.6	1.5	4.7	350	43
2050	36	47	68	83	.2	.6	4.5	350	39
2052	38	51	76	86	.4	.7	5.3	350	38
2054	38	53	87	100	.5	1.0	6.2	350	39
2056	43	60	103	108	4	1.8	6.3	355	43
2058	22	39	94	114	.5	2.1	6.6	360	49
2100	23	41	78	106	.6	1.8	6.8	"	47
2102	36	52	95	123	.6	1.7	6.7	"	51
2104	55	76	129	129	.5	2.2	6.6	"	59
2106	55	84	136	137	.6	1.9	6.8	"	MSG
2108	68	97	143	138	.6	2.2	6.8	"	"
2110	76	106	143	136	.6	2.8	6.1	"	79
2112	69	97	136	133	.6	2.8	6.0	"	72
2114	56	83	125	128	.6	3.3	6.7	"	53
2116	46	80	128	128	.8	3.4	7.0	"	45
2118	55	88	138	135	.7	3.8	6.9	"	45
2120	56	87	136	135	.7	3.3	6.8	"	45
2122	64	92	129	132	.6	4.6	7.0	"	48
2124	93	123	144	135	.7	4.5	7.1	"	69
2126	97	126	148	142	.6	4.3	6.9	"	59
2128	81	104	139	150	.4	3.0	6.7	"	59
2130	63	89	134	142	.5	2.8	6.7	"	62
2132	62	93	136	136	.6	2.9	7.0	"	63
2134	55	85	136	127	.7	1.9	7.4	"	60
2136	91	119	150	126	.7	2.9	7.6	350	59
2138	117	144	157	134	.8	3.7	7.7	345	51
2140	123	153	156	142	1.0	3.5	7.8	340	41
2142	141	168	186	171	.5	3.1	7.3	340	43

February 13, 1960 (Continued)

Time, EST	Anemometer Revolutions				Temperature Difference, °C			Wind Dir. Degrees	% Mod.
2 min. period, ending	0.5m	1m	2m	4m	1m-0.5m	2m-0.5m	4m-0.5m		
2144	133	161	203	197	.5	2.0	6.2	335	41
2146	133	160	187	187	.5	2.0	5.8	335	38
2148	111	138	152	MSG	.5	2.5	4.8	340	38
2150	105	131	145	"	.6	2.9	4.7	340	43
2152	105	132	155	"	.6	2.8	5.9	345	50
2154	101	132	146	"	.7	2.9	6.3	345	51
2156	80	109	137	"	.6	3.0	6.2	350	50
2158	45	63	119	"	.5	1.9	5.9	350	51
2200	59	71	110	130	.4	2.5	6.3	350	48
2202	50	58	69	113	.7	1.5	4.6	355	43
2204	45	52	64	109	.4	1.3	3.4	350	38
2206	54	68	96	99	.4	.6	5.1	350	37
2208	40	52	90	104	.4	.8	5.4	350	40

February 14, 1960

1930	1	13	53	67	2.5	5.6	7.6	055	23
1932	4	14	49	68	1.4	4.0	7.3	060	26
1934	24	29	48	77	1.2	4.0	7.1	070	32
1936	29	34	34	90	1.2	4.5	8.1	080	27
1938	4	21	20	90	1.4	4.8	7.9	080	30
1940	5	17	35	94	1.4	5.4	7.8	095	40
1942	1	13	36	94	1.4	5.3	8.5	100	34
1944	0	14	47	93	1.4	5.9	8.7	090	24
1946	2	10	50	94	1.5	5.4	8.4	095	24
1948	1	1	46	86	1.3	5.2	7.9	095	31
1950	2	1	41	72	1.1	5.1	7.7	105	24
1952	14	7	29	60	1.3	4.3	7.0	110	18
1954	17	27	2	48	1.7	3.6	7.4	"	14
1956	18	31	3	38	1.9	3.3	7.0	"	15
1958	10	25	1	39	1.9	2.9	7.1	"	12
2000	1	16	0	34	1.9	3.5	7.3	"	13
2002	1	14	1	35	1.9	2.8	6.3	"	12
2004	3	22	13	30	2.0	2.9	5.8	170	12
2006	8	26	13	16	1.2	2.8	5.0	170	10
2008	1	16	4	28	1.7	2.7	5.2	155	15
2010	3	0	18	67	1.2	3.3	5.8	150	20
2012	1	1	20	74	.8	3.6	5.4	155	16
2014	1	2	12	70	1.2	3.3	5.4	160	18
2016	14	17	11	46	.7	2.5	5.1	170	12
2018	11	18	3	42	1.4	2.0	4.7	170	12
2020	1	3	1	53	.6	2.5	4.6	165	16
2022	2	3	12	76	1.1	2.9	5.0	175	16
2024	7	12	35	88	1.1	3.0	5.0	175	10

February 14, 1960 (Continued)

Time, EST	Anemometer Revolutions				Temperature Difference, °C			Wind Dir. Degrees	% Mod.
2 min. period, ending	0.5m	1m	2m	4m	1m-0.5m	2m-0.5m	4m-0.5m		
2026	2	14	55	111	1.1	3.8	5.3	170	16
2028	6	24	75	129	1.0	3.1	5.1	160	23
2030	39	60	100	MSG	.7	2.1	3.8	155	22
2032	69	91	120	"	.8	1.7	2.4	150	20
2034	73	93	121	"	.6	1.3	2.2	150	27
2036	60	78	104	"	.5	1.3	2.1	150	28
2038	52	69	95	"	.6	1.2	2.4	150	24
2040	49	68	93	"	.5	1.2	2.0	155	26
2042	49	68	97	"	.5	1.4	2.0	155	20
2044	55	74	103	"	.7	1.4	2.1	155	19
2046	53	72	97	"	.7	1.2	1.9	165	19
2048	66	78	101	"	.5	1.4	1.7	155	16
2050	67	86	108	"	.7	1.3	1.9	145	18
2052	51	70	94	"	.4	1.1	1.3	150	20
2054	45	61	83	"	.4	1.0	1.2	155	19
2056	44	64	93	"	.6	1.4	2.0	160	17
2058	42	60	86	"	.7	1.4	2.0	165	18
2100	42	51	66	"	.2	.6	1.3	170	16
2102	37	49	70	105	.4	1.1	1.5	175	13
2104	56	79	103	141	.4	1.2	1.8	180	13
2106	76	93	116	150	.5	.8	1.5	170	16
2108	67	83	108	143	.4	.8	1.5	160	19
2110	95	115	140	169	.4	1.0	1.4	165	25
2112	121	138	159	187	.2	.6	.8	170	28
2114	88	105	126	158	.4	.7	1.2	170	21
2116	72	84	99	121	.5	.6	1.2	180	17
2118	76	91	113	132	.5	1.0	1.4	170	25
2120	80	93	113	133	.2	.8	1.1	160	22
2122	95	115	136	156	.4	1.0	1.5	160	21
2124	71	88	111	123	.6	.8	1.3	165	16
2126	75	86	100	109	.4	.6	1.0	170	16
2128	52	63	80	89	.6	1.1	1.3	165	15
2130	44	61	83	99	.5	1.3	1.7	170	12
2132	51	67	87	109	.7	1.2	1.7	170	10
2134	45	61	83	101	.6	1.3	1.7	165	8
2136	27	42	59	78	.8	1.4	1.8	160	MSG
2138	10	12	28	48	.8	1.5	2.0	160	6
2140	24	5	2	22	.7	1.1	2.2	160	10
2142	23	29	26	9	1.1	1.7	2.1	160	9
2144	21	22	19	10	1.2	1.3	2.0	170	6
2146	29	24	14	13	.7	1.1	1.7	170	10
2148	38	51	49	29	.7	1.5	1.5	360	7
2150	36	48	50	33	.7	.8	1.8	360	6
2152	36	39	31	19	.5	1.1	1.1	360	7

February 14, 1960 (Continued)

Time, EST	Anemometer Revolutions				Temperature Difference, °C			Wind Dir.	%
2 min. period, ending	0.5m	1m	2m	4m	1m-0.5m	2m-0.5m	4m-0.5m	Degrees	Mod.
2154	15	15	17	9	.6	1.0	1.4	360	7
2156	18	22	32	22	.4	1.0	1.3	"	10
2158	26	35	31	16	.5	1.2	1.4	"	9
2200	13	24	24	4	.5	1.2	1.4	"	8
2202	12	18	14	9	.6	1.3	1.5	"	9
2204	9	9	18	13	.7	1.3	1.7	005	6
2206	15	25	33	25	.6	1.3	1.4	015	5
2208	21	25	16	23	.6	1.4	1.5	040	4
2210	17	16	15	27	.2	.8	1.5	065	6
2212	13	11	13	5	.5	1.3	1.7	065	10
2214	13	20	20	32	.7	1.4	2.1	120	11
2216	15	14	17	26	.5	1.4	1.4	165	8
2218	10	15	21	22	.7	1.4	1.7	165	8
2220	31	29	26	15	.5	1.1	1.4	020	4
2222	43	49	41	23	.7	1.4	1.3	"	4
2224	31	34	32	25	.7	1.7	1.7	"	4
2226	23	30	27	24	1.1	1.9	2.0	"	5
2228	23	28	25	21	1.1	1.5	1.9	"	8
2230	44	58	60	38	.8	1.2	1.9	330	7
2232	64	84	97	80	.5	1.1	1.7	320	12
2234	59	68	71	64	1.0	1.2	1.5	300	9
2236	55	66	75	79	.6	.8	1.8	300	13
2238	35	45	58	63	.5	1.0	1.7	260	22
2240	26	39	54	84	.4	1.0	1.3	250	20
2242	69	90	109	144	.4	1.1	1.5	"	19
2244	132	152	178	208	.4	.8	1.2	"	22
2246	115	135	164	192	.4	1.0	1.7	"	22
2248	171	188	209	237	.4	.6	.7	"	22
2250	148	166	194	223	.4	.7	1.1	"	21
2252	146	163	187	216	.4	.7	1.2	"	21
2254	142	159	186	218	.4	.7	1.2	"	21
2256	144	162	187	211	.4	.7	1.0	"	20
2258	123	143	169	197	.4	.8	1.3	245	20
2300	125	145	172	200	.4	1.0	1.2	"	20
2302	121	138	168	200	.4	.7	1.1	"	21
2304	133	149	169	191	.2	.7	1.0	"	21
2306	132	152	176	204	.2	.6	.8	250	20
2308	112	130	156	182	MSG	MSG	MSG	250	20

MICROMETEOROLOGICAL AND SCINTILLATION DATA

February 18, 1960

Time, EST	Anemometer Revolutions				Temperature Difference, °C			Wind Dir. Degrees	% Mod.
2 min. period, ending	0.5m	1m	2m	4m	1m-0.5m	2m-0.5m	4m-0.5m		
1408	MSG	MSG	MSG	MSG	-.05	-.1	-.1	MSG	10
1410	"	"	"	"	-.05	-.05	-.1	"	"
1412	"	"	"	"	-.05	-.1	-.2	310	"
1414	383	422	455	479	-.05	-.1	-.1	315	"
1416	297	319	343	361	-.05	-.1	-.1	310	"
1418	301	331	362	390	-.05	-.1	-.2	320	"
1420	358	388	411	439	-.05	-.1	-.1	350	"
1422	348	375	414	439	-.05	-.05	-.1	340	"
1444	275	303	317	334	-.05	-.05	-.1	330	"
1426	353	381	408	428	-.05	-.05	-.1	340	"
1428	366	402	430	456	0	-.05	-.1	345	"
1430	330	358	380	402	-.05	0	-.1	"	"
1432	327	356	389	410	-.05	-.05	-.1	"	"
1434	371	393	430	453	-.05	-.05	-.2	"	"
1436	341	366	395	418	-.05	-.05	-.1	340	"
1438	309	329	356	379	-.05	-.05	-.1	335	"
1440	327	350	376	395	0	-.05	-.2	350	"
1442	313	339	362	382	.05	.05	.05	325	"
1444	321	351	367	374	-.05	-.05	-.1	325	MSG
1446	275	296	314	331	0	0	-.1	330	10
1448	316	340	357	375	0	-.05	-.1	325	10
1450	370	402	433	463	0	-.05	-.1	330	11
1452	330	367	390	418	-.05	-.05	-.1	320	10
1454	361	398	431	462	-.05	-.05	-.1	320	"
1456	376	409	440	471	-.05	-.05	-.1	320	"
1458	383	417	447	460	0	-.05	-.1	315	"
1500	345	378	403	431	-.05	-.05	-.1	320	11
1502	374	416	442	470	0	-.1	-.1	315	"
1504	375	409	444	472	-.05	-.05	-.1	320	"
1506	286	310	329	358	-.05	-.05	-.1	325	"
1508	377	410	443	470	-.05	-.05	-.1	330	12
1510	324	357	387	419	0	-.05	-.1	335	"
1512	360	388	415	446	0	0	-.1	340	"
1514	383	417	448	474	0	0	-.1	350	"
1516	367	400	431	461	0	0	-.1	345	13
1518	329	354	380	407	0	-.05	-.1	340	12
1520	347	378	402	432	0	-.1	-.1	345	13
1522	294	322	354	370	0	-.05	-.1	350	19
1524	337	361	390	412	0	-.05	-.1	345	22
1526	331	363	383	397	-.05	0	-.05	335	22
1528	359	393	422	447	0	0	-.05	345	21
1530	340	373	409	444	0	-.05	-.05	350	22
1532	292	317	343	373	0	-.05	-.05	340	22
1534	312	335	360	383	-.05	-.05	0	335	23

February 18, 1960, (Continued)

Time, EST	Anemometer Revolutions				Temperature Difference, °C			Wind Dir. Degrees	% Mod.
2 min. period, ending	0.5m	1m	2m	4m	1m-0.5m	2m-0.5m	4m-0.5m		
1536	290	318	340	363	0	-.1	0	330	23
1538	314	340	360	381	-.05	-.1	0	340	22
1540	243	269	290	310	0	-.05	-.05	325	20
1542	262	289	316	340	0	0	-.1	340	21
1544	291	320	345	361	0	0	-.05	335	20
1546	240	263	288	301	0	-.05	-.05	325	17
1548	326	359	390	409	0	0	-.05	330	17
1550	291	319	344	360	0	0	-.05	325	20
1552	296	328	355	382	0	0	-.1	330	20
1554	273	299	323	347	0	0	-.1	325	19
1556	239	262	286	307	0	0	-.1	330	19
1558	250	273	291	312	0	-.05	-.05	320	20
1600	301	337	365	384	0	0	-.1	320	19
1602	304	332	356	379	0	0	0	335	17
1604	260	282	302	321	0	0	0	330	17
1606	231	259	277	291	0	0	-.05	325	18
1608	259	281	303	323	0	0	-.05	320	19
1610	290	318	342	359	0	-.05	-.05	320	17

February 19, 1960

2136	302	342	384	426	.1	.2	.3	350	13
2138	341	395	432	462	.1	.2	.2	350	12
2140	312	349	387	415	.1	.2	.2	345	13
2142	338	379	416	447	.1	.2	.3	350	14
2144	323	363	404	441	.1	.3	.4	345	14
2146	311	359	399	433	.1	.2	.3	345	14
2148	330	369	413	444	.1	.2	.3	350	13
2150	307	346	382	408	.1	.2	.2	345	12
2152	294	335	371	402	.05	.1	.2	350	12
2154	305	339	373	404	.05	.2	.3	350	12
2156	380	420	463	493	.05	.2	.2	355	11
2158	361	403	436	468	.1	.2	.2	350	13
2200	352	397	441	481	.05	.2	.2	355	13
2202	328	369	410	444	.05	.1	.1	355	13
2204	281	315	349	377	.05	.1	.2	355	12
2206	303	340	374	408	.05	.1	.2	350	12
2208	277	311	346	370	.05	.1	.1	355	11
2210	285	319	353	389	.05	.1	.1	350	"
2212	273	306	336	360	.05	.2	.2	355	"
2214	240	269	300	328	.05	.1	.1	355	"
2216	323	361	402	441	.05	.1	.2	355	"
2218	298	329	359	392	.05	.1	.2	355	"

February 19, 1960 (Continued)

Time, EST	Anemometer Revolutions				Temperature Difference, °C			Wind Dir. Degrees	% Mod.
2 min. period, ending	0.5m	1m	2m	4m	1m-0.5m	2m-0.5m	4m-0.5m		
2220	310	348	378	408	.1	.1	.1	350	11
2222	329	363	401	423	.05	.1	.1	355	"
2224	295	333	371	398	0	.1	.05	350	"
2226	316	357	384	414	.05	.1	.1	345	"
2228	309	344	380	412	.05	.05	.05	345	"
2230	301	337	374	397	.1	.1	.1	350	"
2232	341	382	423	458	.05	.1	.2	350	"
2234	312	350	389	425	.05	.1	.1	350	"
2236	287	328	359	387	.1	.1	.1	345	12
2238	308	345	381	413	.05	.2	.2	350	12
2240	321	365	403	435	.05	.2	.2	345	12
2242	336	385	424	453	.05	.1	.2	350	11
2244	280	318	346	382	.05	.1	.2	350	11
2246	308	346	384	410	.05	.1	.2	350	11

February 20, 1960

2004	92	107	119	108	MSG	MSG	MSG	050	38
2006	82	103	120	125	1.7	3.6	4.3	090	22
2008	76	88	111	126	2.3	3.0	4.0	110	19
2010	114	132	164	174	.9	2.9	3.9	170	MSG
2012	107	119	145	161	.3	1.2	2.4	185	"
2014	70	82	102	110	1.2	1.4	2.1	195	40
2016	44	61	74	68	2.5	2.7	4.8	200	28
2018	25	60	59	26	4.1	4.9	5.6	"	28
2020	19	45	39	24	4.8	5.2	4.7	"	29
2022	3	22	18	19	5.2	5.3	5.6	"	22
2024	16	24	28	26	1.9	4.4	6.4	240	16
2026	20	25	34	46	1.5	3.0	4.5	300	23
2028	45	45	55	48	2.1	4.2	5.7	300	22
2030	60	65	67	56	3.0	5.7	5.9	325	16
2032	34	54	69	46	2.2	6.3	7.2	"	12
2034	1	14	62	37	2.0	5.8	8.6	"	18
2036	2	3	42	55	1.8	4.4	8.9	"	21
2038	21	16	43	68	1.5	4.0	8.6	335	23
2040	28	14	47	64	1.5	3.5	7.6	340	27
2042	27	26	45	57	2.1	4.3	8.8	360	23
2044	32	35	70	67	2.4	4.6	9.6	010	24
2046	27	47	97	76	2.1	6.4	9.5	010	23
2048	11	34	85	89	2.6	7.0	9.1	010	24
2050	14	29	63	90	2.6	5.4	8.8	015	32
2052	5	17	53	81	3.7	6.6	9.6	"	27
2054	2	11	55	90	3.3	8.7	9.7	"	23

February 20, 1960 (Continued)

Time, EST	Anemometer Revolutions				Temperature Difference, °C			Wind Dir. Degrees	% Mod.
2 min. period, ending	0.5m	1m	2m	4m	1m-0.5m	2m-0.5m	4m-0.5m		
2056	2	28	77	99	4.9	7.8	10.0	015	26
2058	8	37	87	106	4.7	8.1	9.8	015	19
2100	33	47	75	98	2.9	5.7	7.9	010	19
2102	27	38	85	116	2.3	6.4	7.7	040	13
2104	35	44	87	115	1.0	4.9	7.4	045	15
2106	59	66	97	131	.6	3.2	6.5	045	18
2108	60	68	102	138	.5	3.1	7.0	040	MSG
2110	41	57	124	150	1.0	5.2	8.0	040	"
2112	41	69	129	134	2.9	6.6	8.0	025	"
2114	24	41	73	124	2.1	5.2	8.1	020	"
2116	36	41	71	134	1.2	2.8	5.7	020	"
2118	27	48	79	143	1.7	3 8	6.4	015	33
2120	33	50	103	147	2.7	4.8	7.9	015	33
2122	30	48	98	136	3.2	6.7	9.5	020	20
2124	19	33	88	130	2.8	6.1	9.3	020	19
2126	5	17	62	114	2.3	5.8	8.8	020	22
2128	18	26	46	101	2.1	4.4	7.1	015	24
2130	28	30	46	100	1.3	3.8	6.2	015	29
2132	33	37	59	96	1.8	3.1	6.4	015	25
2134	29	44	68	86	2.1	4.7	6.3	010	35
2136	38	54	67	86	2.9	5.4	6.1	005	41
2138	54	62	73	95	2.7	4.4	5.4	015	42
2140	66	63	76	86	1.4	3.9	4.8	015	33
2142	60	59	70	84	.8	4.2	4.9	020	24
2144	60	62	74	82	.3	3.5	4.4	020	16
2146	62	65	85	79	1.0	3.3	5.0	020	19
2148	55	57	86	75	1.6	4.1	5.4	015	17
2150	17	39	66	78	1.7	4.8	6.7	010	22
2152	20	32	60	60	2.1	4.7	6.5	"	16
2154	11	28	48	57	2.0	5.4	6.4	"	12
2156	6	23	50	68	1.2	5.2	7.3	"	20
2158	14	23	57	72	1.2	6.1	8.2	"	20
2200	27	37	54	66	1.7	4.6	7.1	350	36
2202	37	55	68	78	2.2	3 8	7.3	325	40
2204	42	57	78	95	1.2	3.4	7.5	330	46
2206	38	50	88	104	.8	2.3	6.4	340	48
2208	66	77	110	99	.4	2.5	5.4	345	55
2210	34	45	78	105	.4	2.1	5.6	360	49
2212	49	54	70	99	.6	1.8	4.2	010	56
2214	30	45	57	81	1.1	2.5	3.6	005	53
2216	64	75	82	87	.3	1.7	2.8	350	50
2218	77	87	91	101	.5	2.2	3.2	350	36
2220	71	81	85	95	.7	2.2	3.4	360	33
2222	78	87	93	99	.4	2.6	3.7	360	31

February 20, 1960 (Continued)

Time, EST	Anemometer Revolutions				Temperature Difference, °C			Wind Dir. Degrees	% Mod.
2 min. period, ending	0.5m	1m	2m	4m	1m-0.5m	2m-0.5m	4m-0.5m		
2224	91	95	102	99	.3	2.4	4.4	360	33
2226	71	78	83	81	.3	3.1	5.0	360	32
2228	42	50	60	47	.1	2.3	4.4	360	24
2230	26	33	46	45	.1	.7	3.0	345	20
2232	24	28	36	51	.1	.5	2.9	330	28
2234	30	36	41	51	.2	.6	3.4	340	MSG
2236	18	30	46	59	.5	1.4	3.7	350	22
2238	7	22	45	51	.7	1.9	3.6	005	20
2240	4	9	28	37	.9	1.9	3.3	"	17
2242	5	12	33	41	.3	1.6	3.1	"	16
2244	26	29	49	60	.4	1.3	3.1	"	16
2246	41	44	57	65	.6	1.9	3.0	010	20
2248	40	42	53	64	.8	2.1	2.9	010	19
2250	30	34	44	51	.8	2.3	2.8	010	15
2252	36	33	44	50	.3	1.3	1.9	020	11
2254	32	34	52	43	.4	1.1	2.2	030	12
2256	20	23	39	57	.6	1.6	3.3	025	14
2258	17	30	39	55	.7	2.1	3.3	010	16

February 23, 1960

2048	65	66	92	127	MSG	MSG	MSG	330	27
2050	59	71	111	128	"	"	"	330	18
2052	53	81	107	126	"	"	"	335	16
2054	43	81	101	113	"	"	"	335	27
2056	62	97	102	123	"	"	"	335	18
2058	77	118	120	135	"	"	"	300	16
2100	70	117	123	154	6.1	8.3	9.7	335	16
2102	89	127	142	157	6.2	7.9	8.6	335	20
2104	96	123	136	150	5.3	6.0	6.4	345	29
2106	85	116	131	150	3.7	5.7	7.2	"	22
2108	72	111	136	153	5.6	7.5	7.8	"	15
2110	73	100	136	155	3.6	7.4	8.6	"	13
2112	93	125	166	201	3.7	5.9	9.1	360	34
2114	97	145	186	201	3.8	8.0	9.0	360	36
2116	80	130	166	191	3.4	6.9	7.3	360	42
2118	60	101	169	201	3.6	7.1	6.6	355	49
2120	107	155	197	228	2.8	4.3	5.0	360	45
2122	124	166	206	237	2.2	3.8	4.3	355	44
2124	141	181	229	262	1.9	3.1	4.1	005	43
2126	164	204	250	281	1.3	2.8	3.1	"	41
2128	187	224	268	309	1.0	1.9	2.9	"	39
2130	182	220	257	298	1.1	2.1	3.2	"	39

MICROMETEOROLOGICAL AND SCINTILLATION DATA

February 23, 1960 (Continued)

Time, EST	Anemometer Revolutions				Temperature Difference, °C			Wind Dir. Degrees	% Mod.
2 min. period, ending	0.5m	1m	2m	4m	1m-0.5m	2m-0.5m	4m-0.5m		
2132	159	197	244	286	1.1	2.8	3.5	360	39
2134	157	195	242	289	1.2	2.5	3.7	005	39
2136	147	188	234	271	1.4	3.0	3.3	"	39
2138	154	188	230	264	1.3	2.3	2.9	"	37
2140	154	190	229	268	1.0	2.0	2.9	"	36
2142	181	214	253	286	1.0	1.8	2.2	"	35
2144	185	216	253	297	.8	1.6	2.2	"	34
2146	211	244	278	316	.5	1.6	2.1	"	33
2148	169	201	240	282	1.0	1.8	2.5	"	34
2150	149	180	221	266	1.1	2.5	2.8	360	35
2152	170	201	234	274	1.1	1.9	2.5	005	36
2154	186	220	255	290	.7	1.7	2.6	005	35
2156	163	197	238	270	1.1	2.3	2.8	360	33
2158	158	193	232	271	1.2	2.2	2.5	355	37
2200	179	210	244	272	.9	2.0	1.6	355	37
2202	178	213	248	280	.9	1.5	2.5	355	35
2204	182	215	259	295	.9	1.9	2.4	360	33
2206	186	218	250	274	1.0	1.6	2.0	355	35
2208	160	191	226	261	1.2	1.6	2.7	355	34
2210	147	183	225	258	1.0	2.1	2.9	355	33
2212	171	205	243	277	1.0	2.1	2.1	360	35
2214	136	170	212	250	1.0	2.1	3.0	"	32
2216	134	166	201	232	1.1	2.2	3.0	"	31
2218	144	172	208	244	.9	1.9	2.6	"	32
2220	184	212	238	258	.8	1.8	1.7	"	31
2222	183	211	237	261	1.0	1.6	1.8	"	32
2224	168	200	231	260	.9	1.6	1.9	355	33
2226	144	175	205	228	1.0	2.0	2.3	355	32
2228	145	171	197	216	.8	1.8	2.3	360	33
2230	162	192	225	249	1.0	1.8	2.7	355	33
2232	149	184	218	256	1.3	2.3	3.1	350	33
2234	189	226	260	294	.8	2.0	2.2	350	34
2236	258	294	332	364	.7	1.1	1.7	005	31
2238	285	327	365	405	.5	.8	1.5	"	30
2240	207	238	284	317	.7	1.4	2.4	"	32
2242	259	294	333	373	.8	1.3	1.8	"	32
2244	206	239	274	306	.7	1.5	1.9	"	32
2246	183	211	249	284	.7	1.4	2.2	360	31
2248	222	258	295	328	.5	1.2	1.6	005	28
2250	214	246	282	318	.7	1.3	1.7	005	28
2252	183	213	243	277	.5	1.1	1.7	005	26
2254	176	203	241	276	.7	1.4	1.8	360	30
2256	201	230	264	300	.7	1.2	1.7	005	28
2258	187	220	253	285	.7	1.0	1.7	005	26
2300	184	211	242	280	.5	.9	1.7	010	26

MICROMETEOROLOGICAL AND SCINTILLATION DATA

February 24, 1960

Time, EST	Anemometer Revolutions				Temperature Difference, °C			Wind Dir. Degrees	% Mod.
2 min. period, ending	0.5m	1m	2m	4m	1m-0.5m	2m-0.5m	4m-0.5m		
2010	71	92	99	100	1.1	2.1	2.8	MSG	19
2012	70	95	105	110	1.4	2.7	3.3	330	22
2014	81	109	128	132	.9	2.3	3.3	330	23
2016	83	107	131	144	.5	1.6	2.7	335	25
2018	78	104	126	156	.5	1.6	2.6	345	25
2020	83	105	135	166	.5	1.3	2.4	345	23
2022	85	108	134	164	.7	1.3	2.1	340	19
2024	95	113	141	165	.4	.8	1.6	345	20
2026	99	115	133	152	.2	.5	.9	350	16
2028	105	124	145	157	.2	.5	.8	355	14
2030	114	132	152	166	.2	.5	.8	350	14
2032	97	113	127	140	.3	.7	.7	345	13
2034	73	93	114	129	.4	1.1	1.2	340	13
2036	86	101	121	143	.3	.7	1.1	335	14
2038	85	103	121	135	.3	.5	.9	335	13
2040	75	94	113	124	.3	.8	1.1	330	14
2042	77	97	113	130	.3	.9	1.1	335	13
2044	72	91	108	129	.4	.8	1.0	"	13
2046	81	100	123	144	.3	.7	.9	"	13
2048	90	111	131	146	.3	.7	.9	"	13
2050	72	88	103	122	.4	.7	1.0	"	14
2052	67	86	105	123	.3	.9	1.0	340	13
2054	69	91	111	130	.3	.5	1.0	335	13
2056	79	94	109	127	.3	.7	.8	335	14
2058	69	85	104	120	.3	.7	.8	345	13
2100	79	96	113	126	.3	.7	.7	350	12
2102	73	90	104	115	.2	.3	.5	"	11
2104	67	82	101	116	.2	.4	.7	"	13
2106	65	83	97	109	.2	.5	.9	"	13
2108	62	82	100	119	.3	.7	.9	"	14
2110	59	76	96	116	.2	.5	.8	"	12
2112	69	85	96	109	.2	.3	.5	"	14

February 27, 1960

1824	MSG	MSG	MSG	MSG	2.7	2.6	3.5	MSG	28
1826	"	"	"	"	2.5	3.3	3.9	315	26
1828	63	96	110	126	2.5	3.7	4.2	315	26
1830	60	91	104	119	3.4	3.5	3.7	310	23
1832	57	88	109	126	3.3	3.7	4.4	310	22
1834	50	87	112	129	3.0	4.4	4.2	310	22
1836	51	87	113	129	3.4	4.2	5.0	305	26
1838	45	83	111	128	3.2	5.8	5.6	305	22
1840	43	87	105	118	5.2	5.8	6.4	305	24

February 27, 1960 (Continued)

Time, EST	Anemometer Revolutions				Temperature Difference, °C			Wind Dir. Degrees	% Mod.
2 min. period, ending	0.5m	1m	2m	4m	1m-0.5m	2m-0.5m	4m-0.5m		
1842	39	82	99	119	5.5	7.4	7.2	310	28
1844	38	90	108	125	7.3	7.0	7.9	310	24
1846	34	80	107	129	5.1	6.9	8.1	310	20
1848	27	84	111	131	6.2	8.1	8.9	315	20
1850	21	75	100	116	5.2	8.9	9.4	320	17
1852	5	45	79	106	5.7	8.6	9.5	325	18
1854	24	46	80	103	4.9	8.8	8.9	310	21
1856	62	75	87	106	3.8	5.4	4 7	295	36
1858	68	79	91	102	3.2	5.8	6.6	285	38
1900	63	72	104	135	2.8	6.0	8.5	275	41
1902	33	56	103	135	2.2	7.6	9.8	275	45
1904	45	90	115	137	3.5	8.3	9.8	280	43
1906	31	77	101	125	3.8	6.7	8.4	285	29
1908	9	30	95	120	2.3	6.2	8.8	290	25
1910	25	49	86	133	2.4	5.3	8.2	290	27
1912	10	36	84	112	2.6	6.5	8.3	295	32
1914	5	10	40	81	2.5	5.9	8.8	295	28
1916	18	26	42	67	2.3	6.8	9.4	300	19
1918	14	17	53	64	3.2	7.7	10.2	305	16
1920	33	27	43	66	3.0	5.3	9.2	310	15
1922	26	27	61	74	2.4	5.0	9.0	320	18
1924	35	33	65	84	3.2	5.7	9.2	330	19
1926	11	14	57	79	3.6	6.5	10.2	330	20
1928	1	3	55	76	3.5	8.2	11.1	325	20
1930	15	16	49	82	4.0	6.3	10.2	320	22
1932	12	8	40	77	2.4	5.5	10.1	335	22
1934	13	2	18	54	2.3	5.6	10.4	335	16
1936	38	17	30	51	1.5	4.3	8.8	335	14
1938	35	45	36	72	2.2	4.0	9.2	345	12
1940	14	34	46	65	4.9	6.8	11.4	345	17
1942	15	46	91	85	4.4	6.2	11.5	325	58
1944	33	50	93	102	.9	3.4	9.6	320	51
1946	20	41	119	107	1.0	4.1	9.8	320	52
1948	7	31	120	111	.9	4.2	10.5	320	50
1950	32	75	121	105	1.5	7.4	10.5	315	60
1952	20	58	126	107	.9	5.6	11.1	310	67
1954	64	105	134	112	1.3	6.6	9.8	315	37
1956	66	116	123	123	2.4	8.1	10.2	305	48
1958	35	73	125	124	1.9	7.7	10.7	"	45
2000	46	83	106	113	1.7	8.2	9.6	"	43
2002	19	61	108	97	1.9	7.6	9.7	"	38
2004	18	51	101	92	1.4	5.7	9.1	315	28
2006	34	80	100	97	2.8	6.4	8.8	320	26
2008	18	62	111	109	2.1	6.8	9.5	315	23

February 27, 1960 (Continued)

Time, EST	Anemometer Revolutions				Temperature Difference, °C			Wind Dir. Degrees	% Mod.
2 min. period, ending	0.5m	1m	2m	4m	1m-0.5m	2m-0.5m	4m-0.5m		
2010	30	75	133	118	1.7	6.7	9.7	310	30
2012	70	112	149	127	2.1	6.2	8.5	310	32
2014	78	121	139	127	2.0	6.5	8.9	305	33
2016	88	134	137	129	2.3	7.0	9.3	"	33
2018	82	128	132	129	2.5	7.4	9.4	"	33
2020	78	124	133	127	2.4	7.5	9.4	"	35
2022	69	112	131	124	2.0	7.6	9.8	"	35
2024	73	117	131	120	2.1	8.0	9.9	"	33
2026	69	110	130	118	1.7	7.7	9.7	"	35
2028	67	108	130	117	1.7	7.6	9.9	"	33
2030	61	103	131	117	1.8	7.2	10.2	"	33
2032	66	108	128	118	1.3	7.8	9.8	"	39
2034	84	124	127	117	2.4	7.8	9.6	"	39
2036	85	124	135	120	2.5	7.2	9.6	310	38
2038	74	113	134	122	1.5	7.7	9.9	305	44
2040	79	119	127	119	2.1	7.9	9.8	305	44
2042	75	117	134	122	2.2	7.4	9.7	310	49
2044	58	100	135	122	1.9	7.1	9.3	"	49
2046	48	81	126	124	1.4	5.5	9.4	"	43
2048	71	110	143	129	1.4	6.2	9.4	"	42
2050	84	125	147	126	1.5	6.2	8.8	"	44
2052	85	120	145	126	1.4	6.2	8.8	"	42
2054	MSG	MSG	MSG	MSG	1.3	7.1	9.3	"	40

February 29, 1960

2012	MSG	MSG	MSG	MSG	5.6	8.8	10.1	280	26
2014	61	96	138	175	5.0	9.0	10.2	275	22
2016	57	98	142	185	5.5	9.6	11.5	270	22
2018	57	109	135	184	6.0	9.7	11.1	275	23
2020	66	118	143	180	6.0	9.6	11.1	"	23
2022	74	117	146	181	6.6	9.2	10.7	"	24
2024	68	119	146	186	6.1	9.6	10.9	"	27
2026	69	121	147	189	5.7	9.1	10.9	"	26
2028	74	124	153	189	5.5	9.3	10.3	"	27
2030	71	118	152	194	5.1	9.2	10.5	"	29
2032	72	115	155	187	4.4	8.9	9.9	"	28
2034	73	119	167	182	4.1	8.1	9.6	280	27
2036	60	109	156	170	5.5	8.9	9.4	285	26
2038	62	108	145	174	5.5	8.2	8.6	290	27
2040	62	101	139	163	5.3	8.4	8.8	"	29
2042	61	102	130	155	6.5	8.2	9.9	"	28
2044	67	104	129	152	5.2	7.2	8.6	"	33

February 29, 1960 (Continued)

Time, EST	Anemometer Revolutions				Temperature Difference, °C			Wind Dir. Degrees	% Mod.
2 min. period, ending	0.5m	1m	2m	4m	1m-0.5m	2m-0.5m	4m-0.5m		
2046	61	95	131	154	4.9	8.0	9.1	290	33
2048	56	98	132	155	6.6	7.9	8.8	"	35
2050	53	98	134	162	5.3	8.6	8.5	"	37
2052	57	98	140	170	4.5	7.1	8.6	"	37
2054	64	98	141	175	4.2	6.4	7.4	"	40
2056	56	101	147	183	3.8	7.6	8.3	"	39
2058	58	108	163	206	3.4	7.8	8.3	295	40
2100	65	114	169	216	3.6	6.6	7.9	290	39
2102	62	111	166	207	3.3	6.6	8.2	285	37
2104	58	102	157	196	3.3	6.4	8.4	290	36
2106	59	99	157	195	3.9	7.2	7.8	290	39
2108	63	106	153	188	3.8	6.5	8.0	285	37
2110	56	93	146	194	4.7	8.0	8.0	"	34
2112	53	95	149	199	4.6	8.8	8.8	"	34
2114	60	102	158	199	4.4	9.2	9.2	"	34
2116	65	107	149	199	MSG	MSG	MSG	280	34
2118	49	94	133	189	"	"	"	275	32
2120	71	108	137	173	"	"	"	280	30
2122	61	99	141	176	"	"	"	280	28
2124	62	107	140	189	"	"	"	275	30
2126	57	100	142	186	"	"	"	280	30
2128	49	92	125	172	"	"	"	280	27
2130	68	93	123	166	"	"	"	275	26
2132	60	103	131	160	5.5	6.4	8.0	270	24
2134	64	107	145	170	4.9	7.3	9.1	265	24
2136	54	95	140	168	5.3	7.6	9.4	265	22
2138	56	91	135	174	5.0	7.5	9.3	265	20
2140	61	111	136	177	5.1	7.1	9.0	265	21

March 1, 1960

1942	7	15	28	23	1.6	4.5	4.7	240	MSG
1944	6	4	21	20	3.2	5.8	6.9	"	"
1946	20	28	22	27	3.0	5.5	7.6	"	"
1948	10	23	17	26	3.4	5.5	8.1	"	"
1950	3	20	12	21	3.8	5.2	8.8	"	"
1952	18	16	14	21	3.4	5.4	9.5	"	"
1954	18	31	28	18	4.4	7.7	10.7	"	"
1956	32	54	42	35	4.9	7.7	8.8	"	"
1958	34	59	43	30	6.4	7.8	9.5	080	"
2000	7	49	33	30	3.3	8.3	9.8	"	"
2002	13	49	40	31	3.4	9.2	9.3	"	"
2004	10	41	27	19	4.8	10.1	9.3	"	"

March 1, 1960 (Continued)

Time, EST	Anemometer Revolutions				Temperature Difference, °C			Wind Dir.	%
2 min. period, ending	0.5m	1m	2m	4m	1m-0.5m	2m-0.5m	4m-0.5m	Degrees	Mod.
2006	11	26	30	17	4.5	9.3	10.7	080	MSG
2008	20	36	42	32	4.7	9.1	9.5	065	"
2010	2	12	23	23	4.2	8.6	10.7	045	"
2012	2	3	25	28	2.6	8.7	10.5	045	"
2014	5	11	30	34	2.9	9.1	11.2	045	"
2016	47	62	62	53	2.3	8.0	10.0	070	32
2018	23	38	53	53	4.1	9.1	7.2	045	34
2020	17	29	44	55	3.6	7.8	8.0	010	48
2022	45	71	76	72	3.0	5.1	8.2	315	MSG
2024	19	52	59	69	3.2	6.6	7.9	310	43
2026	34	62	70	60	5.3	5.0	7.0	330	39
2028	32	56	82	75	1.6	7.1	8.1	335	41
2030	17	33	62	72	1.0	4.6	8.5	330	42
2032	31	44	70	54	1.0	4.1	7.9	330	51
2034	5	17	47	56	1.5	3.2	8.1	330	51
2036	15	23	36	68	1.5	3.7	8.1	320	45
2038	9	12	20	51	1.4	4.4	10.1	310	34
2040	15	26	45	67	2.2	5.0	9.8	"	32
2042	2	26	48	63	2.9	5.6	10.6	"	39
2044	16	42	62	75	2.1	3.4	9.6	"	54
2046	3	10	46	63	1.7	5.9	11.1	300	63
2048	19	28	37	76	1.4	2.1	9.1	310	76
2050	14	21	34	81	1.7	3.3	9.6	310	53
2052	9	20	42	87	2.1	4.6	10.0	310	51
2054	3	28	59	80	2.0	4.5	9.7	295	57
2056	4	15	48	72	1.9	3.7	9.6	295	80
2058	7	20	54	72	1.0	3.0	9.1	300	80
2100	11	24	54	66	1.0	3.2	9.7	305	72
2102	23	34	70	71	.7	3.6	9.8	300	67
2104	25	36	50	85	1.0	1.7	6.4	305	37
2106	11	23	57	102	1.4	2.6	7.8	335	37
2108	23	47	90	88	.8	4.1	9.0	300	35
2110	38	51	78	92	.7	3.1	8.9	295	69
2112	10	28	75	84	1.2	5.3	10.0	295	80
2114	12	28	75	92	.9	3.7	10.3	300	77
2116	10	33	94	99	.9	6.6	10.3	300	72
2118	7	35	97	102	1.0	7.4	9.9	295	72
2120	4	34	101	96	1.3	6.4	10.3	300	70
2122	5	17	80	99	1.2	4.2	10.6	305	48
2124	30	52	102	103	1.1	4.2	8.2	315	48
2126	17	50	103	99	1.0	5.2	9.3	315	41
2128	15	52	116	95	.9	5.9	11.1	305	65
2130	2	38	107	94	1.1	6.1	11.8	300	50
2132	MSG	MSG	MSG	MSG	1.2	4.0	11.2	300	59

March 1, 1960 (Continued)

Time, EST	Anemometer Revolutions				Temperature Difference, °C			Wind Dir. Degrees	% Mod.
2 min. period, ending	0.5m	1m	2m	4m	1m-0.5m	2m-0.5m	4m-0.5m		
2134	MSG	MSG	MSG	MSG	1.2	3.4	11.0	300	50
2136	5	13	75	88	1.0	3.3	10.8	305	40
2138	1	15	89	103	1.5	3.9	10.4	315	41
2140	1	16	98	99	1.6	5.5	11.2	315	62
2142	5	27	107	108	1.6	5.7	10.8	315	63
2144	11	13	82	106	1.1	4.1	10.4	325	60
2146	6	22	97	109	1.4	5.4	10.5	325	82
2148	19	25	82	111	1.0	3.8	10.7	325	59
2150	25	25	89	101	.8	3.8	10.4	330	62
2152	27	32	92	103	.2	2.5	10.3	335	69
2154	24	36	78	114	.3	2.2	10.3	335	59
2156	37	41	98	108	.3	2.9	9.8	335	67
2158	39	50	103	104	.2	4.6	10.5	340	62
2200	47	66	108	101	.7	6.5	10.5	"	65
2202	27	41	99	97	.3	5.6	11.3	"	62
2204	25	36	82	100	.4	3.7	11.0	"	72
2206	30	49	98	107	.9	6.1	11.2	"	79
2208	14	33	93	103	.7	4.6	11.4	"	69
2210	31	48	98	102	.7	6.3	11.0	"	74
March 2, 1960									
1840	MSG	MSG	MSG	MSG	1.3	2.1	2.3	MSG	20
1842	81	114	158	184	1.4	2.6	3.2	"	18
1844	79	116	162	184	1.4	2.9	3.2	"	19
1846	92	124	166	189	1.5	2.6	3.4	"	19
1848	111	*141	184	MSG	1.2	2.6	3.2	"	20
1850	125	*151	189	"	.9	1.9	2.7	"	19
1852	144	*174	216	"	.8	1.7	2.1	"	19
1854	143	*170	212	"	.9	1.8	2.2	"	18
1856	143	*167	205	"	.8	1.7	2.1	"	18
1858	115	*139	176	"	1.1	1.8	2.3	"	21
1900	123	*144	179	"	.8	1.9	2.5	"	21
1902	120	*141	176	"	1.0	1.4	2.4	"	23
1904	132	*167	193	"	.8	2.0	2.1	"	22
1906	133	*168	195	"	.8	1.8	2.4	"	24
1908	131	*168	196	"	1.1	1.6	2.4	"	24
1910	134	*170	201	"	.9	1.9	2.4	"	24
1912	122	*150	189	"	1.2	2.1	2.4	"	25
1914	125	*155	196	"	1.1	2.1	2.6	"	24
1916	145	*169	208	"	.8	1.8	2.2	"	24

*Interpolated.

March 2, 1960 (Continued)

Time, EST	Anemometer Revolutions				Temperature Difference, °C			Wind Dir. Degrees	% Mod.
2 min. period, ending	0.5m	1m	2m	4m	1m-0.5m	2m-0.5m	4m-0.5m		
1918	MSG	MSG	MSG	MSG	1.1	2.0	2.4	MSG	25
1920	"	"	"	"	.9	1.5	2.3	"	24
1922	"	"	"	"	.9	1.8	2.4	"	24
1924	167	*200	236	"	1.0	1.9	2.0	"	24
1926	143	*171	210	"	.7	1.7	2.2	"	23
1928	148	*178	220	"	.9	1.7	2.1	"	23
1930	160	*192	226	"	.8	1.6	2.1	"	24
1932	147	*176	217	"	.9	1.8	2.3	"	23
1934	182	*213	249	"	.8	1.6	1.9	"	22
1936	172	*200	234	"	.8	1.4	1.7	"	22
1938	170	*200	230	"	.7	1.4	1.8	"	24
1940	183	*211	245	"	.5	1.3	2.0	"	25
1942	162	*195	231	"	.8	1.4	1.7	"	27
1944	187	*215	251	"	.7	1.2	1.8	"	28
1946	188	*217	253	"	.8	1.6	1.6	"	26
1948	185	*213	247	"	.5	1.2	1.7	"	23
1950	187	*215	250	"	.5	1.2	1.6	"	21
1952	190	*217	256	"	.8	1.2	1.5	"	21
1954	181	*209	249	"	.5	1.2	1.5	"	22
1956	192	*216	252	"	.5	1.3	1.5	"	22
1958	183	*212	248	"	.7	1.1	1.6	"	21
2000	205	*234	261	"	.4	.9	1.3	"	20
2002	197	*227	259	"	.5	.9	1.5	"	20
2004	201	*230	253	"	.4	.8	1.2	"	20
2006	194	*225	257	"	.4	1.0	1.3	"	19
2008	178	*206	242	"	.5	1.0	1.4	"	18
2010	194	*220	249	"	.4	.8	1.1	"	18
2012	196	*227	258	"	.4	.9	1.0	015	18
2014	196	*222	248	"	.4	.8	1.0	"	18
2016	203	*233	263	"	.4	.8	1.1	"	17
2018	201	*228	258	"	.3	.7	1.0	"	17
2020	213	*241	266	"	.3	.7	.9	020	16
2022	213	*241	265	"	.3	.7	.9	"	16
2024	209	*239	268	"	.2	.5	1.0	"	15
2026	216	*246	275	"	.3	.7	.8	"	16
2028	199	*227	257	"	.3	.7	.8	"	15
2030	204	*232	255	"	.3	.7	.8	"	15
2032	205	*234	261	"	.3	.5	.8	"	14
2034	218	*241	264	"	.2	.5	.8	015	14
2036	230	*251	273	"	.2	.5	.7	"	14
2038	213	*241	269	"	.3	.4	.5	"	14
2040	211	239	265	"	.2	.4	.8	"	13

*Interpolated.

MICROMETEOROLOGICAL AND SCINTILLATION DATA

March 7, 1960

Time, EST	Anemometer Revolutions				Temperature Difference, °C			Wind Dir. Degrees	% Mod.
2 min. period, ending	0.5m	1m	2m	4m	1m-0.5m	2m-0.5m	4m-0.5m		
1824	88	119	144	166	2.2	2.8	3.1	305	35
1826	85	118	143	163	2.2	2.5	3.2	305	32
1828	74	110	135	155	2.3	3.0	3.6	305	32
1830	70	100	119	141	2.2	3.4	4.2	300	29
1832	57	96	120	141	3.5	4.4	4.9	"	37
1834	55	87	115	135	3.0	4.6	4.9	"	31
1836	50	80	107	126	3.5	4.7	4.8	"	25
1838	50	75	91	121	2.9	4.2	5.6	"	21
1840	42	68	81	98	2.9	3.8	5.3	"	16
1842	38	60	82	102	3.0	5.5	6.1	"	26
1844	55	72	76	86	2.0	2.4	3.6	"	24
1846	49	68	78	80	2.2	3.9	4.0	295	20
1848	29	63	75	MSG	5.0	6.2	6.9	295	20
1850	13	*45	77	"	6.1	7.2	7.4	290	18
1852	7	*35	85	"	5.7	7.7	8.3	285	15
1854	13	*35	86	"	6.2	8.2	8.5	285	17
1856	14	*40	83	"	5.0	8.2	8.5	280	21
1858	2	*30	75	"	3.9	8.9	9.1	270	18
1900	3	*38	81	"	4.1	9.5	10.0	275	18
1902	17	*45	77	"	3.0	8.9	9.7	285	24
1904	10	*30	66	"	3.7	8.3	9.0	295	26
1906	8	*28	65	"	4.0	8.5	9.6	305	32
1908	11	*20	62	"	1.9	6.1	7.6	305	33
1910	10	*20	65	"	2.4	6.2	8.2	310	35
1912	6	*18	55	"	2.3	6.4	8.7	300	30
1914	2	*10	51	"	2.2	7.3	8.8	320	29
1916	9	*17	61	"	2.0	5.8	7.7	"	33
1918	16	*36	58	"	2.9	4.8	7.7	"	32
1920	11	*21	66	"	2.1	5.4	7.5	"	28

*Interpolated

March 8, 1960

0550	MSG	MSG	MSG	MSG	0	1.9	7.9	MSG	34
0552	"	"	"	"	.4	1.6	7.6	"	43
0554	"	"	"	"	.3	1.9	8.6	"	41
0556	"	"	"	"	.8	5.3	9.8	"	99
0558	"	"	"	"	1.2	5.0	10.1	"	119
0600	"	"	"	"	.7	3.3	8.5	"	80
0602	20	38	49	65	1.3	3.0	8.3	340	47
0604	0	29	46	48	1.6	3.2	9.3	340	48

March 8, 1960 (Continued)

Time, EST	Anemometer Revolutions				Temperature Difference, °C			Wind Dir. Degrees	% Mod.
2 min. period, ending	0.5m	1m	2m	4m	1m-0.5m	2m-0.5m	4m-0.5m		
0606	0	21	39	41	1.4	3.3	10.3	335	45
0608	"	24	37	43	1.1	2.2	8.7	325	48
0610	"	27	40	52	.8	2.2	8.4	"	74
0612	"	13	22	45	.8	1.9	9.0	"	89
0614	25	37	42	43	.4	1.7	9.3	"	82
0616	9	24	44	38	.3	2.0	9.2	"	72
0618	0	11	31	43	.1	2.2	8.8	"	69
0620	4	34	42	68	.5	1.6	8.8	315	79
0622	43	49	72	59	.1	1.3	9.1	310	82
0624	27	35	67	57	.2	2.5	9.7	305	69
0626	0	23	46	59	.2	2.3	9.3	"	69
0628	0	26	54	47	-.2	2.2	9.0	"	76
0630	20	36	61	50	-.3	2.5	8.5	"	70
0632	7	27	54	64	.1	2.2	9.2	310	63
0634	0	23	51	56	.1	2.2	9.6	305	62
0636	"	26	47	44	.2	2.1	9.6	"	63
0638	"	26	44	36	.2	1.8	9.2	"	48
0640	"	37	44	28	.1	2.1	8.1	315	40
0642	"	43	43	38	1.8	4.1	9.8	330	40
0644	"	39	37	30	3.2	4.8	10.7	"	25
0646	"	30	27	30	3.4	4.4	11.0	"	31
0648	"	23	37	33	2.8	3.7	10.4	"	44
0650	"	31	48	49	1.9	2.6	9.6	"	56
0652	"	27	47	52	1.1	2.4	9.5	"	72
0654	"	21	39	50	-.1	1.8	9.6	335	80
0656	"	32	54	57	.2	2.0	9.2	"	74
0658	10	44	56	54	-.3	1.4	8.2	"	67
0700	1	20	43	58	.8	2.1	8.7	"	50
0702	0	17	36	51	.1	2.2	8.9	"	40
0704	"	12	31	44	.5	2.5	9.3	330	45
0706	"	17	32	49	.7	2.8	9.9	340	57
0708	"	23	29	45	.9	2.6	9.5	MSG	53
0710	7	24	33	31	.7	2.6	9.6	"	45
0712	25	35	32	33	1.9	3.7	10.5	"	47
0714	26	30	29	37	2.7	4.0	10.6	"	50
0716	25	14	30	36	1.7	3.1	10.4	"	57
0718	10	13	32	37	2.0	3.5	10.5	"	47
0720	5	17	33	33	.9	2.9	9.7	"	40
0722	0	18	32	37	1.0	3.4	10.2	"	51
0724	0	14	31	44	1.8	3.8	10.5	"	51
0726	0	17	38	49	1.4	3.8	9.6	"	51
0728	11	31	50	62	.5	2.3	8.3	"	63
0730	12	24	61	52	.8	3.8	9.5	"	69
0732	26	33	49	50	-.3	3.1	7.3	"	55

March 8, 1960 (Continued)

Time, EST	Anemometer Revolutions				Temperature Difference, °C			Wind Dir. Degrees	% Mod.
2 min. period, ending	0.5m	1m	2m	4m	1m-0.5m	2m-0.5m	4m-0.5m		
0734	25	38	58	48	.7	2.9	8.3	MSG	53
0736	51	65	74	61	1.2	3.3	6.6	"	34
0738	78	84	74	72	3.0	4.4	7.7	"	32
0740	55	58	71	51	3.2	5.0	9.1	"	37
0742	20	43	63	55	2.6	4.5	9.1	"	35
0744	18	44	70	57	1.8	5.2	8.6	"	37
					March 14, 1960				
0948	17	20	24	32	-.3	-1.5	-4.1	100	10
0950	13	16	20	28	.9	-1.9	-3.7	"	11
0952	15	16	18	28	.7	-3.3	-5.0	"	10
0954	17	18	19	29	.5	-4.0	-4.6	"	10
0956	13	13	12	20	-.7	-2.8	-2.5	"	11
0958	11	9	11	17	2.2	-.3	.2	"	12
1000	15	17	19	20	1.5	-.4	.7	"	12
1002	11	11	15	19	.9	-.1	3.0	"	12
1004	1	1	8	12	.9	0	1.6	"	11
1006	4	1	14	19	1.1	-2.3	.2	"	11
1008	11	13	20	22	1.9	-1.8	-.1	"	11
1010	6	5	15	15	.9	-2.8	-1.0	"	12
1012	5	2	2	3	.7	-1.0	1.5	"	12
1014	4	3	2	1	1.8	1.2	6.2	"	12
1016	8	4	3	0	2.2	2.8	5.7	"	10
1018	1	1	1	2	MSG	MSG	MSG	"	10
1020	9	8	15	10	.7	-3.7	.3	"	10
1022	24	23	24	23	1.3	-1.6	3.4	"	12
1024	29	32	34	35	1.0	-.3	3.1	"	14
1026	14	12	15	17	.3	-.3	1.0	"	17
1028	11	7	11	11	.9	-.2	1.7	"	15
1030	16	19	25	31	.7	-1.4	-.5	"	16

MICROMETEOROLOGICAL AND SCINTILLATION DATA
(Willow Run Field Station)

January 25, 1961

Time, EST	Anemometer Revolutions				Air Temp.°C	Temperature Difference,°C		Wind Dir. Degrees	% Mod.
2 min.period, ending	0.5m	1m	2m	4m	C.5m	2m-0.5m	4m-0.5m		
1956	22	35	44	43	-13.5	.8	1.5	020	14
1958	20	27	34	35	-13.5	.9	.9	045	11
2000	10	14	22	30	-13.9	1.2	1.9	"	10
2002	16	16	22	25	-14.7	1.2	2.8	"	8
2004	2	6	5	16	-15.4	.9	2.8	"	8
2006	10	26	14	8	-15.8	.8	2.3	"	6
2008	5	29	28	26	-16.3	1.1	2.9	"	8
2010	20	37	33	30	-16.6	1.7	3.0	010	14
2012	14	31	36	38	-16.7	2.1	3.6	355	10
2014	21	35	39	43	-16.6	2.3	3.3	360	10
2016	17	33	40	47	-15.9	1.9	2.8	005	12
2018	10	30	37	43	-14.9	1.8	2.1	010	18
2020	14	10	18	32	-15.1	1.5	2.8	"	8
2022	33	23	18	23	-15.6	1.5	2.9	"	9
2024	22	28	25	23	-15.5	1.2	2.8	"	5
2026	13	19	19	23	-15.8	.9	2.6	020	3
2028	20	24	29	31	-15.8	1.5	2.8	020	5
2030	4	13	29	40	-16.0	1.1	2.8	020	9
2032	8	19	23	32	-16.1	2.2	2.6	030	6
2034	14	25	26	40	-15.9	1.3	1.9	045	10
2036	11	14	26	40	-15.8	1.2	2.1	060	8
2038	11	15	31	42	-15.7	1.1	1.9	"	6
2040	14	20	30	40	-15.4	.8	1.8	"	17
2042	12	21	41	52	-15.5	.7	1.7	"	14
2044	12	29	47	54	-15.6	.8	1.9	"	17
2046	26	35	51	58	-15.4	.5	1.9	210	23
2048	23	33	51	59	-15.4	.6	1.9	"	14
2050	7	20	46	56	-15.4	.6	1.8	"	6
2052	3	8	29	52	-15.7	.5	2.2	"	4
2054	5	11	36	52	-15.9	.4	2.5	160	6
2056	7	10	33	50	-15.2	-0.1	2.6	110	8
2058	6	23	43	47	-15.3	.8	2.5	090	6
2100	38	54	62	57	-14.2	1.1	1.2	090	8
2102	40	50	58	67	-13.4	.6	.8	090	10
2104	30	37	48	54	-13.0	.3	.5	130	10
2106	16	26	33	37	-13.0	.5	.8	210	17
2108	33	29	25	27	-14.4	.7	1.9	"	23
2110	44	56	68	58	-15.2	.3	2.0	"	22
2112	23	36	55	53	-15.3	.6	2.0	"	19
2114	16	28	52	67	-15.2	.4	1.8	"	13
2116	1	7	33	53	-15.5	.4	2.0	"	8

MICROMETEOROLOGICAL AND SCINTILLATION DATA
(Willow Run Field Station)

February 6, 1961

Time, EST	Anemometer Revolutions				Air Temp.°C	Temperature Difference,°C		Wind Dir. Degrees	% Mod.
2 min.period ending	0.5m	1m	2m	4m	1.0m	2m-1m	4m-1m		
1946	7	25	73	107	-10.1	3.6	6.9	255	35
1948	11	27	80	110	-9.9	3.7	6.9	250	27
1950	35	47	85	100	-8.2	2.9	5.2	250	28
1952	44	58	83	101	-7.7	2.8	4.3	255	27
1954	58	79	98	102	-7.1	2.7	3.4	255	32
1956	48	66	83	101	-7.6	2.6	3.3	260	32
1958	25	41	75	92	-8.1	2.8	3.4	260	27
2000	20	35	67	109	-8.3	1.6	3.7	260	24
2002	6	22	59	108	-8.8	1.6	4.8	265	21
2208	67	98	130	142	-10.6	2.5	4.3	035	29
2210	64	102	140	155	-10.2	2.9	4.0	025	30
2212	74	89	118	149	-8.7	1.4	2.0	025	35
2214	71	91	124	150	-9.3	1.3	2.7	025	30

February 8, 1961

1406	102	MSG	131	148	MSG	MSG	MSG	005	18
1408	53	"	61	65	"	"	"	350	12
1410	86	"	100	110	"	"	"	010	12
1412	67	"	84	95	"	"	"	010	14
1414	81	"	101	108	5.9	-.1	.2	360	12
1416	118	"	151	169	6.6	-.1	.1	325	13
1418	164	189	216	243	5.5	0	.2	320	14
1420	MSG	MSG	MSG	MSG	5.2	0	.1	015	14
1422	141	163	178	197	5.2	.1	.1	015	12
1424	166	189	212	239	5.3	.1	.1	035	13
1426	176	199	232	264	5.1	-.1	.1	015	14
1428	160	184	211	238	5.4	-.1	-.1	335	12
1430	178	203	230	258	5.2	0	-.1	340	13
1432	145	165	191	214	5.4	-.1	-.1	355	12
1434	163	186	213	232	5.4	-.1	.1	340	17
1436	132	148	165	194	5.6	-.1	.1	360	20
1438	149	168	187	212	5.5	-.1	-.1	355	18
1440	139	155	178	197	MSG	MSG	MSG	360	14
1442	108	127	142	163	"	"	"	360	14
1444	164	191	215	239	"	"	"	320	14
1446	173	196	224	248	"	"	"	330	14
1448	117	135	151	166	5.4	-.1	0	315	12
1450	107	121	138	148	5.8	-.1	0	320	14
1452	147	169	194	213	5.7	-.1	-.2	335	12

MICROMETEOROLOGICAL AND SCINTILLATION DATA
(Willow Run Field Station)

February 8, 1961 (Continued)

Time, EST	Anemometer Revolutions				Air Temp.°C	Temperature Difference,°C		Wind Dir. Degrees	% Mod.
2 min.period, ending	0.5m	1m	2m	4m	1.0m	2m-1m	4m-1m		
1454	143	161	179	202	5.7	-.1	0	345	14
1456	118	137	158	174	5.8	-.1	0	350	16
1458	130	146	163	181	5.7	-.1	0	350	14
1500	146	167	188	202	5.8	0	-.1	360	12
1502	139	161	178	197	5.9	0	0	350	14
1504	175	197	220	240	5.8	.1	.2	350	16
1506	183	210	230	250	5.7	.1	.3	330	14
1508	157	184	207	231	5.6	0	.1	310	14
1510	142	162	182	193	5.7	-.1	0	300	12
1512	178	205	240	274	5.8	-.1	0	310	14
1514	181	211	237	262	5.7	0	.1	300	14
1516	150	170	195	219	5.8	-.1	.1	325	14
1518	151	176	198	219	5.9	0	.2	360	14
1520	150	171	195	219	5.9	.1	.2	360	14
1522	162	185	205	219	5.9	.2	.2	360	14
1524	162	190	210	225	5.9	0	.2	350	14
1526	175	201	232	263	5.8	-.1	.1	360	14
1528	138	159	181	207	5.9	0	.1	340	14
1530	173	198	226	250	5.8	0	.1	330	18
1532	119	136	149	154	5.9	-.1	.1	330	21
1534	85	99	109	122	6.1	0	-.1	320	12
1536	132	151	184	208	6.2	-.1	.1	320	13
1538	117	133	149	166	5.9	-.1	-.1	330	12
1540	141	166	190	210	6.2	-.1	0	330	13

February 14, 1961

1958	31	47	69	107	-.5	1.2	1.2	285	32
2000	20	36	61	101	-.6	1.2	1.4	285	28
2002	29	45	70	108	-.5	1.2	1.3	290	26
2004	33	48	69	107	-.6	1.3	1.3	280	25
2006	43	57	76	108	-.5	1.4	1.4	280	20
2008	35	47	62	85	-.5	1.3	1.6	275	26
2010	37	44	60	88	-.8	1.5	1.4	"	28
2012	32	36	44	69	-.5	1.5	1.7	"	24
2014	28	33	43	69	-1.1	1.6	1.8	"	22
2016	13	20	37	64	-1.0	1.9	1.8	265	25
2018	7	21	36	60	-.9	1.4	1.7	270	25
2020	12	20	32	56	-.9	1.4	1.6	265	22
2022	15	19	35	61	-.9	1.7	1.7	270	20
2024	11	16	31	58	-1.1	1.7	1.6	270	24
2026	27	39	55	84	-.7	1.0	.9	280	32

MICROMETEOROLOGICAL AND SCINTILLATION DATA
(Willow Run Field Station)

February 14, 1961 (Continued)

Time, EST	Anemometer Revolutions				Air Temp.°C	Temperature Difference,°C		Wind Dir. Degrees	% Mod.
2 min.period, ending	0.5m	1m	2m	4m	1.0m	2m-1m	4m-1m		
2028	26	36	56	92	-.5	1.2	.9	280	33
2030	16	30	54	84	-.8	1.4	1.0	280	33
2032	12	31	59	95	-.9	1.5	.9	280	31
2034	33	45	67	101	-.6	1.2	.9	270	29
2036	38	52	78	115	-.8	1.4	.9	270	MSG
2038	51	68	90	119	-.6	1.3	.9	270	"
2040	50	71	98	124	-.7	1.5	.9	275	"
2042	32	54	87	116	-.9	1.8	1.3	275	40
2044	38	59	88	125	-1.1	1.6	1.1	275	39
2046	49	70	96	127	-.8	1.4	1.1	280	42
2048	36	55	82	120	-.8	1.6	1.4	285	35
2050	34	45	66	102	-1.1	2.4	2.1	305	26
2052	31	41	54	79	-1.4	2.9	2.8	305	20
2054	34	38	50	78	-1.3	2.6	2.4	320	21
2056	44	48	57	81	-.4	1.9	1.9	320	9
2058	62	79	94	102	-.2	1.3	1.9	325	17
2100	57	87	101	109	-1.1	1.0	1.5	345	24
2102	45	72	93	106	-.7	1.0	1.8	335	16
2104	38	67	90	101	-1.8	1.6	2.2	335	13
2106	38	72	92	97	-1.4	1.4	1.7	350	17
2108	34	66	88	94	-1.1	1.0	1.7	350	16
2110	32	59	88	95	-1.2	1.6	2.2	355	24
2112	45	74	99	110	-1.3	1.9	2.1	010	22
2114	61	86	104	116	-1.0	1.6	2.0	010	24
2116	58	86	105	123	-1.6	1.9	2.2	015	25
2118	67	96	115	140	-.9	1.4	2.1	020	36
2120	64	90	114	137	-.8	1.7	2.3	020	31
2122	52	76	103	122	-.9	2.1	2.5	020	30
2124	54	69	111	134	-1.3	2.1	2.3	020	28
2126	58	89	130	158	-1.4	2.3	2.6	020	33
2128	59	83	116	150	-.9	1.8	2.6	005	30
2130	49	73	102	126	-1.0	1.9	2.6	005	22
2132	26	34	55	90	-1.4	2.6	3.4	015	16
2134	38	30	14	48	-.9	2.2	3.4	005	19
2136	32	23	5	28	-.1	1.2	3.2	010	13
2138	22	15	3	27	.5	.9	3.3	010	12
2140	9	3	6	38	-.2	2.5	3.9	010	10
2142	15	18	25	39	-.3	2.4	4.3	005	28
2144	32	33	30	42	-.4	.6	2.6	350	34
2146	39	46	45	45	-.4	.8	2.7	325	33
2148	18	34	44	51	-.8	1.7	2.9	315	35
2150	29	41	49	58	-.9	1.3	2.6	305	32
2152	8	19	41	58	-.9	1.6	2.9	305	23

MICROMETEOROLOGICAL AND SCINTILLATION DATA
(Ford Lake)

February 20, 1961

Time, EST	Anemometer Revolutions				Air Temp.°C	Temperature Difference,°C		Wind Dir. Degrees	% Mod.
2 min.period, ending	0.5m	1m	2m	4m	1.0m	2m-1m	4m-1m		
2000	29	27	23	19	-3.6	-.2	-.3	*	3
2002	41	40	40	37	-3.8	-.1	-.3	*	4
2004	45	42	43	43	-3.9	0	.2	*	4
2006	35	34	32	29	-4.0	.2	.4	*	4
2008	31	26	18	14	-3.9	-.1	-.2	*	5
2010	44	35	31	20	-3.6	-.4	-.9	*	5
2012	49	48	41	32	-3.6	.2	-.3	*	5
2014	37	37	33	23	-3.6	-.1	-.5	*	3
2016	21	20	20	12	-3.9	-.1	-.5	*	3
2018	33	35	29	21	-4.3	.1	.1	*	3
2020	30	31	34	29	-4.2	.1	.2	*	3
2022	45	44	41	37	-3.9	.1	-.2	*	3
2024	44	45	44	38	-4.1	-.1	-.5	*	3
2026	23	21	20	18	-4.5	-.1	-.2	*	3
2028	15	15	14	6	-4.5	.1	-.3	*	3
2030	3	7	8	7	-5.2	.2	.1	*	3
2032	14	15	18	9	-5.4	.1	-.2	*	2
2034	3	2	5	8	-5.3	.1	.1	*	2
2036	22	20	18	13	-5.2	0	.5	*	2
2038	23	19	14	17	-5.3	.4	.9	*	2
2040	27	24	23	16	-4.8	-.1	-.3	*	3
2042	53	52	45	32	-4.4	-.2	-.5	*	4
2044	46	45	39	25	-4.1	-.1	-.8	*	6
2046	50	50	48	31	-4.3	-.1	-.5	*	6
2048	47	51	52	41	-4.6	.3	.1	*	6
2050	60	61	58	55	-4.3	.3	.3	*	8
2052	53	52	53	52	-4.3	.3	.2	*	8
2054	54	52	52	49	-4.5	.2	.5	*	8
2056	62	62	65	58	-4.7	.9	.9	*	8
2058	64	61	60	60	-4.6	.8	.8	*	8
2100	50	50	51	62	-4.4	.5	.7	*	11
2102	51	51	54	59	-4.3	.2	.5	*	7
2104	47	47	50	54	-4.6	.3	.7	*	7
2106	52	52	54	57	-4.4	.6	.7	*	6
2108	68	68	70	65	-3.9	.2	.3	*	8
2110	71	70	73	78	-4.1	.2	.4	*	9
2112	67	69	73	76	-4.2	.2	.4	*	8
2114	66	65	66	67	-3.9	.2	.5	*	7
2116	95	101	107	110	-3.8	.3	.4	*	8
2118	93	97	102	108	-3.9	.3	.6	*	8
2120	65	71	79	91	-3.9	.2	.4	*	7

*Average wind direction northeast for entire period.

MICROMETEOROLOGICAL AND SCINTILLATION DATA
(Ford Lake)

February 20, 1961 (Continued)

Time, EST	Anemometer Revolutions				Air Temp.°C	Temperature Difference,°C		Wind Dir. Degrees	% Mod.
2 min. period, ending	0.5m	1m	2m	4m	1.0m	2m-1m	4m-1m		
2122	65	70	76	90	-4.2	.3	.4	*	7
2124	71	74	79	87	-4.3	.2	.4	*	8
2126	52	53	58	67	-4.3	.2	.5	*	6
2128	61	64	72	78	-4.1	.1	.3	*	5
2130	60	64	72	83	-4.2	.3	.5	*	5
2132	69	69	73	76	-3.9	.2	.3	*	6
2134	65	68	70	81	-4.2	.1	.2	*	6
2136	65	71	84	103	-4.5	.3	.6	*	6
2138	57	65	80	108	-4.8	.4	.9	*	5
2140	60	63	74	99	-5.0	.4	.8	*	5
2142	52	56	63	82	-5.5	.4	.9	*	4
2144	41	43	49	65	-5.3	.4	.7	*	4
2146	45	49	56	74	-4.9	.2	.4	*	3
2148	40	42	50	72	-4.7	.2	.4	*	3
2150	45	49	59	71	-4.8	.3	.6	*	4
2152	46	50	61	71	-5.1	.3	.6	*	4
2154	43	48	58	74	-5.1	.5	.8	*	5
2156	44	48	58	71	-4.9	.3	.6	*	4
February 21, 1961									
1504	**	**	**	**	5.8	.3	.3	**	9
1506	**	**	**	**	6.0	0	-.1	**	13
1508	**	**	**	**	5.4	.3	.3	**	13
1510	**	**	**	**	MSG	.2	.6	**	14
1512	**	**	**	**	"	.6	.9	**	12
1514	**	**	**	**	"	.7	.6	**	11
1516	**	**	**	**	"	.7	.8	**	9
1518	**	**	**	**	"	.7	1.5	**	9
1520	**	**	**	**	"	1.1	1.9	**	9
1522	**	**	**	**	"	.9	2.2	**	10
1524	**	**	**	**	"	.9	2.0	**	8
1526	**	**	**	**	"	.5	.6	**	9
1528	**	**	**	**	"	.3	.9	**	6

*Average wind direction northeast for entire period.

**Wind speed and direction system malfunction.

MICROMETEOROLOGICAL AND SCINTILLATION DATA
(Willow Run Field Station)

March 15, 1961

Time, EST	Anemometer Revolutions				Air Temp.°C	Temperature Difference,°C		Wind Dir. Degrees	% Mod.
2 min.period, ending	0.5m	1m	2m	4m	1.0m	2m-1m	4m-1m		
1934	349	409	468	530	1.1	.2	.3	MSG	22
1936	334	389	439	491	1.0	.2	.3	"	22
1938	285	333	383	438	.8	.2	.3	"	24
1940	294	343	392	435	.7	.2	.3	"	24
1942	322	382	436	491	.8	.2	.3	"	25
1944	304	353	411	463	.7	.2	.3	"	24
1946	342	405	465	524	.8	.2	.3	"	25
1948	295	345	401	459	.8	.2	.3	305	26
1950	251	300	347	396	.5	.2	.4	305	27
1952	214	255	299	349	.2	.3	.4	310	27
1954	248	295	340	375	.3	.2	.4	310	27
1956	218	260	296	339	.2	.2	.4	310	27
1958	215	255	299	341	-.1	.2	.6	305	27
2000	236	279	326	377	-.1	.2	.4	305	28
2002	201	243	285	328	0	.3	.5	310	27
2004	237	284	330	380	-.2	.3	.6	305	28
2006	249	296	336	374	-.2	.2	.4	305	29
2008	198	239	275	319	-.5	.3	.5	300	30
2010	228	275	325	361	-.5	.2	.4	305	30
2012	254	295	337	391	-.4	.3	.4	305	29
2014	293	345	399	455	.3	.2	.4	300	29
2016	256	302	348	400	.1	.3	.4	310	29
2018	282	329	368	415	-.1	.2	.4	305	27
2020	274	326	379	433	-.2	.3	.4	305	27
2022	261	311	350	392	-.1	.2	.4	305	27
2024	301	351	397	445	-.2	.2	.3	300	28
2026	260	305	343	380	-.3	.2	.3	310	27
2028	216	256	293	339	-.5	.2	.5	310	26
2030	269	321	368	409	-.6	.2	.4	305	27
2032	256	302	343	391	-.5	.2	.5	315	27
2034	218	255	305	360	-.8	.3	.4	305	27
2036	194	234	271	314	-1.0	.3	.5	310	28
2038	244	298	336	378	-1.1	.3	.5	305	28
2040	272	314	350	392	-.9	.3	.4	310	27
2042	249	291	334	371	-.9	.3	.4	305	27
2044	250	299	333	375	-1.2	.3	.4	310	27
2046	267	316	364	416	-1.2	.2	.5	310	27
2048	259	306	362	424	-1.1	.3	.5	315	28
2050	275	329	374	435	-1.2	.2	.5	310	27
2052	250	306	356	400	-1.2	.3	.4	310	27
2054	240	281	320	365	-1.6	.3	.4	305	26
2056	255	301	346	391	-1.4	.2	.4	305	26
2058	282	326	377	426	-1.5	.2	.4	210	25

MICROMETEOROLOGICAL AND SCINTILLATION DATA
(Willow Run Field Station)

March 15, 1961 (Continued)

Time, EST	Anemometer Revolutions				Air Temp.°C	Temperature Difference,°C		Wind Dir. Degrees	% Mod.
2 min.period, ending	0.5m	1m	2m	4m	1.0m	2m-1m	4m-1m		
2100	251	306	354	409	-1.6	.2	.4	310	26
2102	258	300	351	399	-1.7	.3	.4	315	26
2104	258	306	347	396	-1.9	.2	.4	310	26
2106	273	317	360	409	-1.9	.2	.4	310	24
2108	251	294	335	381	-2.1	.2	.4	310	23
2110	240	282	318	357	-2.1	.2	.3	315	22
2112	260	306	346	387	-2.0	.2	.3	310	20
2114	226	266	300	335	-1.9	.2	.3	315	21
2116	222	266	305	351	-2.2	.2	.4	305	22
2118	206	243	281	322	-2.2	.2	.4	315	23
2120	247	289	336	387	-2.4	.2	.4	310	25
2122	205	247	290	326	-2.5	.2	.4	"	26
2124	182	217	258	306	-2.9	.3	.6	"	27
2126	184	217	251	292	-3.1	.3	.5	"	26
2128	192	226	264	301	-3.1	.3	.4	"	26
2130	222	265	300	349	-2.9	.3	.3	"	24
2132	207	247	286	337	-2.7	.2	.3	315	22
2134	182	217	252	276	-2.9	.2	.3	310	21
2136	194	230	268	305	-3.2	.2	.4	"	23
2138	232	275	324	370	-3.2	.2	.4	"	26
2140	194	233	266	312	-3.4	.2	.5	"	27
2142	177	213	248	289	-3.6	.3	.5	"	27
2144	167	201	232	273	-3.9	.3	.6	"	28

March 16, 1961

1436	MSG	MSG	MSG	MSG	-.9	-.4	-1.0	320	MSG
1438	"	"	"	"	-.9	-.5	-.9	340	85
1440	272	317	346	378	-.4	-.5	-.9	315	94
1442	321	377	428	491	-1.5	-.3	-.8	320	95
1444	307	361	412	464	-2.5	-.3	-.2	330	78
1446	377	444	520	580	-.9	-.7	-.9	335	53
1448	350	405	460	511	-1.5	-.4	-1.0	340	83
1450	340	387	445	501	.1	-.5	-1.0	350	83
1452	367	418	476	514	.2	-.6	-.7	350	83
1454	339	392	440	485	-.6	-.4	-.7	345	83
1456	327	377	426	466	-.9	-.3	-1.2	345	90
1458	345	402	454	510	-.8	-.3	-.9	345	85
1500	402	463	519	555	-.8	-.3	-.7	350	77
1502	420	493	560	616	-.7	-.3	-.9	340	78
1504	375	433	487	541	-.7	-.5	-.8	320	90
1506	377	437	489	543	-.9	-.2	-.5	325	90

MICROMETEOROLOGICAL AND SCINTILLATION DATA
(Willow Run Field Station)

March 16, 1961 (Continued)

Time, EST	Anemometer Revolutions				Air Temp.°C	Temperature Difference,°C		Wind Dir. Degrees	% Mod.
2 min.period, ending	0.5m	1m	2m	4m	0.1m	2m-1m	4m-1m		
1508	357	411	465	510	-1.3	-.1	-.8	320	88
1510	358	420	479	521	-.7	-.2	-.6	320	88
1512	325	380	430	480	-.7	-.2	-.9	325	92
1514	333	390	438	483	-.6	-.3	-.6	305	87
1516	322	375	410	441	-.7	-.2	-.3	315	95
1518	357	415	458	506	-1.7	-.1	-.4	325	92
1520	334	388	438	491	-.8	-.2	-1.0	330	85
1522	414	488	570	644	-.5	-.4	-1.0	350	80
1524	335	392	440	492	-1.4	-.2	-.6	330	87
1526	283	327	374	422	-.8	-.4	-.5	330	92
1528	374	443	505	562	-1.2	-.3	-.6	340	88
1530	406	475	535	602	-1.8	-.3	-.6	330	72
1532	394	469	538	589	-1.0	-.3	-.5	340	66
1534	359	422	476	529	-2.1	.2	-.3	335	47
1536	332	386	457	494	-1.9	-.3	-.3	330	75
1538	347	405	458	508	-1.7	.1	-.3	340	63
1540	311	367	420	475	-2.6	.2	.1	340	32
1542	371	435	492	538	-1.2	-.1	-.1	330	63
1544	380	438	498	547	-1.5	-.3	-.8	335	87
1546	348	405	463	520	-1.0	-.3	-.6	350	85
1548	326	368	426	472	-1.6	.1	-.3	345	61
1550	358	418	482	545	-2.3	.2	-.2	345	42
1552	321	374	427	473	-2.0	.2	-.2	345	39
1554	411	470	536	605	-1.4	-.4	-.7	350	73
1556	333	379	427	482	-1.5	-.1	-.5	335	85
1558	315	363	417	467	-.9	-.1	-.6	345	85
1600	349	406	471	541	-1.2	.1	-.6	340	68
1602	427	499	567	638	-1.3	-.1	-.3	355	49
1604	370	426	477	517	-1.4	0	-.2	340	72
1606	339	395	456	503	-1.7	.2	.4	350	66
1608	330	378	416	461	-1.3	.1	-.6	350	70

March 30, 1961

1346	78	86	93	101	6.1	-.7	-.4	285	71
1348	129	137	146	154	5.6	-.3	-.5	015	70
1350	148	169	188	200	6.8	-.5	-.9	325	87
1352	165	188	198	201	6.2	-.6	-.9	295	81
1354	107	115	126	128	5.6	-.5	.2	300	84
1356	129	143	155	172	5.4	-.5	-.8	320	84
1358	111	118	129	139	5.7	-.1	-.8	305	84
1400	168	188	208	219	5.4	-.6	-1.5	320	81

MICROMETEOROLOGICAL AND SCINTILLATION DATA
(Willow Run Field Station)

March 30, 1961 (Continued)

Time, EST	Anemometer Revolutions				Air Temp.°C	Temperature Difference,°C		Wind Dir. Degrees	% Mod.
2 min.period, ending	0.5m	1m	2m	4m	0.1m	2m-1m	4m-1m		
1402	149	167	183	208	6.4	.2	-1.2	360	70
1404	239	277	313	342	6.3	-1.2	-1.7	350	73
1406	216	237	263	286	6.1	-.9	-1.3	355	65
1408	178	197	218	237	5.9	-.9	-1.5	360	68
1410	215	244	268	293	6.7	-.8	-1.3	010	71
1412	149	164	185	205	5.7	-1.0	-1.2	015	74
1414	102	109	119	121	5.4	-.7	-.3	005	71
1416	106	117	137	147	6.6	.1	-.6	030	70
1418	128	146	161	179	6.2	-.7	-.5	025	68
1420	113	125	144	152	6.3	-.6	-1.2	005	78
1422	134	148	164	178	6.4	-.6	-.2	360	84
1424	170	193	222	238	7.6	-.6	-.6	315	78
1426	209	235	259	272	5.8	-.7	-1.0	320	85
1428	69	74	82	83	6.4	-.3	-.8	240	73
1430	123	130	137	139	5.8	-.8	-1.1	255	73
1432	85	93	102	116	7.1	-.9	-1.4	290	81
1434	75	81	89	96	6.7	-.4	-.5	240	76
1436	65	69	71	72	5.7	-.5	-.2	200	64
1438	75	81	89	96	6.1	.2	.1	150	71
1440	59	67	71	76	6.8	-.2	.9	140	81
1442	34	40	45	48	7.3	-.7	-.4	150	74
1444	99	106	116	109	7.3	-.2	-.6	030	68
1446	140	157	168	182	6.7	-.4	-1.3	340	76
1448	124	139	152	166	6.3	-.2	-.6	330	76
1450	265	299	328	351	6.7	-.5	-1.0	310	85
1452	153	180	202	222	6.7	-.9	-1.3	290	85
1538	125	142	162	177	6.1	-.5	-.8	305	85
1540	194	223	242	266	6.6	-.8	-1.2	320	77
1542	125	140	153	162	5.9	-.8	-.9	285	82
1544	97	109	117	130	6.7	-.6	-.4	290	80
1546	157	174	191	205	6.1	-.4	-.3	335	72
1548	108	118	130	139	6.2	-.3	-.3	350	66
1550	123	133	141	150	6.1	-.4	0	005	68
1552	172	189	207	218	5.6	-.5	-1.1	360	59
1554	112	122	128	139	5.9	-.5	-.6	010	70
1556	88	100	106	108	6.0	-.1	-.4	340	63
1558	75	90	96	105	6.3	-.1	0	300	61
1600	161	179	195	202	6.4	-.6	-.5	015	72
1602	182	206	228	251	6.9	-.5	-.9	360	MSG

MICROMETEOROLOGICAL AND SCINTILLATION DATA
(Willow Run Field Station)

March 30, 1961 (Continued)

Time, EST	Anemometer Revolutions				Air Temp.°C	Temperature Difference,°C		Wind Dir. Degrees	% Mod.
2 min.period, ending	0.5m	1m	2m	4m	1.0m	2m-1m	4m-1m		
1702	137	160	177	191	5.8	-.2	MSG	215	40
1704	158	183	204	215	5.9	-.4	"	215	37
1706	165	193	221	241	6.8	-.2	"	245	40
1708	178	203	232	254	6.1	-.3	"	260	40
1710	148	177	202	217	6.1	-.1	"	270	39
1712	MSG	MSG	MSG	MSG	5.5	-.3	"	250	37
1714	"	"	"	"	5.7	-.2	"	240	37
1716	"	"	"	"	5.8	-.1	"	260	38
1718	176	207	235	255	5.5	-.1	"	240	35
1720	129	147	165	184	5.3	-.2	"	240	33
1722	168	199	220	233	5.3	-.1	"	225	33
1724	105	117	132	148	5.3	-.3	"	235	30
1726	91	100	108	114	5.2	-.3	"	185	25
1728	34	36	37	44	5.6	-.2	"	205	24
1730	41	45	52	58	5.7	-.1	"	170	25
1732	107	118	124	132	6.5	-.2	"	240	28
1734	98	112	123	134	6.8	-.2	"	215	24
1736	70	84	98	103	6.8	-.1	"	235	23
1738	72	80	89	98	6.8	-.1	"	235	24
1740	78	88	98	105	6.8	-.1	"	230	23
1742	113	127	143	151	6.9	-.1	"	250	23
1744	111	127	142	152	6.8	-.1	-.1	260	19
1746	86	98	113	120	6.8	-.1	-.3	255	17
1748	100	115	126	129	6.6	0	-.1	245	17
1750	75	89	99	107	6.6	-.1	-.1	220	16
1752	65	77	90	103	6.6	-.1	-.2	220	12
1754	150	175	205	225	6.5	0	-.1	210	11
1756	133	159	191	210	6.6	0	-.1	250	10
1758	127	147	168	181	6.4	0	-.2	225	9
1800	104	128	148	165	6.4	.1	-.1	235	7
1802	111	131	150	164	6.4	.1	0	235	7
1804	87	103	113	128	6.4	.1	0	270	6
1806	70	86	99	109	6.4	0	-.1	275	4
1808	53	65	80	98	6.3	.1	.1	235	4
1810	64	78	99	120	6.2	.1	.1	215	4
1812	83	96	109	121	6.2	.2	.1	195	5
1814	58	70	82	94	6.2	.2	.1	185	5
1816	91	108	121	130	6.2	.2	.2	190	10
1818	75	91	106	120	6.0	.3	.3	250	14
1820	88	110	133	152	5.8	.3	.3	250	18
1822	81	98	115	132	5.6	.3	.5	250	20
1824	76	95	117	141	5.4	.4	.5	235	21
1826	109	133	163	190	5.5	.3	.5	225	25

MICROMETEOROLOGICAL AND SCINTILLATION DATA
(Willow Run Field Station)

March 30, 1961 (Continued)

Time, EST	Anemometer Revolutions				Air Temp.°C	Temperature Difference,°C		Wind Dir. Degrees	% Mod.
2 min.period, ending	0.5m	1m	2m	4m	1.0m	2m-1m	4m-1m		
1828	125	154	185	219	5.2	.3	.5	215	26
1830	130	157	181	202	5.7	.4	.5	220	28
1832	77	95	121	155	5.1	.3	.8	215	31
1834	58	79	102	132	4.5	.4	1.0	215	31
1836	58	81	109	140	4.4	.7	1.2	220	32
1838	64	94	134	171	4.2	.9	1.8	215	34
1840	60	88	125	163	3.7	.9	1.7	205	51
1842	65	89	126	171	3.1	1.2	2.6	200	39
1844	66	96	138	179	3.4	1.3	2.2	200	39
1846	59	85	124	172	3.1	1.0	2.3	200	37
1848	62	84	118	155	2.9	1.2	2.2	200	29
1850	51	72	103	137	2.2	1.4	2.4	200	30
1852	43	61	90	132	2.2	1.5	2.7	205	MSG
1854	38	57	88	132	1.9	1.6	2.9	205	"
1856	42	62	98	133	2.3	1.7	2.6	205	16
1858	51	75	103	139	2.7	1.2	1.9	200	14
1900	55	80	103	136	2.1	1.4	2.2	195	15
1902	55	80	102	129	2.5	1.5	2.0	190	19
1904	52	77	104	118	2.4	1.6	2.6	190	16
1906	40	64	90	115	1.8	1.7	2.8	190	11
1908	42	65	87	114	2.1	1.5	2.6	190	14
1910	38	54	75	93	1.4	1.2	3.4	190	15
1912	48	67	79	83	3.6	.9	.8	230	38
1914	45	61	75	83	3.5	.7	.8	215	23
1916	42	63	78	88	3.2	.9	1.2	210	15
1918	35	54	83	106	2.2	1.6	2.5	215	17
1920	43	67	86	125	2.7	.9	1.8	220	32
1922	36	51	92	119	1.5	1.7	3.4	210	20
1924	34	51	80	105	.9	2.0	4.0	200	8
1926	54	78	99	111	1.6	2.8	3.0	195	4
1928	64	93	105	121	2.5	1.7	2.0	195	14
1930	51	79	115	133	.7	2.6	3.6	195	23
1932	36	65	101	125	.9	3.2	4.2	195	17
1934	38	67	99	107	1.7	2.1	3.2	190	7
1936	44	68	93	96	1.8	1.8	2.8	180	15
1938	77	117	140	146	3.0	1.6	1.3	130	35
1940	116	153	175	195	2.5	.6	.9	110	26
1942	120	144	170	183	2.3	.3	.6	125	27
1944	119	144	178	209	2.0	.4	.9	125	26
1946	132	158	186	201	2.0	.6	.8	135	24
1948	121	144	183	205	1.9	.5	1.0	130	25
1950	110	138	172	198	2.1	.7	.8	140	26

MICROMETEOROLOGICAL AND SCINTILLATION DATA
(Willow Run Field Station)

March 30, 1961 (Continued)

Time, EST	Anemometer Revolutions				Air Temp.°C	Temperature Difference,°C		Wind Dir. Degrees	% Mod.
2 min.period, ending	0.5m	1m	2m	4m	1.0m	2m-1m	4m-1m		
1952	102	126	157	188	2.0	.6	.7	140	24
1954	125	151	183	207	2.1	.7	.8	155	25
1956	136	169	198	228	2.4	.6	.7	150	26
1958	122	156	192	226	1.9	.6	.8	160	26
2000	111	141	172	196	1.5	.6	1.3	170	29
2002	112	141	177	213	1.7	.6	1.1	170	27
2004	121	153	190	229	1.3	.6	.9	170	26
2006	104	136	173	225	.7	.5	1.4	180	26
2008	105	131	165	220	.4	.7	1.4	180	25
2010	92	120	157	212	.2	.7	1.6	180	26
2012	92	121	157	216	.3	.7	1.7	180	26
2014	84	109	148	210	0	.8	2.0	180	27
2016	80	109	143	200	-.1	.6	2.0	180	29
2018	89	116	154	214	-.2	.8	1.8	180	27
2020	88	117	157	201	.2	.8	1.7	175	30
2022	94	124	163	196	.6	.9	1.6	170	34
2024	88	121	157	194	1.0	.9	1.3	175	31
2026	89	118	151	173	1.5	.8	.9	160	30
2028	91	122	150	170	1.7	.7	.8	150	28
2030	93	116	143	165	1.4	.6	.7	160	29
2032	86	114	149	188	1.1	.6	1.2	160	30
2034	102	129	167	196	1.3	.8	1.2	170	30
2036	86	115	152	191	.7	.8	1.5	170	32
2038	91	119	156	195	.7	.7	1.4	170	30
2212	MSG	MSG	MSG	MSG	-1.0	2.1	1.8	185	MSG
2214	36	54	80	114	-.9	1.8	1.3	180	"
2216	23	39	80	115	-1.5	2.3	1.8	175	"
2218	35	55	89	120	-1.3	1.9	1.2	180	"
2220	26	42	80	111	-1.3	1.9	1.6	180	"
2222	28	46	75	106	-.9	1.8	1.4	185	19
2224	28	47	79	107	-1.0	1.8	1.3	185	18
2226	29	42	73	104	-1.5	1.9	1.7	190	17